# The role of Four-and-a-half LIM domain protein 2 in dendritic cell migration

Dissertation

zur
Erlangung des Doktorgrades (Dr. rer. nat.)
der
Mathematisch-Naturwissenschaftlichen Fakultät
der
Rheinischen Friedrich-Wilhelms-Universität Bonn

vorgelegt von
Katharina König
aus
Hamm

Bonn
August 2011

With authorization of the Faculty of Mathematics and Natural Sciences of the Rheinische Friedrich-Wilhelms-University of Bonn

The study presented here was conducted at the Institute of Pathology of the University Hospital Bonn.

| | |
|---|---|
| First Referee (Thesis Advisor): | Prof. Dr. Reinhard Büttner |
| Second Referee: | Prof. Dr. Percy Knolle |
| Third Referee: | Prof. Dr. Waldemar Kolanus |
| Fourth Referee: | Prof. Dr. Dieter Fürst |

Tag der Promotion: 20. Dezember 2011
Erscheinungsjahr: 2012

# Table of contents

# Abstract

We identified the four-and-a-half LIM domain protein 2 (FHL2) as a novel regulator of CCL19-induced dendritic cell (DC) migration. Initiation of migration is a hallmark of DC function and plays a central role in the induction and regulation of immune responses. *In vivo*, DCs continuously acquire Ag in the periphery and migrate to draining LNs, under the influence of local environmental chemotactic factors like CCL19/21 or sphingosine 1-phosphate (S1P). We investigated the role of S1P- and RhoA regulated FHL2 in this process.

We found reduced nuclear localization of FHL2 in mature bone marrow-derived DCs (BMDCs), compared with immature BMDCs, following stimulation with CCL19. Furthermore, in vitro-generated murine FHL2-/- BMDCs displayed a significantly increased migratory speed, directionality, and migratory persistence toward the chemokine CCL19 compared with wild-type BMDCs. Moreover*, in vivo*, FHL2-/- BMDCs showed increased migration toward lymphoid organs. FHL2-/- BMDCs increased the expression of S1P receptor 1, which was associated with greater Rac activation. An S1PR1 antagonist and knock-down of S1PR1 abrogated the increased migratory speed of FHL2-/- BMDCs. Our results identify FHL2 as an important novel regulator of DC migration via regulation of their sensitivity toward environmental migratory cues like S1P and CCL19.

# Zusammenfassung

Dendritische Zellen (DZ) spielen eine entscheidende Rolle in der Initiierung und Regulierung adaptiver und angeborener Immunantworten. In der Peripherie nehmen unreife DZ ständig Antigen auf, prozessieren es und wandern zu den drainierenden Lymphknoten, um T Zellen ihr spezifisches Antigen zu präsentieren. Die Migration der DZ zu den Lymphknoten spielt eine wichtige Rolle in der Ausübung ihrer Aufgabe als Antigen präsentierende Zellen. Man weiß, dass das Aktin Zytoskelett bei der Ausübung von Migration eine entscheidende Rolle spielt. Wir haben herausgefunden, dass das Four-and-a-half-Lim only protein (FHL2), das an Integrinen bindet und als Koaktivator von Transkriptionsfaktoren wirkt, an der Zellmigration von DZ beteiligt ist.

FHL2 findet sich in reifen aus murinen Knochenmark gewonnen dendritischen Zellen (KMDZ) nach Stimulation mit CCL19 an der Membran statt im Zellkern wieder, wie es bei immaturen KMDZ der Fall ist. Geschwindigkeit, Direktionalität und Persistenz von aus FHL2-defizienten KMDZ ist *in vitro* und *in vivo* signifikant erhöht. FHL2-/- prägen nicht konstitutiv den Chemokin Rezeptor CCR7, andere Maturationsmarker aus oder erhöhte Zytokin Produktion. Weiterhin hat FHL2 keinen Einfluss sowohl auf Rezeptor vermittelte als auch pinozytotische Antigenaufnahme und Präsentation von Ovalbumin zu T Zellen. Dafür weisen FHL2-defiziente KMDZ morphologisch einen reifen Phänotyp auf. Der Sphingosin-1-Phosphat Rezeptor 1ist in FHL2-/- KMDZ erhöht, was wohl zu einer höheren Rac Aktivierung führt.

Anhand dieses Models wird zum ersten Mal ein Mechanismus beschrieben, der migratorische Geschwindigkeit unabhängig von der DZ Maturierung kontrolliert.

# 1. Introduction

## 1.1 Cell migration

Cell migration plays a central role in both normal and pathological processes, including embryonic development, wound healing, tumor metastasis, and inflammation (Chan et al., 2007). For example, leucocytes move toward inflammation, infection and injury, guided by gradients of chemokines or bacterial products. Angiogenic endothelial cells migrate toward ischaemic tissues which produce growth factors, such as vascular endothelial growth factor (VEGF). Fibroblasts migrate toward platelet-derived growth factor (PDGF) and other factors produced in wounds to facilitate healing. In metastasis, tumor cells migrate from the initial tumor mass into the circulatory system, which they subsequently leave and migrate into a new site (Moissoglu and Schwartz, 2006). Cell migration is a multistep process involving changes in the cytoskeleton, cell-substrate adhesions and the extracellular matrix (ECM) which will be discussed below.

### 1.1.1 The Cytoskeleton

In most animal cells, the cytoskeleton is the essential component in creating motility-driving forces, and in coordinating the entire process of movement. The cytoskeleton is a polymer network, composed of three distinct biopolymer types: actin, microtubules (MT) and intermediate filaments (IF), which are differentiated principally by their rigidity (Ananthakrishnan and Ehrlicher, 2007).
Actin is the most abundant protein in many eukaryotic cells, which is arranged in semiflexible polymers (Gittes et al., 1993). The filaments are double helical polymers of globular subunits all arranged head-to-tail to give the filament a molecular polarity (Fig. 1.1), whereas growth at the barbed end is favored over the other and actin filaments in cells are strongly oriented with respect to the cell surface, barbed ends outward (Pollard and Borisy, 2003).

MTs are the stiffest of the biopolymers (Dogterom et al., 2005) and exhibit similar dynamics to those of actin: They are functionally polar, treadmill, and can impart a force through polymerization. IFs are much more flexible than actin filaments and MTs. There are different classes of IFs such as vimentin, desmin, keratin, lamin and neurofilaments. Unlike actin filaments or MTs, IFs are not polarized, do not treadmill, do not generally depolymerize under physiological conditions.

These three kinds of biopolymers build an internal cellular scaffold, known as the cytoskeleton – an organized and coherent structure that is formed by connecting these filaments via entanglements, and also crosslinking, bundling, binding motor and other proteins. These cytoskeletal assemblies then work together as a composite, dynamic material in cell functions such as structural integrity, shape, division, and organelle transport and cell motility. With respect to motility, although the other polymer assemblies in the cell also aid in coordinating movement and powering translocation, the actin cytoskeleton is regarded as the essential engine that drives cell protrusion, the first step of movement (Ananthakrishnan and Ehrlicher, 2007).

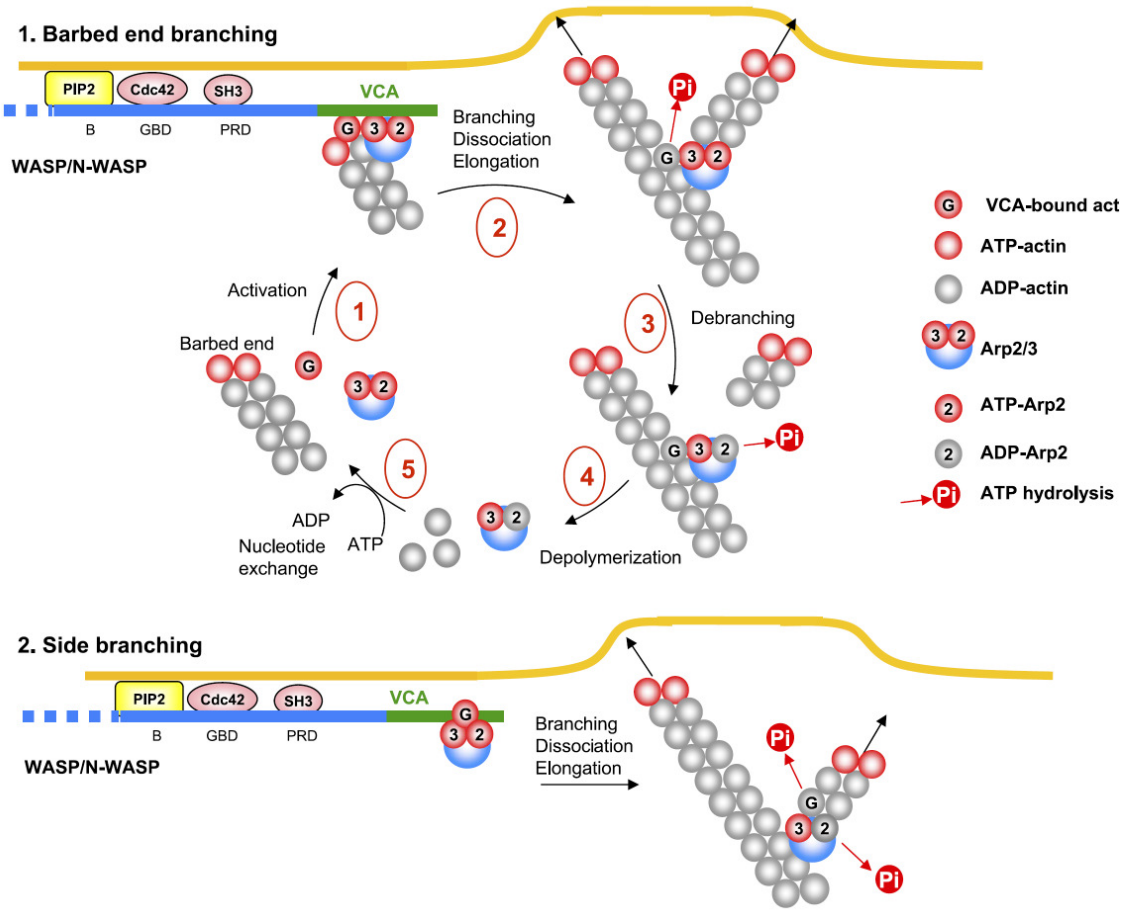


**Figure 1.1: The dendritic nucleation model of actin dynamics at the leading edge of motile cells.** Top: the barbed end branching model. (1) The branching complex made of G-actin, Arp2/3, and WASP/N-WASP (or WAVE isoforms) binds to the barbed end of the filament. This incorporation is mediated by the actin subunit of the branching complex. (2) Arp2/3 nucleates a lateral branch. The growth of the filaments drives membrane protrusion. (3) ATP hydrolysis on Arp2 induces debranching. (4) After depolymerization of the branched filament, Arp2/3 and actin are released. (5) Nucleotide exchange is required to recycle actin and Arp2/3. Bottom: the side branching model. This model proposes that Arp2/3 activated by the COOH-terminal domain of WASP/N-WASP (or WAVE isoforms) binds to the side of an actin filament. In this activated state, Arp2-Arp3-G-actin mimics an actin nucleus to initiate a lateral branch (Le Clainche and Carlier, 2008).

### 1.1.2 Components and structure of the actin cytoskeleton

Actin filaments *in vivo* can assemble into different structures such as networks and bundles, which is carried out with the help of numerous accessory proteins (Pollard et al., 2000). Cells contain a pool of unpolymerized actin monomers, globular actin (G-actin), bound to profilin and thymosin-β4. Signaling pathways activate nucleation-promoting factors such members of the Wiskott-Aldrich Syndrome Protein (WASp) family of proteins to stimulate Actin-Related

Proteins2/3 (Arp2/3) complex to initiate a new filament in 70° angle (Fig. 1.1; Amann and Pollard, 2001). Cofilin facilitates subunit dissociation from the pointed end of actin filaments and induces filament severing and is essential for promoting filament treadmilling at the front of migrating cells. Also, actin filaments themselves bind Adenosine-5'-triphosphate (ATP), and hydrolysis of ATP stimulates destabilization of the polymer (Le Clainche and Carlier, 2008; Pollard and Borisy, 2003). All these proteins and many more work together to coordinate actin network formation and bring about leading edge motility in several steps.

Although multicellular organisms contain a wide array of actin filament assemblies, the actin structures that play fundamental roles in cell migration can be roughly divided into three categories: lamellipodial actin network at the leading edge of the cell, unipolar filopodial bundles beneath the plasma membrane, and contractile actin stress fibers in the cytoplasm (Ridley et al., 2003).

The lamellipodium contains a network of short, branched actin filaments that produce the physical force for protrusion of the leading edge. The formation of new actin filaments at the leading edge is promoted by the Arp2/3 complex (Mullins et al., 1998; Svitkina and Borisy, 1999). Filopodia are thin cellular processes organized into long parallel bundles rope-like bundles (Welch and Mullins, 2002).

In contrast to relatively well characterized lamellipodia and filopodia, the assembly mechanisms of actin stress fibers are still poorly understood. Stress fibers are contractile actomyosin bundles, which are essential for cell adhesion to the substratum and for changes in cell morphology, specifically the retraction of the trailing edge during migration. Stress fibers are composed of relatively short actin filaments with alternating polarity (Hotulainen and Lappalainen, 2006).

### 1.1.3 Pushing the cell forward

After sensing the signal, the cell starts moving in response to the signal. If the signal is a chemoattractant, actin polymerizes in the region of the cell closest to

the signal, whereas if the signal is a chemorepellant, the cell moves away by polymerizing actin in the opposite side. As the extending edge moves forward, the cell constantly monitors the signal direction and tailors its direction of motion accordingly. The central dogma of cell motility divides movement into four sequential steps (Fig. 1.2).

To migrate, cells must acquire a spatial asymmetry enabling them to turn intracellularly generated forces into net cell body translocation, i.e. a clear distinction between cell front and rear (Sullivan et al., 1984). Long, flexible actin filaments cannot sustain a pushing force without buckling. Cells overcome this problem by creating a dense array of short-branched filaments namely lamellipodia and filopodia, respectively. The membrane does not remain stationary but undergoes constant Brownian motion i.e. random thermal fluctuation. Polymerization of actin filaments towards the cell membrane at the leading edge can subsequently apply an elastic force on the membrane and push it forward. Actin filaments move rearward with respect to the substrate, and generally in a direction opposite to the movement of the cell, known as retrograde flow (Ananthakrishnan and Ehrlicher, 2007; Lauffenburger and Horwitz, 1996).

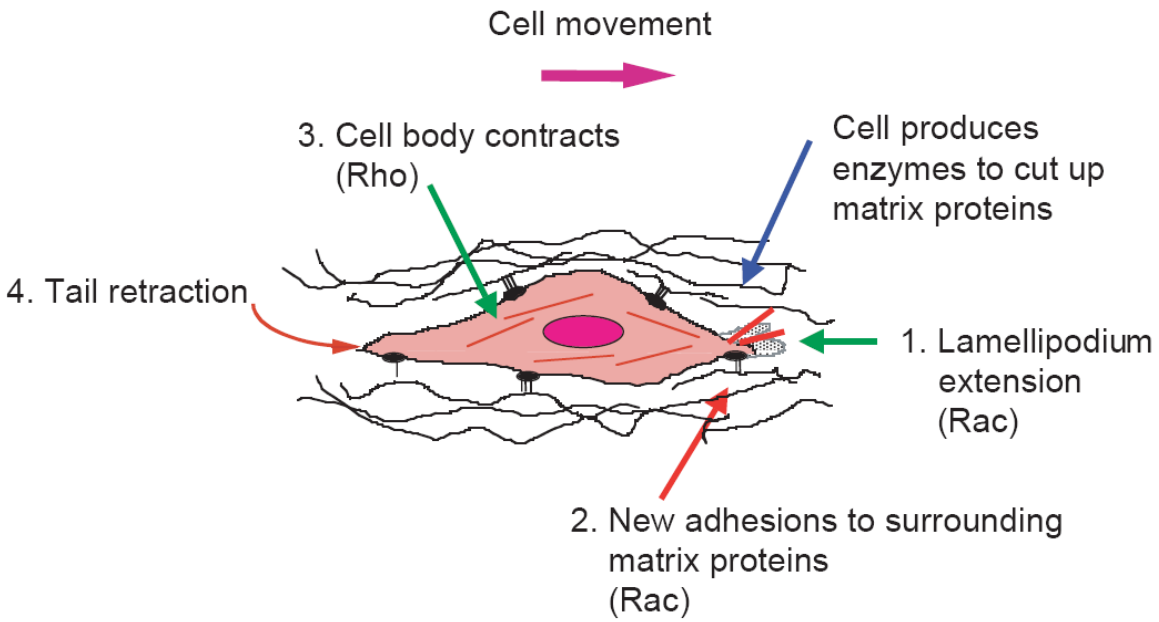


**Figure 1.2: The central dogma of cell motility divides movement into four sequential steps.** Cells (1) extend a lamellipodium at the leading edge, (2) make new adhesive contacts, (3) contract to move the cell body forward, and (4) detach the trailing edge. These attachments prevent the protruding leading edge from retracting. Thus forward movement requires that new adhesive contacts form at the leading edge and old ones break in the trailing edge (Ridley, 2001).

### 1.1.4 Small Rho GTPases

Many different intracellular signaling molecules have been implicated in cell migration, including $Ca^{2+}$-regulated proteins, mitogen-activated protein kinase cascades, protein kinases C, phosphatidylinositide kinases, phospholipases C and D, and tyrosine kinases (Ridley, 2001). However, one particular family of proteins seems to play a pivotal role in regulating the biochemical pathways most relevant to cell migration, the Ras homolog gene family (Rho) guanosine triphosphate (GTP)ases (Raftopoulou and Hall, 2004).

Rho-family proteins make up a major branch of the Ras superfamily of small GTPases. All members contain sequence motifs characteristic of all GTP-binding proteins, and are thought to cycle between active GTP-bound and inactive guanosine diphosphate (GDP)-bound states. The GDP/GTP cycling of Rho-family proteins is controlled mainly by three distinct functional classes of regulatory protein: Guanine nucleotide exchange factors (GEFs), GTPase activating protein (GAPs), and Guanine nucleotide dissociation inhibitors (GDIs) (Figure 1.3). When bound to GTP, they are active and interact with their downstream target proteins, which include protein kinases, lipid-modifying enzymes, and activators of the Arp2/3 complex (Charest and Firtel, 2007; Raftopoulou and Hall, 2004).

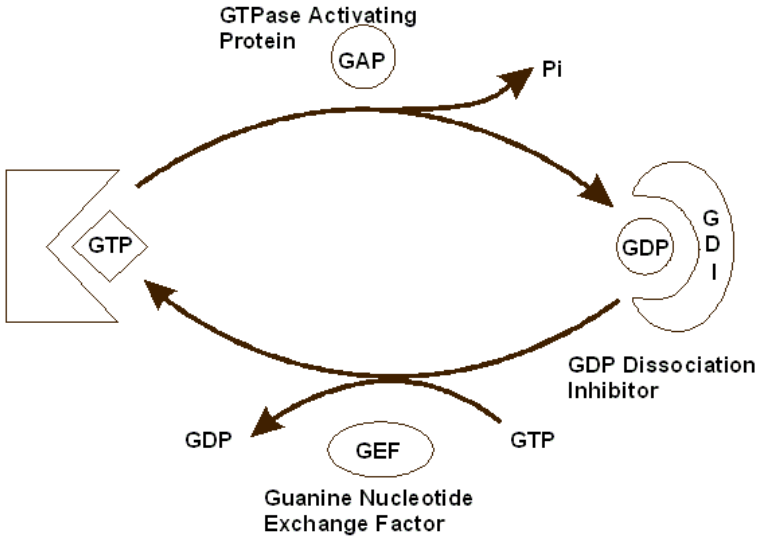


**Figure 1.3: Three distinct regulatory proteins control GDP/GTP cycling.** GEFs stimulate the weak intrinsic exchange activity of Rho-family proteins to promote an exchange of the bound GDP for GTP; GAPs stimulate the intrinsic GTP hydrolysis activity of Rho-family proteins and thereby promote formation of the inactive GDP-bound protein and GDIs inhibit Rho proteins by blocking nucleotide exchange, and thus the binding of effectors and GAPs to GTP-bound Rho GTPases (Wennerberg and Der, 2004).

Rho GTPases are pivotal regulators of actin and adhesion organization and control the formation of lamellipodia and filopodia. The major targets for Ras-related C3 Botulinum Toxin Substrate (Rac) and Cell Division Cycle 42 (CDC42) that mediate actin polymerization in protrusions are the WASP/ WASP-family verprolin-homologous protein (WAVE) family of Arp2/3 complex activators (Cory and Ridley, 2002). Rac stimulates Arp2/3-complex-induced actin polymerization by interacting with a complex of insulin receptor tyrosine kinase substrate p53 (IRSp53) and WAVE proteins. Rac can also induce actin filament uncapping by generating phosphatidylinositol 4,5-bisphosphate locally or, Rac acts via p21-activated kinases to stimulate LIM domain kinase, which inhibits cofilin-induced actin depolymerization (Ridley, 2001).

The interaction of CDC42 with WASP together with binding to phosphatidylinositol-4,5-bisphosphate (PtdIns(4,5)P2), relieves the autoinhibited conformation of WASP proteins and subsequently leads to activation of the ARP2/3 complex (Mattila and Lappalainen, 2008; Svitkina et al., 2003).

Stress fiber assembly is regulated by a signaling cascade involving the RhoA small GTPases. The GTP bound form of RhoA activates Rho-associated kinase (Friedl and Brocker, 2000), which in turn promotes stress fiber formation by inhibiting actin filament depolymerization and by inducing contractility (Hotulainen and Lappalainen, 2006; Jaffe and Hall, 2005).

## 1.2 The immune system

Vertebrates have developed systems of immune defense enabling them to cope with the constant threat posed by environmental pathogens. The mammalian immune system represents a multilayered defense system comprising both innate and adaptive immune responses, characterized by the increasing complexity of their antigen-recognition systems (Moser and Leo, 2010).

Innate immunity uses the genetic memory of germline-encoded receptors to recognize the molecular patterns of common pathogens (Janeway and Medzhitov, 2002). Adaptive immunity, akin to somatic memory, is a complex system by which the body learns to recognize a pathogen's unique antigens and builds an antigen specific response to destroy it. The effective development

of the overall immune response depends on careful interplay and regulation between innate and adaptive immunity.

### 1.2.1 Innate versus adaptive immunity

Cells of the innate immune system are able to detect an invading pathogen through a limited set of germ-line encoded receptors. The innate immune system uses various Pattern recognition receptors (PRRs) that are expressed on the cell surface, in intracellular compartments, or secreted into the blood stream and tissue fluids and recognize a series of conserved molecular structures expressed by pathogens. These pathogen-associated molecular patterns (PAMPs; Akira et al., 2006) are distinctive for a set of pathogens and include components of microbial membranes, cell walls, proteins, deoxyribonucleic acid (DNA) and ribonucleic acid (RNA). On the basis of function, PRRs may be divided into endocytic PRRs or signaling PRRs. Signaling PRRs include the large families of membrane-bound Toll-like receptors (TLRs) and cytoplasmic NOD-like receptors (Medzhitov, 2001). Endocytic PRRs promote the attachment, engulfment and destruction of microorganisms by phagocytes, without relaying an intracellular signal.

Due to the limited diversity of PRRs, pathogens displaying a high mutation rate can easily escape recognition from the innate immune system (Bowie and Unterholzner, 2008). Moreover, the ability of several pathogens such as viruses to replicate intracellularly renders their detection and elimination particularly challenging. The adaptive immune system constitutes a humoral and cellular part, B cells and T cells, respectively, which show high specificity and are at the same time very versatile due to their expression of receptors recognizing non-conserved molecules. The possibility of the T and B cell receptor to undergo genetic recombination allows a small number of genes to form a nearly infinite number of receptors which will then be able to recognize a molecule never encountered before. B cells can also undergo somatic hypermutation which makes antibodies more and more specific and increases their affinity over time. Importantly, the adaptive immune response is able to form a memory, conferring life long protection from the respective pathogen to the organism. However, cells of the adaptive immune system cannot reliably discriminate

between self and non-self with potentially deleterious consequences to the organism. Therefore adaptive immune responses must be educated by the innate immune system and tightly controlled (Palm and Medzhitov, 2009). Any conversation between innate and adaptive immunity requires accurate and effective translation of the innate signals of infection or damage. Central to this translation is the dendritic cell (DC).

### 1.2.2 Dendritic cells

DCs next to macrophages and B cells belong to professional antigen presenting cells (APC). DC are the most potent APC that facilitate T cell activation and play a major role in the initiation and regulation of innate and adaptive immune responses to antigens (Kikuchi et al., 2005). They are a heterogeneous population that are derived from bone marrow (BM) progenitors, which may differentiate into circulating precursors that later home to peripheral tissue as immature myeloid DC (Sánchez-Sánchez et al., 2006). Myeloid DC are found in an immature state in epithelia and in the interstitial space of most solid organs (Sánchez-Sánchez et al., 2006) where they constantly sample their microenvironment for foreign and host antigens (Burns et al., 2004). After antigen engulfment they turn from highly efficient antigen capturing cells into APC with the capacity to prime T cells after they have migrated to the draining lymph nodes (LN).

### 1.2.3 Antigen uptake and processing

Immature DCs endocytose avidly through a variety of mechanisms, including ‘nonspecific’ uptake by constitutive macropinocytosis and ‘specific’ uptake via receptor-mediated endocytosis and phagocytosis (Trombetta and Mellman, 2005). Macropinocytosis represents a critical antigen uptake pathway allowing DCs to rapidly and nonspecifically sample large amounts of surrounding fluid. Phagocytosis, in contrast, is initiated by the engagement of specific receptors, triggering a cascade of signal transduction, which is required for actin polymerization and effective engulfment (Lanzavecchia, 1996). Receptor-

mediated endocytosis allows the uptake of macromolecules through specialized regions of the plasma membrane, termed coated pits, and includes Fc, complement, heat shock proteins, scavenger and members of the c-type lectin family (Guermonprez et al., 2002).

After antigen engulfment, DCs assemble small peptide epitopes of the pathogen or extracellular material in antigen–major histocompatibility complexes (MHC) and their skills to capture antigen declines (Johannessen et al., 2006). MHC molecules are cell-surface glycoproteins with a peptide-binding groove that allows intracellularly loaded peptides to be presented at the cell surface, where the combined ligand can be recognized by T cells receptors. There are two classes of MHC molecules, MHC class I and MHC class II, which bind peptides from proteins degraded in different intracellular compartments.

MHC class I molecules bind peptides from proteins degraded in the cytosol i.e. derived from viruses and present these at the cell surface, where they are recognized by cluster of differentiation (CD)8 T cells (Banchereau and Steinman, 1998). These peptides which are usually 8 to 10 amino acids (aa) long are translocated into the endoplasmatic reticulum (ER) by a heterodimeric ATP-binding protein called transporters associated with antigen processing (TAP), and are then available for binding by partially folded MHC class I molecules that are held tethered to TAP (Ohl et al., 2004). In contrast, MHC class II molecules present peptides, which are at least 13 aa long, from pathogens and their products originating in the vesicular system to the cell surface, where they are recognized by CD4 T cells (Janeway et al., 2005). In addition, DCs have the ability to present exogenous antigens internalized through the endocytic pathway to CD8 T cells. The mechanisms responsible for so called cross-presentation are critical for initiating CD8 T cell responses to antigens that would not otherwise gain access to the MHC class I presentation pathway in DC (Jensen, 2007).

### 1.2.4 Maturation

The main function of DC in the induction of an adaptive immune response is to carry antigen from the periphery to lymphoid organs for presentation to T cells (Fig. 1.4). The interface between an APC and lymphocyte is called

immunological synapse, which consists of a central cluster of T cell receptors surrounded by a ring of adhesion molecule.

A signal from pathogens, often referred to as a danger signal, induces DCs to enter a developmental program, called maturation, which transforms DCs into efficient APCs and T cell activators (Guermonprez et al., 2002). Immature DCs display a phenotype reflecting their specialized function as antigen-capturing cells. They are highly endocytic and express relatively low levels of surface MHC I and MHC II class molecules and costimulatory molecules such as CD80, CD86 and CD40 (Tan and O'Neill, 2005). Bacterial and viral products, as well as inflammatory cytokines and other nonself-molecules, induce DC maturation through direct interaction with specific DC surface receptors. The transition of immature to a mature DC is accompanied by a change of their phenotype which equips the DC to efficiently stimulate T cells. These phenotypic changes include increased production of MHC-peptide complexes, markers necessary of T cell binding, costimulatory molecules, and production of growth factors such as Interleukin-12 (IL-12), chemokines, and cytokines (Fig. 1.5; Steinman et al., 2003).

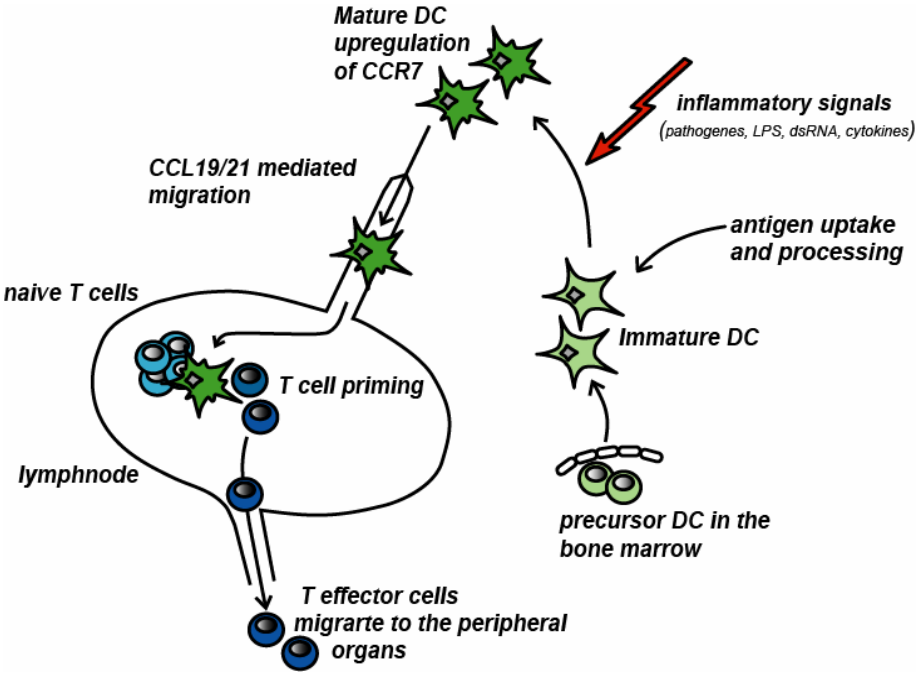


**Figure 1.4: The migratory pathway of DC under steady-state and inflammatory conditions.** DC reside in the periphery where continuously sample their environment for antigen. After antigen engulfment and concomitantly signaling via PRRs DC undergo a huge transition, which will equip them to present antigen to T cells in the draining LN. They highly upregulate CCR7 that will guide them the way towards CCL19 produced in the draining LN.

The interaction of naive T cells with DCs can lead to different forms of immune response depending on the type of DC and its activation state (Steinman et al., 2003). Under steady state conditions, the outcome of T cell stimulation by DC can be apoptosis, anergy, or the development of regulatory T cells, which can result in T cell tolerance (Tan and O'Neill, 2005). Under conditions of infection or inflammation, DC encounter signals via TLR or other danger signals including proinflammatory cytokines and bacterial or viral products such as lipopolysaccharides (LPS), CpG motifs, and double-stranded RNA. These factors may induce maturation and activation of DC, rendering them immunogenic.

The maturation state of DC is considered as a key determinant of the outcome of T cell activation leading to T cell tolerance or T cell immunity. DC with an immature phenotype are likely tolerogenic to T cells, and mature DC are immunogenic, but some level of maturation of DC is required for tolerance induction (Tan and O'Neill, 2005).

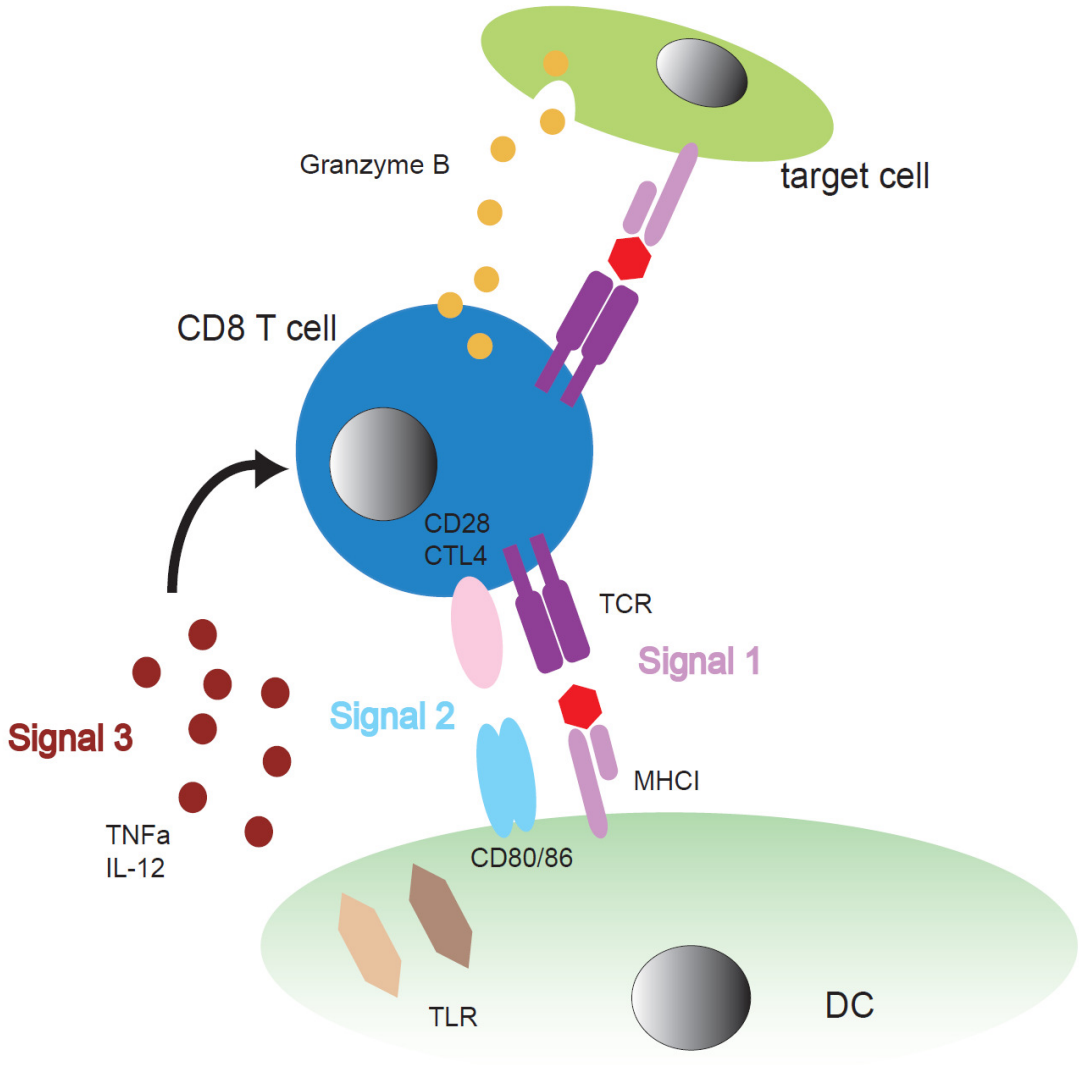


**Figure 1.5: T cell stimulation requires three DC-derived signals.** Signal 1 is the antigen-specific signal that is mediated through T-cell receptor triggering by MHC class-associated peptides processed from pathogens after internalization through PRRs. Signal 2 is the costimulatory signal, mainly mediated by triggering of CD28 by CD80 and CD86 that are expressed by DCs after ligation of PRRs. Signal 3 is the polarizing signal that is mediated by various soluble or membrane-bound factors, such as IL-12 (Kapsenberg, 2003).

### 1.2.5 The migratory phenotype of DC

During the process of migration also the morphology of DC changes. Migration of DC from sentinel sites to lymphoid tissue entails the initiation and coordination of a complex series of cytoskeletal rearrangements resulting in polarized protrusion, formation of new adhesion points, and detachment (Burns et al., 2004). Immature DCs are characterized by a relatively small cell body, but very long membrane processes. These processes are known as filopodia

and are involved in anchorage to ECM. The dendrites are temporarily retracted during DC migration, as immature DC differentiate into the mature state after antigen uptake. DC morphology in the periphery is believed to increase the efficiency of antigen contact and uptake, while within lymphoid tissue it may maximize contact with T cells (Swetman et al., 2002). After antigen capture with subsequent migration to the LN, filopodia vanish, the membrane ruffles, lamellipodia and veils develop, which assist in detachment from the surface (Calle et al., 2004).

In stark contrast to the situation found in the majority of resident connective tissue cells, migrating DCs possess neither stress fibers nor large focal adhesions. Instead, the cytoplasm contains a delicate tracery of microfilament bundles that concentrate at a series of discrete foci at the substratum interface termed podosomes (Adams, 2002). DCs, like all leukocytes, use amoeboid cell migration mechanisms to traffic within peripheral and lymphoid tissues (Friedl and Weigelin, 2008). Amoeboid migration is characterized by the acquisition of cell polarity, which then drives the development of a leading edge followed by the cell body and a posterior tail known as the uropod. Generally, polarization occurs in response to migration-promoting factors such as chemokines, which signal via G protein-coupled receptors.

The formation of protrusions at the leading edge of DC is controlled by Rac and Cdc42 (Swetman et al., 2002), whereas Rho signaling regulates cytoskeletal reorganization upon DC maturation leading to cell contraction at the trailing edge of cells. Furthermore, Cdc42 activity is associated with the formation of filopodia in immature DC, while Rac activity induces the loss of filopodia and formation of lamellipodia in mature DC. This formation of lamellipodia in mature DC is thought to allow their rapid migration into the secondary lymphoid organs (Burridge and Wennerberg, 2004).

Mechanistically, it was believed that migration of leukocytes, including DCs, relied upon interactions between surface receptors, such as integrins, and their ligands in the extracellular environment. However, it was demonstrated that DC locomotion occurred through alignment of the cell body to surrounding cell surfaces and/or ECM proteins independently of integrins (Lammermann et al., 2008). Rather, cell movement is achieved by ‘squeezing and flowing’ of the

actin cytoskeleton, a process that appears to utilize weak-to-non-adhesive interactions and thus propels the DC along the path of least resistance towards the polarizing agent (Roediger et al., 2008).

### 1.2.6 Chemokine, CC Motif, receptor 7 (CCR7)

During the maturational processes, DCs also change their surface expression profile of chemokine receptors. Chemokines are small proteins that can bind G protein-coupled chemokine receptors (Yanagawa and Onoe, 2002), that confer DC the ability to detect and move directionally toward a chemotactic stimulus (Riol-Blanco et al., 2005).

During the migration to the draining LN under inflammatory as well as under steady-state conditions, DC chemokine receptors CCR2 or CCR5 are downregulated that facilitate entry into inflamed tissues, while CCR7 is upregulated (Sallusto et al., 1998). CCR7 is essential for DC migration into dermal lymphatics and guidance to the draining LN (Ohl et al., 2004; Saeki et al., 1999). CCR7 has two ligands, chemokine, CC MOTIF, ligand 19 (CCL19) and CCL21 that are highly expressed by stromal cells in the T cell rich areas in the LN (Sánchez-Sánchez et al., 2006), endothelial cells, and DCs themselves (MartIn-Fontecha et al., 2003), and they each participate in the migration of DCs from peripheral tissues like skin to LNs (Robbiani et al., 2000). Because the two CCR7 ligands, CCL19 and CCL21, are expressed in the T cell area of secondary lymphoid organs, DCs migrate toward these ligands and finally aggregate in afferent lymphatic vessels and the T cell area of secondary lymphoid organs (Dieu-Nosjean et al. 1999).

## 1.3 Four-and-a-half lim domains 2 (FHL2)

FHL2 belongs to the family of Four-and-a-half LIM only proteins which consist of five members: FHL1–4 and Activator of CREM in testis (ACT). Common synonymes are SLIM 3 and DRAL standing for 'Downregulated in Rhabdomyosarcoma Lim Protein', which how it was called by Genini et al. (1997), because they used subtractive cloning to isolate a gene that is downregulated during transformation of normal myoblasts to rhabdomyosarcoma cells.

### 1.3.1 Structure and expression of FHL2

The FHL2 gene encodes a 279 aa polypeptide with an observed mass of 32kD (Morgan and Madgwick, 1996), which was confirmed by Muller et al. (2000) and El Mourabit et al. (2003). The protein sequence contains four complete LIM domains and the second half of a fifth LIM domain (Fig. 1.6). The presence of a LIM domain is emerging as a hallmark of proteins that can associate with both the actin cytoskeleton and the transcriptional machinery (Johannessen et al., 2006).

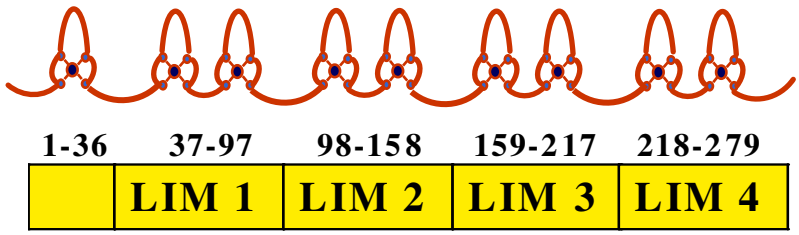


**Figure 1.6: Structure of FHL2.** The LIM domain is a cysteine-rich motif with the consensus sequence $CX_2CX_{16-23}HX_2$ $CX_2CX_2CX_{16-21}CX(C,H,D)$ that coordinately binds two zinc atoms and mediates protein–protein interactions.

Northern blotting revealed that FHL2 is expressed at highest levels in heart and ovary, and at lower levels in skeletal muscle, prostate, testis, small intestine, and colon. Analysis of the expression pattern in normal human tissues revealed that FHL2 is expressed at high levels in the heart and skeletal muscle but also at lower levels in most other tissue, suggesting an important function in the specification of heart muscle cells (Genini et al., 1997). Therefore Chu et al.

(2000a), generated a mouse carrying a null mutation of the FHL2 gene, but failed to proof their hypothesis since FHL2 deficient mice are viable and maintain normal cardiac function both before and after acute mechanical stress induced by aortic constriction (Chu et al., 2000b).

### 1.3.2 Function of FHL2

FHL2 was shown by several other groups to be involved in various other cellular processes which can exert its function via two different mechanisms (Fig. 1.7). Stimulation of the Rho signaling pathway induces translocation of FHL2 to the nucleus (Morlon and Sassone-Corsi, 2003; Muller et al., 2002), where it acts as either transcription coactivator or corepressor in interaction with numerous transcription factors including the androgen receptor, AP1, CREB, PLZF, SKI, β-catenin, FOXO1, Runx2, Id2 and serum response factor (SRF; Chen et al., 2003; Fimia et al., 2000; Gunther et al., 2005; Hamidouche et al., 2008; Labalette et al., 2004; Martin et al., 2002; Morlon and Sassone-Corsi, 2003; Muller et al., 2000; Paul et al., 2006; Philippar et al., 2004; Wei et al., 2003; Yang et al., 2005). SPP-induced FHL2 activation is mediated by Rho GTPases, but not by the GTPases Cdc42, Rac1 or Ras, and depends on Rho-kinase (Morlon and Sassone-Corsi, 2003; Muller et al., 2002). FHL2 may participate in a regulatory mechanism that coordinates cellular responses controlled by NF-κB transcription factor (Stilo et al., 2002). All these data allude to FHL2 to play an important role in the modification of the transcriptional level of various genes.

FHL2 has the capacity to interact, both in yeast and in mammalian cells, with itself, with the cytoplasmic domain of integrin α3A, α3B, α7A, and several β subunits, and with integrin-binding proteins (Wixler et al., 2000). This was investigated further by authors of Samson et al. (2004), who identified FHL2 and FHL3 as novel α7β1 integrin-interacting proteins. Immunofluorescence studies with cells expressing full-length FHL proteins or their deletion mutants showed that FHL2 and FHL3 but not FHL1 colocalize with integrins at cell adhesion sites. Further, their recruitment to the membrane results from binding to either the alpha- or the beta-chain of the integrin receptor.

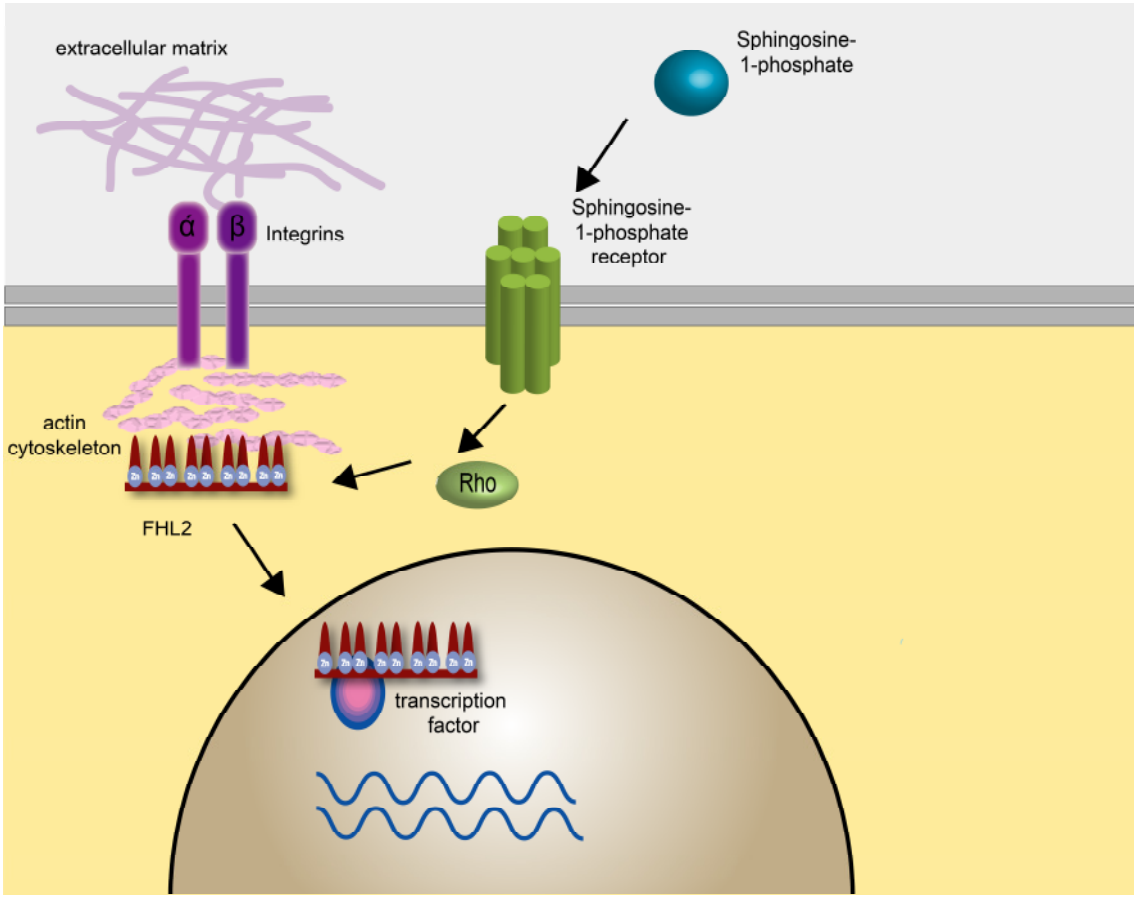


**Figure 1.7: FHL2 plays a dual role within the cell.** FHL2 can act as a co-activator of several transcription factors upon stimulation e.g. by Sphingosin-1-phosphate (S1P). Secondly, it binds to integrins which link the ECM and the actin cytoskeleton.

### 1.3.3 FHL2 affiliates with actin associated proteins and structures

FHL2 acts as an adaptor protein, regulating integrin trafficking, function or signaling pathways associated with cytoskeleton related genes, therefore may also play in migration. Co-localization of FHL2-(green fluorescent protein) GFP at focal adhesions was observed in C2C12, H9C2 myoblast as well as a nonmyogenic cell line, HepG2 cells. Moreover, FHL2 was observed along with F-actin and focal adhesion of C2C12 and H9C2 myotubes (Li et al., 2001). Cytoskeleton-associated proteins were shown to co-localize with FHL2 in cell lamellipodia (El Mourabit et al., 2004). FHL2 colocalizes to Grb7, which is an adaptor molecule and overexpression has been linked to enhanced cell migration and metastasis (Siamakpour-Reihani et al., 2009). Using mesenchymal stem cells from wt and FHL2-knockout mice, it was shown that inactivation of FHL2 leads to impaired assembly of ECM proteins on the cell

surface and to impaired bundling of focal adhesions (Park et al., 2008). A Disintegrin And Metalloproteinase (ADAM)-17 is a metalloprotease-disintegrin responsible for the ectodomain shedding of several transmembrane proteins, which colocalizes with FHL2 to the actin-based cytoskeleton (Canault et al., 2006).

Impaired cutaneous wound healing occurs in FHL2-deficient mice, which furthermore show collagen contraction and cell migration are severely impaired in FHL2-deficient cells. Consequently, the expression of alpha-smooth muscle actin is delayed in wounds of FHL2-deficient mice and the expression of p130Cas, which is essential for cell migration, is reduced in FHL2-deficient cells (Wixler et al., 2007). These results show impaired intestinal wound healing in FHL2-deficient mice is due to disturbed collagen III metabolism (Kirfel et al., 2008).
In a different study high levels of Lysine specific demethylase 1 (LSD1), nuclear expression of the FHL2 coactivator, high Gleason score and grade, and very strong staining of nuclear p53 correlate significantly with relapse during follow-up. This suggests that LSD1 and nuclear FHL2 may serve as novel biomarkers predictive for prostate cancer with aggressive biology and point to a role of LSD1 and FHL2 in constitutive activation of AR-mediated growth signals (Kahl et al., 2006).

## 1.4 Sphigosine-1-Phosphate Receptors (S1PR)

FHL2 translocates into the nucleus upon binding of S1P and can act as a coactivator of transcription factors like AR or CREB/CREM in a cell type specific manner (Muller et al., 2002). S1P is a potent lysosphospholipid with a wide range of biological activities (Spiegel and Milstien, 2000) including regulation of cytoskeletal rearrangement and cell migration via the actions of five G-protein-coupled receptors termed S1PR1-5, also known as endothelial differentiation gene (EDG), which mediate their functions through coupling of the receptor to heterotrimeric G-proteins (Takuwa et al., 2002). S1P is produced by platelets and red blood cells and circulates in the plasma at concentration of $10^{-7}$ M. S1P possess chemoattractive property for a variety of immune cells (Graeler and

Goetzl, 2002; Idzko et al., 2002), and has an impact of the egress of B and T cells from the LN and thymus (Matloubian et al., 2004). Furthermore, S1P is responsible for correct positioning of B cells and DC within the spleen (Cinamon et al., 2004; Czeloth et al., 2007).

S1PR1 and S1PR3 usually promote cell migration via $G_i$ pathways and Rac activation leading to lamellipodia formation (Paik et al., 2001), which observation could be extended to a variety of other cell types (Becker et al., 2010; Gil et al., 2010; Liu et al., 2010). In contrast to S1PR2 which has a repellent effect on cell migration antagonizing Rac, stimulating $G_{12/13}$ and Rho activation causing assembly of stress fibers (Fig. 1.8; (Arikawa et al., 2003; Okamoto et al., 2000; Sugimoto et al., 2003; Takashima et al., 2008).

S1PR1-4 are expressed by a variety of immune cells, whereas expression of S1PR5 is mainly confined to cells of the central nervous system (Im et al., 2000). S1P is the ligand for the five S1PRs, where S1PR1-4 are differentially expressed in T cells (Graeler and Goetzl, 2002) and bone marrow-derived dendritic cells (BMDC; Maeda et al., 2007). Depending on the maturation status of DC, they show a differential expression pattern of the S1PRs (Czeloth et al., 2005; Maeda et al., 2007; Rathinasamy et al., 2010), which can either have an stimulatory or inhibitory regulation of migration (Sugimoto et al., 2003). This migratory effect is reflected by the expression pattern of S1PRs in DC causing a slower migratory behavior in their immature state leading to high migratory speed during maturation. Czeloth et al. (2005) showed that immature BMDC lack expression of S1PR1, and display only minor expression of S1PR3. These are highly upregulated after the maturation of BMDC, whereas expression of S1PR2 and 4 declines.

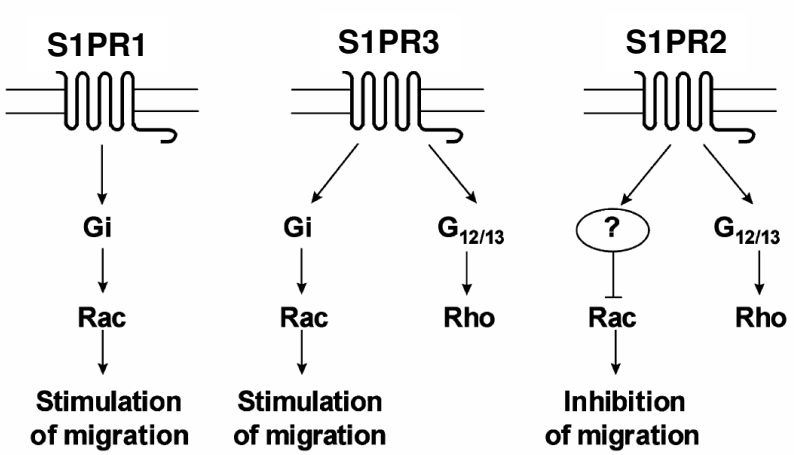


**Figure 1.8: The coupling of the three S1P receptors to the Rho family GTPases.** Both S1PR1 and S1PR3 mediate stimulation of Rac via $G_i$, leading to cell migration, whereas S1PR2 mediates inhibition of Rac activity through an unknown mechanism, leading to inhibition of cell migration. S1PR3 and S1PR2 stimulate RhoA activity most likely via $G_{12/13}$, however, stimulation of RhoA activity does not seem to be required for cell migration al least in CHO cells (Takuwa, 2002).

## 1.5 Objective

DCs are the first cells of defense against invading pathogens in an adaptive immune response. Therefore, DCs need to carry antigen, which they have taken up in the periphery, to the draining LN. Here, DCs present their antigen in MHC molecule to T cells. The communication between DC and T cell are very important in determining what kind of immune response is elicited, namely tolerance or immunity. Both can have detrimental effects for the organism: autoimmunity or no killing of the threatening pathogen. If a DC can reach the LN in a sufficient period of time, this is very critical to accomplish that task properly. FHL2 could play an important role in the mechanism of DC migration, since it is known to play in important role in fibroblast migration and subsequently wound healing and tumor formation.

In this thesis the following questions will be addressed:

1. What role does FHL2 play in DC migration?
2. By which mechanism does FHL2 effect DC migration if at all.
3. Does FHL2 play a role in other DC functions such as antigen uptake, antigen presentation and DC morphology?

# 2. Materials and Methods

## 2.1 Materials

### 2.1.1 Equipment

| | |
|---|---|
| Accurate Scales | PL-3001 (Mettler, Toledo, Greifensee, Schweiz); BP211S (Sartorius;,Göttingen) |
| Autoclave | Tuttnauer 3870, Tuttnauer 5075 ELV (Biomedis, Gießen) |
| Blotting Unit | XCell II Blot Module (Invitrogen, Karslruhe) |
| Bunsenburner | LABOGAZ 206 (Roth, Karlsruhe) |
| Cell Separation | AutoMACS (Miltenyi, Bergisch Gladbach) |
| Developer | X-Omat 1000 Processor (Kodac, Rochester, USA) |
| Electrophoresis Unit | XCell *Sure*Lock Mini-Cell (Invitrogen, Karlsruhe) |
| Electroporation | Gene Pulser Xcell Electroporation System (Biorad, München) |
| ELISA reader | $EL_X800$ (BioTek Instruments, Bad Friedrichshall |
| Flow Cytometer | FACS Canto (Becton Dickinson, Heidelberg) |
| Fluorescence Microscope | IX71 (Olympus, Hamburg) |
| Freezer (-20°C) | 7081-598-03 (Liebherr, Biberach an der Riss) |
| Freezer (-80°C) | HERAfreeze (Hereaus, Hanau) |
| Ice machine | ZBE 70-35 (Ziegra, Isernhagen) |
| Incubator | Cytoperm 2, BBD 6220 (Heraus, Hanau) |

| | |
|---|---|
| Laminar Flow Hood | HERAsafe, HERAguard (Heraeus, Hanau) |
| Luminometer | Centro LB 960 Berthold (VWR, Darmstadt) |
| Magnetstirrer | RCT (IKA, Staufen) |
| Microscope | Axiovert 40Cn (Zeiss, Oberkochen) |
| Microwave | Microwave 800 (Severin, Sundern) |
| Mini Centrifuge | Galaxy Mini (VWR, Darmstadt) |
| Motorized rotor homogenizer | Fastprep (Sartorius, Göttingen) |
| Orbital Shaker | VXR basic Vibrax (Ika, Staufen) |
| pH Meter | Blueline pH 12 (Schott, Mainz) |
| Power supply | Consort E835 (Rhys Scientific Ltd,,Lancashire, UK) |
| Real-Time PCR System | 7900HT (Applied Biosystems, Darmstadt) |
| Refrigerator (+4°C) | 7081-312-04 (Liebherr, Biberach an der Riss) |
| Rocking Shaker | Duomax 1030 (Heidolph, Schwabach) |
| Scale | 440-45N (Kern, Balingen) |
| Spectrophotometer | NanoDrop ND-1000 (PeqLab, Erlangen) |
| Speed Rotator | Intelli-Mixer RM-2 Elmi LV-1006 (Elmi, Riga, Latvia) |
| Table Centrifuge | 5417R (Eppendorf, Hamburg) |
| Thermal cycler | MJ Research PTC-200 Peltier Thermal cycler (Biozym, Oldendorf) |
| Thermomixer | Thermomixer (Eppendorf, Hamburg) |
| Timelapse Microscopy | IX81 (Olympus, Hamburg) |
| Vortex | Genie 2 (Scientific Industries, New York, USA) |
| Waterbath | WB/OB7-45 WBU45 (Memmert, Schwabach) |

### 2.1.2 Consumables

| | |
|---|---|
| 384 Microreader plate | Thermo Fisher Scientific, Langenselbold |
| Beaker 25ml, 100ml, 500ml | TGI, Ilmenau |
| Chamber Slide2 well Permanox | Nalge Nunc International, New York, USA |
| Cell Culture flasks 75cm$^2$ | Corning, Wiesbaden |
| Cell strainer 40µm | Becton Dickinson, Heidelberg |
| Centrifuge round bucket 500ml | Heraeus, Hanau |
| Conical Tubes 15ml, 50ml | Greiner, Solingen. Corning; Wiesbaden |
| Cover slips | Leica, Wetzlar |
| Cover Slips, ∅13 mm | Assistent, Sondheim |
| Electroporation Cuvette | Biorad, München |
| Erlenmeyer flask 50ml, 100ml, 250ml, 500ml, 1l | Schott, Mainz |
| Falcon round-bottom tubes | Becton Dickinson, Heidelberg |
| Filterflasks 1L 0.2µm | Corning, Wiesbaden |
| Filter paper Whatmann 3MM | Schleicher & Schuell, Dassel |
| High performance Chemiluminiscence film | GE Healthcare, München |
| Lysing Matrix D | Q-Biogen, Heidelberg |
| Microplates flat bottom 96, 48 well | Corning, Wiesbaden |
| PCR tubes 0.2ml | Greiner, Frickenhausen |
| Microplates round-bottom 96 well | Greiner, Frickenhausen |
| Needle, 21G, 25G | Becton Dickinson, Heidelberg |
| Neubauer Counting chamber | Roth, Karlsruhe |
| Nitrocellulose membrane 0.2µm | BioRad, München |
| Nunc Cryo tubes | Thermo Fisher Scientific, Langenselbold |
| Nylon Wool | Dunn Labortechnik, Asbach |
| Petri dish, non tissue culture treated 10cm, 5cm | Greiner, Frickenhausen |

| | |
|---|---|
| Petri Dish 15cm | TPP, Trasadingen, Schweiz |
| Pipette accu-jet | Brand, Wertheim |
| Pipettes 0.2-2µl, 0.5-10µl, 2-20µl, 20-100µl, 30-200µl, 100-1000µl | Eppendorf, Hamburg |
| Snap cap microcentrifuge tube 500µl, 1ml, 2ml | Eppendorf, Hamburg |
| Strainer, metal, 100µm | University Bonn, Department „Feinmechanik“ |
| Stripes Serological Pipets | Corning, Wiesbaden |
| Syringe 1ml, 5ml, 10ml | Becton Dickinson, Heidelberg |
| Threaded bottles100ml, 250ml, 500ml, 1l, 2l | Schott, Mainz |
| Transwell 5µm, 24 well | Corning, Wiesbaden |
| Ultrapure water system | Reinstwassersysteme, Leverkusen. NANOpure Diamond, Barnstead |
| µ-Slide Chemotaxis | IBIDI, München |

### 2.1.3 Chemicals (liquid)

| | |
|---|---|
| Acetic acid ($CH_3COOH$) | Merck, Darmstadt |
| Acetone ($C_3H_6O$) | Merck, Darmstadt |
| Bradford reagent | BioRad, München |
| β-mercaptoethanol ($C_2H_6OS$) | Merck, Darmstadt |
| Citric acid ($C_6H_8O_{7)}$ | Merck, Darmstadt |
| Dimethyl sulfoxide ($C_2H_6OS$) | Sigma, Steinheim |
| Ethanol ($C_2H_6O$) | Merck, Darmstadt |
| Glycerol 87% ($C_3H_8O_3$) | Merck, Darmstadt |
| Hydrochloric acid (HCl) | Merck, Darmstadt |
| Hydrogen peroxide ($H_2O_2$) | Roth, Karlsruhe |
| Methanol ($CH_4O$) | KMF, Lohmar |
| Tween 20 ($C_{58}H_{114}O_{26}$) | KMF, Lohmar |

### 2.1.4 Chemicals (solid)

| | |
|---|---|
| Agarose ($C_{12}H_{18}O_9$ ) | Biozym, Oldendorf |
| 2,2'-azino-bis(3-ethylbenzo-thiazoline-6-sulphonic acid) ($C_{18}H_{18}N_4O_6S_4$) | Sigma, Steinheim |
| Bovine serum albumin | Biolabs, SIGMA |
| Bromophenol blue ($C_{19}H_{10}Br_4O_5S$) | Fluca, Steinheim |
| Deoxycholic acid ($C_{24}H_{40}O_4$) | Roth, Karkruhe |
| Ethylenediaminetetraacetic acid ($C_{10}H_{16}N_2O_8$ ) | Merck, Darmstadt |
| Gelatine | Sigma, Steinheim |
| Milk powder | Merck, Darmstadt |
| Nonidet P-40 | Roth, Karlruhe |
| Saponin | Merck, Darmstadt |
| Sodiumazid ($NaN_3$) | Sigma, Steinheim |
| Sodium chloride (NaCl) | Merck, Darmstadt |
| Sodium dodecyl sulfate ($NaC_{12}H_{25}SO_4$) | Roche, Berlin |
| Sodium hydrogen phosphate ($Na_2HPO_4$) | Merck, Darmstadt |
| Sodium hydroxide (NaOH) | Merck, Darmstadt |
| Tris(hydroxymethyl)aminomethane ($C_4H_{11}NO_3$) | Merck, Darmstadt |
| Triton X-100 ($C_{14}H_{22}O(C_2H_4O)_n$) | Merck, Darmstadt |
| Paraformaldehyde ($OH(CH_2O)_nH$ (n = 8 - 100)) | Fluca, Steinheim |
| Xylencyanol ($C_{25}H_{27}N_2NaO_6S_2$) | Roth, Karlsruhe |

### 2.1.5 Reagents

| | |
|---|---|
| 5x First strand Buffer | Invitrogen, Karlsruhe |
| 10x PCR Rxn Buffer | Invitrogen, Karlsruhe |

| | |
|---|---|
| 100bp Molecular Ruler | BioRad, München |
| 10x RT Buffer | Invitrogen, Karlsruhe |
| Affinity purified mouse CCL19-Fc fusion protein | eBioscience, San Diego, USA |
| AllStars negative control siRNA | Qiagen, Hilden |
| Antibody diluent | Dako, Hamburg |
| Calibrate beads | Becton Dickenson, Heidelberg |
| Dithiothreitol | Invitrogen, Karlsruhe |
| dNTP Mix | Invitrogen, Karlsruhe |
| Ethidium bromide solution | Fluca, Steinheim |
| LPS | Sigma, Steinheim |
| Magnesium chloride | Invitrogen, Karlsruhe |
| Mini Complete | Roche, Berlin |
| Mounting medium | Dako, Hamburg |
| Normal mouse serum | Sigma, Steinheim |
| Normal rat serum | Sigma, Steinheim |
| Oligo(dt)-Primer$_{12-15}$ | Invitrogen, Karlsruhe |
| Prostaglandin E2 | Sigma, Steinheim |
| Protein G PLUS-Agarose | Santa Cruz Biotechnology, Heidelberg |
| Proteinase K solution | Qiagen, Hilden |
| PureCol Collagen | Sigma, Steinheim |
| RLT Buffer | Qiagen, Hilden |
| RNase-free water | Qiagen, Hilden |
| Rnase OUT | Invitrogen, Karlsruhe |
| S1PR1 siRNA | Qiagen, Hilden |
| SuperScript III Reverse Transcriptase | Invitrogen, Karlsruhe |
| Taq DNA polymerase | Invitrogen, Karlsruhe |
| Protein G PLUS-Agarose | Santa Cruz Biotechnology, Heidelberg |

### 2.1.6 Antibody coated beads

| | |
|---|---|
| CD4 (L3T4) MicroBeads | Miltenyi Biotec, Bergisch Gladbach |
| CD8 (Ly-2) MicroBeads | Miltenyi Biotec, Bergisch Gladbach |
| CD11c MicroBeads | Miltenyi Biotec; Bergisch Gladbach |

### 2.1.7 Fluorochrome labeled ligands

| | |
|---|---|
| $Dextran^{FITC}$ | Sigma, Steinheim |
| $OVA^{Alexa647}$ | Invitrogen, Karlsruhe |
| $Phalloidin^{Alexa488}$ | Invitrogen, Karlsruhe |
| $Phalloidin^{Alexa546}$ | Invitrogen, Karlsruhe |
| $Phalloidin^{Alexa647}$ | Invitrogen, Karlsruhe |

### 2.1.8 Fluorochromes

| | |
|---|---|
| Carboxyfluorescein succinimidyl ester ($C_{25}H_{15}NO_9$) | Molecular Probes, Karlsruhe |
| 4',6-diamidino-2-phenylindole | Invitrogen, Karlruhe |
| SNARF-1 carboxylic acid, acetate, succicimidyl ester | Molecular Probes, Karslruhe |

### 2.1.9 Enzymes

| | |
|---|---|
| Collagenase A | Sigma, Steinheim |

### 2.1.10 Proteins

| | |
|---|---|
| Ovalbumin | Serva, Heidelberg |

### 2.1.11 Inhibitors

| | |
|---|---|
| Brefeldin A | eBioscience, San Diego, USA |
| CCG-1432 | Cayman Chemical, Tallinn, Estonia |
| Fasudil hydrochloride | Tocris Bioscience, Bristol, United Kingdom |
| Monensin | eBioscience, San Diego, USA |
| SEW8271 | Cayman Chemical, Tallinn, Estonia |
| S1P | Sigma, Steinheim |

| | |
|---|---|
| Y27632 | Merck, Darmstadt |

### 2.1.12 Cytokines and Chemokines

| | |
|---|---|
| Recombinant IL-2 | Peprotech, Hamburg |
| Recombinant Mouse MIP-3/CCL19 | R&D Systems, Wiesbaden-Nordenstadt |
| Recombinant murine TNF-α | Peprotech, Hamburg |

### 2.1.13 Cell culture supplies

| | |
|---|---|
| ACK lysis buffer | Lonza, Köln |
| Fetal calf serum | PAA, Cölbe |
| G418 | PAA, Cölbe |
| IMDM medium | PAA, Cölbe |
| L-Glutamine | Gibco, Karlsruhe |
| Optimem | Invitrogen, Karlsruhe |
| Penicillin/Streptomycin | PAA, Cölbe |
| PBS | PAA, Cölbe |
| RPMI Medium | Gibco, Karlsruhe |
| Trypan blue | Sigma, Steinheim |
| Trypsin-EDTA | PAA, Cölbe |

### 2.1.14 Western Blot supplies

| | |
|---|---|
| MOPS SDS Running Buffer (20x) | Invitrogen, Karlsruhe |
| Novex® Sharp Pre-stained Protein Standard | Invitrogen, Karlsruhe |
| NuPAGE 4-12% Bis-Tris Gel (1.5mmx15 well) | Invitrogen, Karlsruhe |
| NuPAGE LDS Sample Buffer (4x) | Invitrogen, Karlsruhe |
| NuPAGE Transfer Buffer (20x) | Invitrogen, Karlsruhe |

### 2.1.15 Oligonucleotides

All primers are HPLC purified and purchased ready lyophilized at a concentration of 10µM. They were 1:10 diluted in $ddH_20$. SIGMA-Proligo, Steinheim.

**Table 2.1: The list of primers used for the PCRs.**

| Name | Sequence 5' – 3' |
|---|---|
| Myco C | GGGAGCAAACAGGATTAGATACCCT |
| Myco D | TGCACCATCTGTCACTCTGTTAACCTC |
| FHL2 Exon1 F | TTGCTGAAAGACAGGTGTCAGC |
| FHL2 Exon1 R | TTGCAGTCGCAGCCGATGGG |
| b-actin F | CTACGTCGCCCTGGACTTCGAGC |
| b-actin R | GATGGAGCCGCCGATCCACACGG |
| 18s F | ACAGCCAGGTTCTGGCCAACGG |
| 18s R | TGACCGCGGACACGAAGGCCC |
| S1PR1 F | TCTCTGACTATGGGAACTATG |
| S1PR1 R | CCAGGATGAGGGAGATGA |
| S1PR2 F | CCTTAACTCACTGCTCAATCC |
| S1PR2 R | GCTGGAAGATAGGACAGACAG |
| S1PR3 F | ACAAGGTCCGGGTGCTGA |
| S1PR3 R | GTAATGTTC CCGGAGAGTGTC |
| S1PR4 F | GCTATGCCCATTGTCCAGTAG |
| S1PR4 R | GGACCAGGTACTGATGTTCATG |

### 2.1.16 Antibodies

**Table 2.2:** Antibodies used in Western blot or for Immunoprecipitation.

| Antigen | Isotype | Clone | Remark | Company |
|---|---|---|---|---|
| b-actin | IgG, mouse | AC-15 | monoclonal | Sigma |
| FHL2 | IgG, rabbit | | polyclonal | self-produced |
| FHL2 | IgG1, mouse | F4B2-B11 | monoclonal | Novus Bilogicals |

**Table 2.3:** Antibodies used for flow cytometry.

| Antigen | Isotype | Clone | Remark | Company |
|---|---|---|---|---|
| TNF-α | IgG1 k, rat | MP6-XT22 | | eBioscience |
| IL-12 p35 | IgG2a k, rat | 4D10p35 | | eBioscience |
| CD11c | IgG, hamster | N418 | Integrin αX chain | eBioscience |
| CD16/32 | IgG2b k, rat | 2.4G2 | FcγRII/III | self produced |
| MHCI | IgG2a κ, rat | AF6-88.5 | H-2Kb | eBioscience |
| MHCII | IgG2b κ, rat | M5/114.15.2 | I-A b | eBioscience |
| CD40 | IgG2a κ, rat | HM40-3 | | eBioscience |
| CD80 | IgG, hamster | 16-10A1 | B7-1 | eBioscience |
| CD86 | IgG2a κ, rat | GL1 | B7-2 | eBioscience |

**Table 2.4:** Antibodies used for ELISA.

| Antigen | Isotype | Clone | Remark | Company |
|---|---|---|---|---|
| IL-2 | IgG2b, rat | JES6 1A12 | pure | eBioscience |
| IL-2 | IgG2b, rat | JES6 5H4 | biotinylated | eBioscience |

**Table 2.5:** Functional antibody used for *in vivo* injection.

| Antigen | Isotype | Clone | Remark | Company |
|---|---|---|---|---|
| NK 1.1 | IgG2a, mouse | PK136 | pure | self produced |

### 2.1.17 Secondary antibodies

| | |
|---|---|
| Anti-mouse HRP | Sigma, Steinheim |
| Anti-rabbit HRP | Invitrogen, Karslruhe |
| Strepavidin PerCpcy5.5 | eBioscience, San Diego, USA |
| Anti-Human IgG (Fc gamma-specific) | eBioscience, San Diego, USA |
| Anti-mouse IgG-Peroxidase antibody | Sigma, Steinheim |
| anti-mouse$^{\text{Texas Red}}$ | Southern Biotech, Eching |

### 2.1.18 Kits

| | |
|---|---|
| Amersham ECL Western blotting Analysis System | GE Healthcare, München |
| Cell Proliferation Kit I (MTT) | Roche, Berlin |
| mirVana miRNA Isolation | Ambion, Darmstadt |
| NucleoSpin RNAII | Macherey&Nagel, Düren |
| QuantiFast SYBR Green PCR Kit | Qiagen, Hilden |
| Rac1 ELISA Kit | Cytoskeleton, Offenbach |
| RNeasy Midi Kit | Qiagen, Hilden |
| RNeasy Mini Kit | Qiagen, Hilden |

### 2.1.19 Media, Solutions and Buffer

| | |
|---|---|
| 1xTBS-T | 10xTBS was diluted 1:10 in $ddH_2O$<br>0.1% Tween |
| 10xTBS | 1l $ddH_2O$<br>200mM Tris<br>1.4M NaCl<br>adjusted to pH 7.6 with HCl |
| 50xTAE Buffer | 1l $ddH_2O$<br>1M Tris<br>17.51% acetic acid<br>0.5M EDTA |
| Freezing Medium | FCS<br>20% DMSO |
| ABTS buffer | 17.89g citric acid, monohydrate<br>1000ml $H_2O$<br>pH 4.35 |

| | |
|---|---|
| Acetic acid 100mM | 50ml $ddH_20$<br>286µl acetic acid |
| BMDC medium | 500ml IMDM medium<br>8% heat inactivated FCS<br>2µM β-ME<br>1x P/S<br>2mM L-Glutamine. |
| BMDC medium/BSA | 500ml IMDM medium<br>8% heat inactivated FCS<br>2µM β-ME<br>1x P/S<br>2mM L-Glutamine<br>2.5g BSA |
| Coating buffer | 0.1M Sodium hydrogen phosphate in $ddH_20$ |
| EDTA 0.5M | 50ml $ddH_20$<br>18.6g EDTA<br>adjusted to pH8 with 5M NaOH |
| FACS buffer | 500ml 1xPBS<br>0.1% Na azid<br>1% BSA. |
| Freezing Medium | FCS<br>20% DMSO |
| Laemmli buffer | 20% Glycerol, 1.5M Tris-HCl<br>0.01g bromphenolblue |
| Loading dye | 50ml $ddH_2O$<br>0.5ml of 1M Tris (pH8) |

| | |
|---|---|
| | 5µl of 0.5M EDTA (pH8)<br>28.74ml of 87% glycerol<br>0.025g Bromphenol blue<br>0.025g Xylencyanol |
| MACS buffer | 500ml 1xPBS<br>0.1% Na azid<br>1% BSA<br>2mM EDTA |
| RIPA buffer | in dd$H_2O$<br>150mM NaCl<br>0.5% Deoxycholic acid<br>1% NP-40<br>0.1% SDS<br>50mM Tris<br>1 tablet Mini Complete was added to 10ml RIPA buffer |
| T cell medium | RPMI medium<br>8% FCS<br>2µM β-ME<br>1x P/S<br>2mM L-Glutamine. |

### 2.1.20 Software

| | |
|---|---|
| Cell^R Imagingsystem | Olympus, Hamburg |
| FlowJo | FlowJo, Ashland, USA |
| SDS2.2 | Applied Biosystems, Darmstadt |
| Track-it software | Olympus, Hamburg |

### 2.1.21 Cell lines

| | |
|---|---|
| Ag8653 | GMCSF producing hybridoma cell line |

### 2.1.22 Mouse lines

All mice were on the C57BL/6 background. Experimental animals were bred under specific pathogen free (SPF) conditions according to the FELASA guidelines in the central animal facility “Haus für Experimentelle Therapie” (HET) at the University Hospital Bonn. For all experiments mice between 6-20 weeks of age were used in accordance with local animal experimentation guidelines.

| | |
|---|---|
| C57Bl/6 | Inbreed line with MHC class I Haplotype $H_2K$ b |
| FHL2-/- | (Kon et al, 2001) |
| OT-I IxRag | CD8 T cell transgene mouseline, H2KbSIINFEKL-restricted Vα2Vβ5 T cell receptor (Hogquist et al., 1994). |
| OT-II | CD4 T cell transgene mouseline, I-$A^b$ |

## 2.2 Methods

### 2.2.1 Cell Culture

#### 2.2.1.1 Primary cell isolation

All mice used for organ removal to receive primary cells were between 6 and 20 weeks old. Prior to organ removal mice were sacrificed by $CO_2$ mediated asphyxiation. Body Surfaces were cleaned with 70% Ethanol and body cavity was opened under semi sterile conditions with forceps and scissors.

### 2.2.1.2 Production of GMCSF

The myeloma cell line AG8653 produces murine recombinant GMCSF under neomycin (G418) selection, which supernatant was added to the BMDC culture to turn bone marrow precursor cells into DC. Cells were expanded in IMDM medium under G418 selection with a final concentration of 1mg/ml for several days until the cells were about 80 to 90% confluent. Medium was aspirated, the cells were washed with PBS and detached from the plastic surface by Trypsin-EDTA at 37°C for 5min. Reaction was stopped by adding equal volume of medium and centrifuged at 1500rpm for 5min. Cells were washed three times with PBS to remove G418 and in the in the end resuspended in IMDM medium and counted. $5x10^5$ cells were plated on 15cm dishes in 20ml volume of IMDM medium for four days. The supernatant was collected in centrifuge buckets for centrifugation 1500rpm for 10min and filtered through 0.2µm pore size to exclude cells and stored at -20°C.

### 2.2.1.3 Determination of cell number

The harvested cell suspension was diluted with Trypan Blue, and 10µl were applied to the edge of the hemocytometer. It consists of four squares, each made up of another 16 smaller squares. All four big squares were counted, excluding dead cells characterized by a deep blue color and the concentration of the cell suspension was calculated by the help of following formula. In order to get an accurate number, the number of cells in the small square should be between 30 to 200.

Number of cells/ml = Number of counted cells/4 * dilution factor * 10,000

### 2.2.1.4 Generation of bone marrow derived dendritic cells

Femur and tibia from FHL2-/- and wt mice were removed, and fur and muscle tissue carefully subducted with sterile forceps. The end on the bones were cut open and flushed through with IMDM medium, centrifuged at 1500rpm for 5min, resuspended in fresh medium and counted. $5x10^6$ cells were cultured in 10cm

untreated Petri dishes in IMDM medium in a final volume of 10ml supplemented with 30% GMCSF containing supernatant prepared as described in 2.2.1.2. After four days, medium including BMDCs was transferred into a conical tube, washed twice with 3ml PBS and detached with 1mM EDTA/PBS including the cells in the medium. $3x10^6$ cells were plated under the same conditions as described before for further three days. This yielded a 60 to 80% pure CD11c positive BMDC culture as determined by flow cytometry.
Optionally on day seven, maturation was induced with either 100ng/ml LPS for 24 hours or 30ng/ml TNF-α for 48 hours depending on the setup of the experiment. Incubation with several inhibitors was done as described in Results.

### 2.2.2 Molecular Biological methods

#### 2.2.2.1 Mycoplasma PCR

Contamination of cells with mycoplasma can lead to cell death or it could influence the phenotype of the cells, which could change the outcome of experiments. Therefore cells were checked for mycoplasma contamination on a regular basis by PCR with primers covering most strains. Medium of cells was not changed at least for two days. 200µl of medium was taken and heated up for 10min at 95°C. Every PCR reaction was done simultaneously with two positive control samples (Table 2.6).

**Table 2.6:** The recipe of the Mycoplasma PCR and the PCR program.

| Reagents | Concentration | Volume µl |
|---|---|---|
| $ddH_20$ | | 16.8 |
| PCR Rxn Buffer | 10x | 2.5 |
| $MgCl_2$ | 50mM | 1 |
| dNTPs 10mM | 10mM | 0.5 |
| Primer Myco C | 1µM | 1 |
| Primer Myco D | 1µM | 1 |
| Taq DNA polymerase | 5U/µl | 0.2 |
| DNA sample | | 2 |
| **Program:** | Temperature ℃ | Time |
| | 94 | 3min |
| | 94 | 30s |
| | 55 | 30s |
| | 72 | 45s |
| | 33 cycles | |

### 2.2.2.2 Isolation of total RNA from tissue

In order to check for FHL2 expression in several organs RNA was isolated from lung, colon, muscle and heart tissue with the “RNeasy Midi” kit according to manufacturers’ instruction.

100mg of tissue were taken up in 1ml RLT Buffer provided by the manufacturer supplemented with 10% β-ME and placed in a “Lysing Matrix D” vessel and disrupted with a motorized rotor homogenizer for 60s. Heart tissue was incubated in 20mg/ml Proteinase K solution dissolved in $ddH_20$ at 55℃ for 20min to destroy contractile proteins, connective tissue and collagen. The concentration of RNA was determined with “Nano Drop”.

#### 2.2.2.3 Isolation of total RNA from cell culture

Total RNA was isolated out of seven to days BMDC using either the 'RNeasy Mini Kit' or 'NucleoSpin® RNA II' following manufacturers' instruction. For every experiment the same number of cells was loaded on the spin columns and eluted in RNAse free water. The concentration of RNA was determined with 'Nano Drop'.

#### 2.2.2.4 RT-PCR

The conversion of RNA isolated from BMDC cell culture and tissues into cDNA was performed with 'SuperScript™ III Reverse Transcriptase'. For every experiment the same amount of RNA was used varying between 200ng to 1µg depending on the yield of RNA from each sample in a final volume of 11µl of RNase free water. To each reaction 1µl of 10mM dNTP mix (10mM each dATP, dGTP, dCTP and dTTP at neutral pH) and 1µl of 50mM Oligo$(dt)_{12\text{-}18}$ was added to a nuclease-free microcentrifuge tube, and heated for 5min at 65°C and cooled down for a minute on ice. The following components were added to each mixture: 4µl of 5X First-Strand Buffer, 1µl 0.1M DTT, 1µl RNaseOUT™ Recombinant RNase Inhibitor (40U/µl), and 1µl of SuperScript™ III RT (200U/µl); and incubated in a thermocycler for 60min at 60°C and inactivated at 70°C for 15min. The final volume of 20µl was further diluted 1:10 or sometimes 1:20 before used in Real Time PCR.

#### 2.2.2.5 Semi-quantitative RT-PCR

40ng of target cDNA was added to a thin-walled tube and mixed together with 10x PCR Rxn Buffer, 2mM $MgCl_2$, 0.2mM dNTP mix and 1U of Taq DNA Polymerase. 40nM of primers were used for the amplification of Exon1 of FHL2 with FHL2 Exon1 F and R primer. As a positive control β-actin is amplified as well, since it is abundantly and ubiquitously expressed in tissue.
The sample is heated to 94°C to cause denaturation, which is followed by rapidly cooling to 60°C allowing the primers to anneal. During elongation the temperature is raised to 72°C. This course was repeated 33 times.

#### 2.2.2.6 Gel Electrophoresis

To prepare a 1.5% concentrated agarose gel, 2.25g agarose was weighed and mixed with 150ml of 1x TAE Buffer, heated in a microwave until it is dissolved. To visualize DNA products, 20µl of ethidium bromide was added which intercalates into double stranded DNA. It was cooled down for a short period of time, and then cast in the form. 12.5µL of PCR-product together with 2.55µL brom phenol blue loading dye is loaded on 1.5% agarose gel, which was run for 30 min at 150V. The sizes of fragments were compared to 100 bp-ladder creating 10 bands ranging from 100 to 1000 bp.

#### 2.2.2.7 Transfection of BMDC with siRNA

A total of $4x10^6$ in 200µl Optimem medium day 7 BMDCs were put in a cuvette together with 5µg S1PR1 siRNA, as well as with 5µg AllStars Negative Control siRNA. The cuvette was placed in 'Gene Pulser Xcell Electroporation System' to be electroporated with a square wave protocol (300V, 6ms), and plated in 5cm plate dish. 48hrs later, transfected BMDCs were allowed to migrate in a Transwell as described in 2.2.4.2, and in parallel RNA was isolated and converted to cDNA to assess the expression of S1PR1 with qRT-PCR as described in detail in previous and following sections.

#### 2.2.2.8 Quantitative Real-Time PCR

In order to monitor expression levels of RNA in a quantitative way, we used the 'QuantiTect SYBR Green PCR Kit'. SYBR Green is an asymmetrical cyanine dye, which preferentially binds to double stranded DNA and the resulting DNA-dye-complex absorbs blue light ($\lambda_{max}$ = 488nm) and emits green light ($\lambda_{max}$ = 522nm). 5µl of '2x QuantiFast SYBR Green PCR Master Mix' was mixed with 1µl cDNA converted by 'SuperScript™ III Reverse Transcriptase', and 0.5µl each forward and reverse primer each having a final concentration of 50nM and filled up with RNAse free water to get a final volume of 10µl. Every sample was

referenced to a housekeeping gene i.e. 18s. Every sample reaction was set up in triplicates in a 384 well format, and run on the '7900 HT ABI Prism' with the following course of program: 50°C for 2min, 95°C for 10min, 95°C for 15s and 60°C for 1min and the last to steps repeated 40 times. The data were analyzed with SDS2.2.

### 2.2.3 Protein Biochemical methods

#### 2.2.3.1 Sample Preparation for western blot

Heart and skeletal muscle tissue was squeezed through a sieve to obtain single cells. These cells and BMDC harvested on day 7 were washed with PBS. The cells stayed on ice in 100µl of RIPA Buffer and were vortexed in between in order to release proteins. After 30 to 45min the samples were centrifuged for 15min at 15,000rpm to gain the supernatant containing proteins, which were stored in a freezer at -20°C.

#### 2.2.3.2 Protein determination by Bradford Assay

The Bradford assay determines protein concentration based on a shift of absorbance when the former red Bradford reagent is stabilized into Coomassie blue by the binding of protein. The concentration of each sample can be calculated from a calibration curve prepared from the Bradford reagent bound to BSA ranging in concentration from 0 to 10µg. Here, the varying amounts of BSA was pipetted to sterile water in a total volume of 80µl of dd$H_2O$ in 96 well flat bottom ELISA plate and 20µl of Bradford reagent was added to BSA. For the determination of the sample concentration 1µl was added to 20µl Bradford reagent and 79µl sterile water. The amount of the complex formed was read in an ELISA reader at 595nm.

#### 2.2.3.4 SDS-PAGE

SDS-PAGE is a technique used to separate proteins according to their electrophoretic mobility. 20µg of protein were mixed with 'NuPAGE LDS Sample

Buffer (4x)' in a final volume of 20µl filled up with PBS and denatured for 5min at 95°C. Proteins were loaded on 'NuPAGE 4-12% Bis-Tris Gel (1.5mmx15 well)', which is placed in the 'XCell *Sure*Lock Mini-Cell' device filled with 1x MOPS SDS Running Buffer. The size of the proteins is compared to the 'Novex® Sharp Pre-stained Protein Standard' consisting of 12 pre-stained protein bands in the range of 3.5 to 260kDa. Proteins were separated for 1hr at 170V.

#### 2.2.3.5 Western Blot

The separated proteins were transferred from the gel to a Nitrocellulose membrane by the help of the 'XCell II Blot Module' containing 'NuPAGE Transfer Buffer' at 30V for 1hr. The membrane was washed with TBS-T.

#### 2.2.3.6 Detection of FHL2 and β-actin

The membrane was blocked overnight at 4°C in 0.1%MP/TBS-T. Subsequently, the membrane was incubated in 0.1%MP/TBS-T with 50ng/ml monoclonal anti-FHL2 antibody or 200ng/ml monoclonal anti-β-Actin antibody for 1 hour at RT. After washing the membrane five times for 5min in 0.1%MP/TBS-T, the membrane was exposed to 3.25µg/ml anti-mouse IgG (Fab specific)-Peroxidase antibody for 30min at RT. The membrane was washed as described before, which was followed by visualization with the ECL Western blotting detection reagents and analysis system.

#### 2.2.3.7 Immunoprecipitation

For immunoprecipitation (IP), 1mg of total protein prepared as described in 2.2.3.1 of total wt and FHL2-/- BMDC lysates were incubated with 4µg polyclonal Ab directed against FHL2 (a kind gift by R. Schüle, Freiburg, Germany) in total volume of 250µl. The complexes were precipitated using 'protein G PLUS-Agarose' at 4°C overnight. Prior protein G PLUS-agarose was precleared with double volume of RIPA buffer for 1h at 4°C in a Speed shaker

and centrifuged for 5min at 2500rpm. At the next day the complexes were washed three times with RIPA buffer for 5min at 2,500rpm at 4°C, and subsequently boiled in 20µl Laemmli buffer for 10min at 95°C, which was loaded on "NuPAGE 4-12% Bis-Tris Gel (1.5mmx15 well)" to be analyzed for FHL2 expression as described previously in section 2.2.3.5.

### 2.2.3.8 Immunofluorescence

The morphology of $2x10^5$ BMDC was studied when staining for actin cytoskeleton and nucleus on collagen coated cover slips with a diameter of 13mm put in a 24 well plate. Therefore, 3mg/ml Collagen diluted 1:100 in 100mM acetic acid was polymerized for 30min at 37°C and washed twice with $ddH_20$.

BMDC were left to adhere for one hour at 37°C. BMDC were fixed with 4% PFA for 15min on ice, and subsequently permeabilized on ice for one hour in 5%MP/0.1%Triton/1%serum/PBS. Actin filaments were stained with 0.4U/ml phalloidin$^{Alexa546}$ in 0.1%Triton/1%mouse serum/PBS for 30min at 37°C. The nucleus was stained with DAPI in PBS for 15min at 37°C. Finally, the cover slips were put on a microscopic slide with mounting medium preserving the fluorescence. Stained BMDC were viewed with Olympus IX71.

When stained for FHL2 another protocol was followed. Wt BMDCs were also plated on Collagen coated surfaces as described before. Cells were fixed for 15min on ice with PFA, and subsequently permeabilzed for 5min at room temperature in 0.2% Triton/PBS. In between all incubation steps it was washed at least twice with PBS for 5min. Cells were blocked for 2hrs in 0.2%gelatine/PBS. Actin filaments were stained with 1U/ml phalloidin$^{Alexa488}$, and simultaneously FHL2 with monoclonal anti-FHL2 antibody diluted 1:50 in Antibody Diluent for 2hrs at RT. Secondary antibody anti-mouse$^{Texas\ Red}$ directed against FHL2 was, and simultaneously the nucleus was stained with DAPI in diluted 1:1,000 in Antibody Diluent for 2hrs at RT. Finally, the cover slips were put on a microscopic slide with mounting medium preserving the fluorescence. Stained BMDC were viewed with Olympus IX71.

### 2.2.4 Migration assays

#### 2.2.4.1 Timelapse-video microscopy

Prior to use µSlides were coated with Collagen for 30min at 37°C, which was diluted in 100mM acetic acid 1:100 to receive a final concentration of 300µg/ml, and afterwards the slides were washed twice with PBS. $1x10^5$ BMDC in IMDM Medium were allowed to adhere to µSildes for 45 min at 37°C. Timelapse images were taken every 15s for 30min to determine the migratory speed without chemokine stimulation using a Cell^R Imagingsystem. After that a CCL19 gradient was set up with 40µl of 20µg/ml chemokine and the cells were imaged for a further 60min at 37°C.
Migratory speed, directionality and migratory distance were determined using the Track-it software.

#### 2.2.4.2 Transwell Assay

$2.5x10^5$ unstimulated, LPS and TNF-α stimulated BMDC in 100µl BSA/IMDM medium were added to the top chamber of the insert of the Transwell with a pore size of 5µm. The bottom chamber was filled with 600µl IMDM/BSA medium containing 10ng/ml CCL19. Cells were allowed to transmigrate for 3hrs at 37°C, harvested from the bottom chamber using 2mM EDTA/PBS, and stained for CD11c positive cells. In order to quantify the number of cells arrived in the bottom chamber 5,000 Calibrate beads were added to each sample during acquisition with FACS Canto.

#### 2.2.4.3 *In vivo* migration

$10^7$/ml TNF-α matured or nonmatured BMDC were incubated with either 1µM CFSE or 10µM SNARF for 10min at 37°C and reaction was stopped with 10% FCS. FHL2-/- and wt BMDC labeled with CFSE respectively SNARF were mixed in equal proportions and $2x10^6$ BMDC in 20µl PBS were injected to the footpad of wt mice. To exclude any dye specific inhibition a dye switch was conducted. Twenty six hours later the cells were recovered from popliteal LN,

which was minced with the stamp of a syringe and squeezed through a cell strainer to get single cell suspensions. The sample were stained with a CD11c-pacific Blue conjugated mAB for 30min on ice in the dark and analyzed on FACS Canto. In addition the mixture injected into the footpad was acquired to check that an equal proportion was injected and minor changes were considered for the calculation.

#### 2.2.4.4 Determination of survival by MTT Assay

The assay is designed for the spectro-photometric quantification of cell growth and viability based on the cleavage of the yellow tetrazolium salt MTT labeling reagent (1x), to purple formazan crystals by metabolic active cells involving the pyridine nucleotide cofactors NADH and NADPH. Day 7 wt and FHL2-/- BMDC were harvested and $2x10^5$ BMDC were plated in 100µl in 96 well plate flatbottom set up as a six fold determination and left to adhere for one hour which represent the reference group. At the same time BMDC adhered for 24hrs and the same procedure described in the following was applied for both days. BMDC were incubated for 4hrs with 10µl of MTT labeling reagent (final concentration 0.5mg/ml) per well and 100µl Solubilization solution (10% SDS in 0.01 M HCl) is added to each well and let stand overnight in the incubator until complete solubilization of the purple formazan crystals occurs. The spectrophotometrical absorbance of the samples was measured using an ELISA reader at 600nm and reference wavelength at 650nm.

### 2.2.5 Flow cytometry

#### 2.2.5.1 Staining of surface markers

Cells were washed in FACS buffer and incubated with 10µg/ml anti-FcγRII/III mAb to block unspecific binding of the following Ab reagents. PE-labeled mAbs (used at 5–20 µg/ml) against MHC class I, MHCII, and biotinylated mABs against CD40, CD80 and CD86 were used. Furthermore all cells were labeled with CD11c APC conjugated mAB. Isotype controls included purified rat IgG2a, either PE labeled or biotinylated IgG. After incubation with mAbs for 20 min at

4°C and washing in FACS buffer, cells coupled to a biotinylated mAB, were incubated with Strepavidin conjugated PerCPCy5.5. FACS analysis was performed on a flow cytometer FACS Canto. FACS data were analyzed using FlowJo software.

#### 2.2.5.2 Intracellular cytokine staining

$2x10^5$ immature and LPS matured BMDCs plated in a 96 well flat bottom in 100µl IMDM Medium were incubated in the presence of Monensin and Brefeldin A, which were diluted 1:1000, for 5h. After surface staining with CD11c PE, BMDCs were fixed with 4% PFA for 10min on ice, permeabilized with 0.5% saponin/FACS buffer for 15min on ice, and stained with Abs against IL-12 and TNF-α conjugated to Alexa647.

#### 2.2.5.3 Expression of CCR7

CCR7 on BMDC were detected with the purified mouse CCL19-Fc fusion protein as described in (Hargreaves et al., 2001). Briefly, 0.1µg of CCL19-Fc fusion protein in 10µl FACS buffer per sample was incubated for 30min on ice. 1µg of PE goat anti-human IgG Fcγ Fragment, which was pre absorbed in 2% mouse and rat serum in a ratio 1:1, and 50ng CD11c APC were added to the sample to a final volume of 50µl FACS buffer, and incubated for 15min on ice. FACS analysis was performed on a flow cytometer FACS Canto. FACS data were analyzed using FlowJo software.

#### 2.2.5.4 Quantification of F-actin by flow cytometry

On day seven the medium of wt and FHL2-/- BMDC was substituted by medium containing 0.5% FCS for two days. Under both conditions the maturation was induced by TNF-α. BMDC were harvested and the surface was stained with CD11c-PE conjugated mAB, and afterwards stained intracellularly by fixing with 4% PFA for 10min on ice and permeabilizing with 0.5% Saponin/FACS buffer for 15min on ice. F-actin was stained with 0.2U/ml phalloidin conjugated to

Alexa647 in 50µl FACS Buffer for 30min on ice, and analyzed by flow cytometry. All samples were set up in triplicates.

### 2.2.6 Rac1 Activation Assay

The activity of Rac1 was investigated with an ELISA based 'Rac GLISA activation assay' which is coated with RBD domain of Rac1-family effector proteins, where only the active GTP-bound form of the Rac-family protein, but not the inactive GDP-bound form will bind to the plate. The protocol provided by the company was followed with minor changes.
Day 7 BMDCs were serum starved for two days in IMDM medium containing 0.5% FCS. On day 9 BMDC were completely serum starved for at least 4h, harvested and $5x10^6$ were lysed in 100µl G-LISA Buffer prepared according to manufacturer's instructions and immediately frozen in liquid nitrogen. 10µl of each sample was removed for measuring the protein concentration with Precision Red™ Advanced protein assay reagent read in an ELISA reader at 600nm. The concentration of lysates was adjusted to 0.5mg/ml and 50µl was used per well set up in triplicates. After antibody incubation the plate was extensively washed with the provided wash Buffer 6 times and in between inverse centrifuged to dry the plate to lower background signal. Signal intensity was measured at a Luminometer at 600nm.

### 2.2.7 Immunological methods

#### 2.2.7.1 Antigen uptake

$2x10^5$ BMDC in 200µl IMDM/medium were left to adhere for one hour at 37°C in a 96 well flatbottom. Medium was replaced by medium supplemented with either 200µg/ml Dextran coupled to FITC or with 2µg/ml OVA labeled Alexa 647, respectively. BMDCs were incubated for 30min at 37°C and as a negative control for the same period of time at 4°C. BMDC were harvested with 2mM EDTA/PBS and stained with a CD11c-PE conjugated mAB. All samples were set up in triplicates and 20,000 events were recorded in a live gate by FACS Canto and evaluated by FlowJo software.

#### 2.2.7.2 Purification of CD11c positive cells out of BMDC culture

For T cell co culture assays the BMDC culture was purified for the CD11c positive cells only by AutoMACS separation. On day 7 BMDC were harvested and $10^8$ in 500µl MACS and 100µl CD11c microbeads for 15min at 4°C incubated, washed twice with MACS buffer and separated from the negative fraction by AutoMACS with the program 'possels'. The positive fraction was counted and used for *in vitro* studies. Staining with anti CD11c antibody and FACS analysis confirmed 95 to 98% purity of cells.

#### 2.2.7.3 Purification of CD8 and CD4 cells

OVA antigen specific CD8 and CD4 positive T cells were isolated out of the spleen of OT-I and OT-II mice respectively. 48hrs before organ harvest the OT-I mouse was injected i.p. with 300µg anti NK1.1 antibody to deplete the NK and NKT cells. Prior 0.6g Nylon Wool in a 10ml syringe was equilibrated with RPMI medium without air bubbles for at least for an hour at 37°C. Spleens were minced through a large pored (250µm) metal sieve with a stamp of a syringe, centrifuged and taken up in 5ml medium, which was then transferred to nylon wool to retain B cells and myeloid cells. After at least 45min at 37°C the enriched T cells were flushed out of the syringe with 20ml medium, centrifuged at 1500rpm for 10min and incubated in 1ml ACK lysis buffer for 2min at room temperature to destroy the red blood cells. For the purification with the AutoMACS, $10^8$ cells from the enriched spleen of the OT-I or OT-II were incubated with 500µl MACS Buffer and 50µl CD8 MicroBeads or CD4 MicroBeads, respectively for 15min at 4°C. The cells were washed twice with MACS Buffer to remove unbound microbeads, send through a cell strainer (40µm pore size) and selected with the AutoMACS using the program 'possels. The positive fraction was further employed in the *in vitro* studies. Staining with CD8 or CD4 antibody and FACS analysis confirmed 95 to 98% purity of cells.

### 2.2.7.4 Antigen presentation

On day 7, $2x10^5$ wt and FHL2-/- BMDCs purified by AutoMacs using CD11c microbeads as described before in 2.2.7.2 were seeded in 100µl per well in a 96 well flatbottom. After at least 45min at 37°C to let them allow adhering, 50µl medium was added to the BMDC containing OVA to reach a final concentration of 0, 0.01, 0.1, or 1mg/ml for 2hrs. A total of $1x10^5$ in 50µl purified naive CD4+ and CD8+ T cells from OT-II and OT-I mice, respectively, were co-cultured with BMDCs. Twenty-four hours later, supernatants were collected and stored at -20°C.

### 2.2.7.5 IL-2 ELISA

Supernatants collected from antigen presentation assay were subjected to a commercially available quantitative IL-2 a read out for T cell activation. A 96 well ELISA plate flatbottom plate was coated with 50µl per well purified anti-IL-2 first antibody diluted 1:500 in Coating Buffer having a final concentration of 1µg/ml and incubated for 1h at 37°C. It was washed for four times with PBS and in between inverse centrifuged (1600rpm, 2min) to dry them more. This washing procedure was performed between all incubation steps. Unspecific binding sites were blocked with 50µl 1%BSA/PBS for 30min at RT. An IL-2 standard curve was established with recombinant IL-2 starting from 40ng/ml in a three fold dilution going down to 6pg/ml in RPMI medium. 100µl of the supernatants of the samples from the antigen presentation assay were added in triplicates to each well, and incubated at 4°C over night. 500ng/ml biotinylated rat anti-mouse IL-2 secondary antibody was diluted 1:1000 in PBS and 50µl added to the samples one hour at 37°C. Streptavidin conjugated with HRP diluted 1:1000 in PBS was added for 30min at 4°C. Peroxidase substrate ABTS was diluted in ABTS buffer to receive a final concentration of 1mg/ml and 2µl 30% $H_20_2$ was added per ml ABTS and the resulting green product is photometrically read in an ELISA Reader at 405nm.

#### 2.2.7.6 T cell proliferation assay

On day 7, $4x10^5$ in 200µl IMDM medium wt and FHL2-/- BMDCs purified by AutoMacs using CD11c microbeads described before, were plated in a 48 well flatbottom per well. After two hours BMDC were pulsed with 100µl OVA with a final concentration of 1mg/ml or medium without OVA for 2 h. Purified CD4+ and CD8+ T cells from OT-II and OT-I mice, respectively, were labeled with 1µM CFSE for 10min at 37°C and the reaction was stopped by FCS. The cells were washed and $2x10^5$ T cells were added to each well in 200µl medium. Three days later, proliferation was assessed by flow cytometry counterstaining with CD4 and CD8 Abs.

### 2.2.8 Statistics

Statistics were calculated with Excel and SPSS. Error bars indicated Standard error of the mean (SEM). The Students T-test was used to analyze data for significant differences. P-values <0.05 were regarded as significant. And indicated in the figures as follows: *$p \leq 0.05$, **$p \leq 0.01$, ***$p \leq 0.001$.

# 3. Results

## 3.1 Nuclear localization of FHL2 is lost in mature but not immature BMDC following stimulation with CCL19

FHL2 deficient mice display wound healing disturbance due to defective migration of fibroblasts (Wixler et al., 2007). On the other hand, loss of FHL2 activity is associated with increased epithelial cell migration in intestinal epithelium, which might allow eliminating of deleterious cells from proliferating crypt more efficiently and reducing the risk of tumorigenesis (Labalette et al., 2010). FHL2 is known to associate with components of the actin cytoskeleton (Li et al., 2001), which could have an effect on the morphology of the cell (Bai et al., 2005). These published observations prompted us to initially study the role of FHL2 as a regulator of DC migration.

In order to study DC functions in the mouse, DCs are usually generated *in vitro* out of BM precursors. In the presence of GMCSF, the hematopoietic stem cell will differentiate into DC defined by the expression of CD11c, a specific integrin alpha x. Therefore we always stained DC for CD11c for flow cytometric analysis, and gated on the CD11c positive population, so that only DCs were analyzed further (Fig 3.1, upper panel). After seven days in culture, BMDC are a heterogenous population: Although no additional external stimulus was present, a small fraction (usually between 10-15% of DC) show high expression levels of maturation markers (Fig. 3.1, lower panel; Petersen et al., 2000). Staining DCs with maturation markers CD86 and MHCII, three populations are visible by flow cytometry: a negative, an intermediate and a positive population. Especially, the number of cells in the gate of the bright population increases, after the addition of maturation reagents like LPS and TNF-α (45.9% and 19.6%, respectively versus 10.4%), which is even higher after the incubation with LPS. This is most likely caused by mitogenic factors present in FCS, because authors of Lutz and Rossner (2007) suspected high levels of glutamic oxaloacetic transaminase and lactate dehydrogenase correlated with a very large proportion of mature DC within the cultures, whereas low levels of these enzymes correlated with an inhibition of DC outgrowth. Other groups could also observe morphological

differences in BMDC culture (Burns et al., 2004). A high proportion of DC even in the absence of LPS provided sufficient stimulus for DC adhesion, polarization, and podosome formation, suggesting partial maturation.

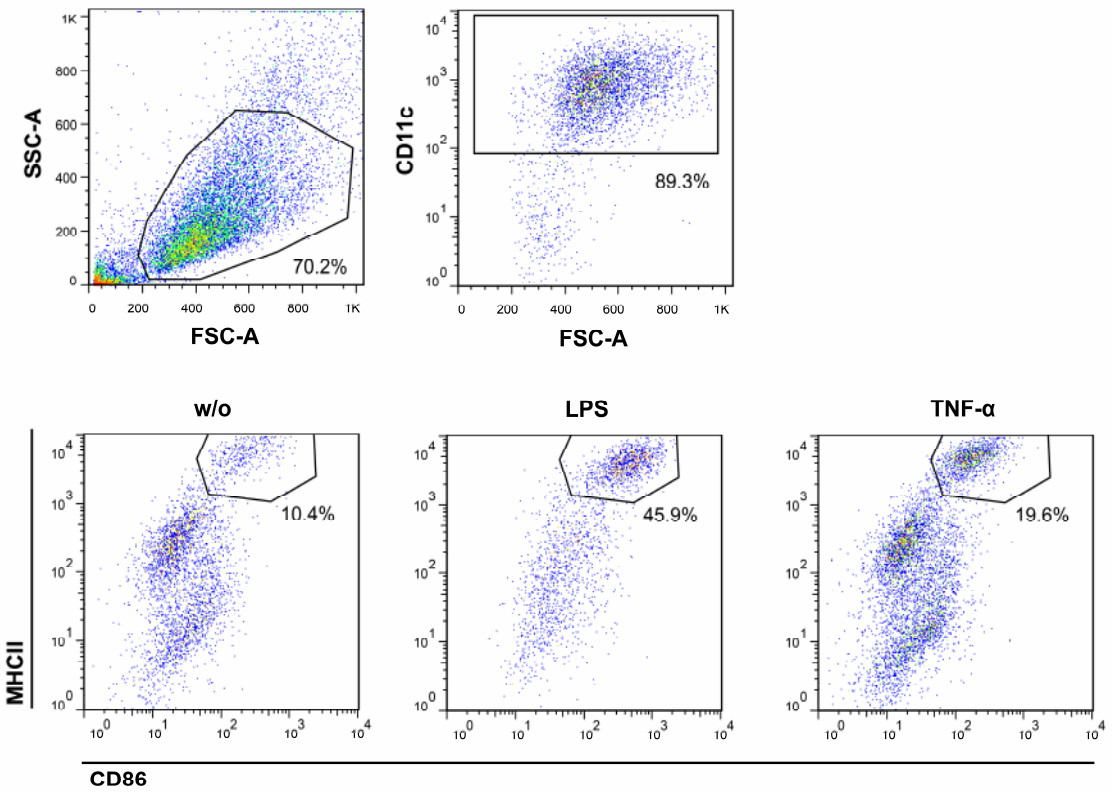


**Figure 3.1: DCs generated out of BM show partial maturation.** A day seven BMDC culture was incubated with 100ng/ml LPS and 30ng/ml TNF-α for 24hrs. BMDCs were harvested as described in Material and Methods 2.2.1.4, stained for CD11c, CD86 and MHCII, and analyzed by flow cytometry. In the upper panel, the gating strategy is depicted that we applied in all experiments: By plotting FSC versus SSC, a live gate was drawn, which contained the presumably living cells. Only these were analyzed for CD11c expression, where we gated on the CD11c positive fraction of cells.

The localization of FHL2 within a cell could give us information of what kind of function FHL2 is playing. FHL2 can act as a co-activator or –repressor of several transcription factors, or it binds to integrins which link the ECM and the actin cytoskeleton. To determine FHL2 expression and the conformation of the actin cytoskeleton we stained immature or LPS-matured wt BMDC for FHL2 and phalloidin. Phalloidin is a toxin derived from a mushroom called death cap that binds to actin filaments much more tightly than to actin monomers, and can give us information about the structure of the actin cytoskeleton within a cell (Cooper, 1987; Sampath and Pollard, 1991). LPS treatment induces via TLR 4 (Akira et al., 2001) a signal cascade that leads to DC maturation. As maturation

progressed an increasing proportion of DC assumed rounded cell morphology with multiple membrane-ruffles covering the surface of the cell (Burns et al., 2004).

We could observe the same observe in the LPS-matured culture where a higher number of DCs have a smaller and rounded appearance compared to the immature culture made visible by phalloidin staining (Fig. 3.2 A). Both immature and mature BMDC express FHL2, which localizes to the nucleus (Fig. 1A, upper and lower left corner). Before we further analyze whether FHL2 has a functional role in DC migration, we wanted to determine localization of FHL2. Therefore, we stained mature and immature BMDC for FHL2 that were stimulated with the CCR7 chemokine receptor ligand CCL19. In immature BMDC, CCL19 treatment did not alter FHL2 localization, which remained mainly in the nucleus (Fig. 3.2. A, upper right corner) Interestingly, CCR7 ligation in mature DC led to loss of nuclear localization of FHL2 redistributing towards the cell membrane, which we could mainly found in small rounded cells of the culture. Together, this indicates that the migratory chemokine CCL19 influences FHL2 localization and strongly suggests a functional role of FHL2 in DC migration.

Before we further functionally addressed the role of FHL2 in CCL19 induced processes in DC migration, we wanted to confirm loss of FHL2 in FHL2-deficient mice (Chu et al., 2000a). Here, we performed RT-PCR on various tissues and *in vitro* generated BMDC of wt C57BL/6 and FHL2-/- mice (Fig. 3.2 B). FHL2 mRNA was highly expressed in the heart, skeletal muscle, gastrointestinal tract, lung and at lower levels in BMDC of wt mice, while expression was lost in FHL2-deficient mice. Moreover, FHL2 protein was not detectable by western blot in heart tissue that has the highest levels of FHL2 expression in wt mice (Chu et al., 2000b), Fig. 3.2 C). Since expression of FHL2 was relatively low in BMDC (Fig. 3.2 B), we performed IP of FHL2 protein with a monoclonal anti-FHL2 ab out of wt and FHL2-/- BMDC protein lysates, and loaded the concentrated lysate on a SDS-PAGE and performed western blot against FHL2. As expected we could confirm that FHL2 expression is not detectable at the protein level in FHL2-/- BMDC (Fig. 3.2 D).

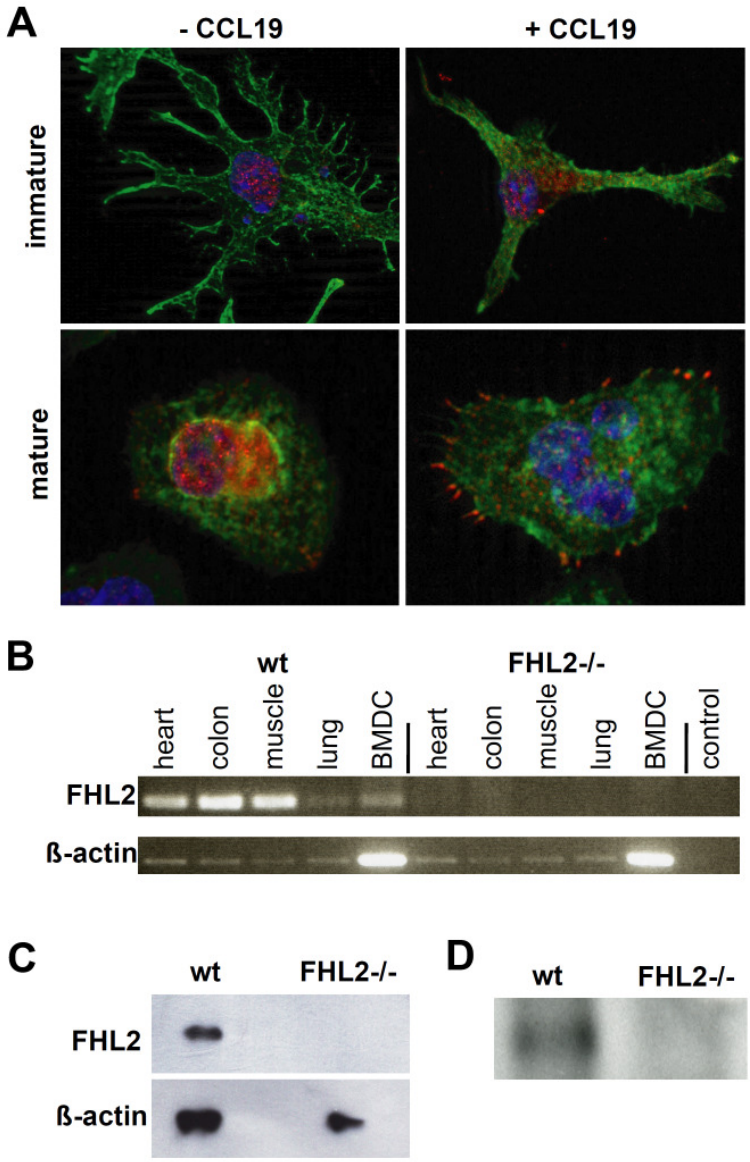


**Figure 3.2: Nuclear expression of FHL2 in mature BMDC is reduced following stimulation with CCL19. (A)** Day 7 BMDC were either matured with LPS (100ng/ml) for one day or left untreated (immature). Subsequently they were left to adhere on glass cover slips in the presence or absence of CCL19 (10ng/ml) for 1h, fixed and stained with a polyclonal FHL2 specific antibody (red), phalloidin (green) and DAPI (blue). **(B)** Detection of FHL2 mRNA by RT-PCR in day 7 wt and FHL2-/- immature BMDC, heart, colon, skeletal muscle and lung using primers for exon 1. As positive control and loading reference ß-actin mRNA was detected. **(C)** Western blot analysis of FHL2 protein in cardiac muscle of wt and FHL2-/- mice. Detection of actin served as loading control. **(D)** IP of FHL2 and following analysis by western blot of wt and FHL2-/- BMDC. The data shown here is representative of three or more independent experiments.

## 3.2 FHL2-/- BMDC display enhanced migratory directionality, speed and persistence *in vitro*

We showed that in mature DCs the actin conformation is changed to a rather small and rounded appearance compared to an immature DC. In the presence of CCL19, FHL2 localizes differently in this cell type rather in the cytoplasm than in the nucleus without CCL19 ligation. So, it seems FHL2 is involved in the conformation of the actin cytoskeleton of DC. The actin cytoskeleton needs to be rearranged in the cell depending on the need for slower or faster migration.

To measure the influence of FHL2 expression on chemotactic directionality, migratory speed and directional persistence of BMDC more closely, we used timelapse video microscopy (Fig. 3.3). Timelapse microscopy can image the same object e.g. a cell at regular time intervals over several hours and compile the images into a movie. So, live-cell imaging enables us to monitor cell movements over time. Images are taken in real time and allows the speed of single cells and the distance they have covered to be measured directly *in vitro*.

Briefly, immature BMDC were transferred into collagen-coated IBIDI µ-slide chambers and images were taken every 15s for a period of one hour after establishing a CCL19 gradient. Quantitative analysis of single BMDC tracks showed that both wt and FHL2-/- BMDC stayed nearly in the same position meaning they show hardly directionality when no chemokine gradient was applied (Fig. 3.3 A, upper left and right corner). Once the chemokine gradient was applied, both wt and FHL2-/- BMDC showed directed migration towards CCL19 from the right (Fig. 3.3 A, lower left and right panel). FHL2-/- BMDC covered a significantly longer distance (mean distance 100µm; n=90), measured as a direct line from their point of origin, than wt BMDC (mean distance 53µm; n=75) (Fig 3.3 B, left panel). This was partly due to a less torturous migratory path (Fig 3.2 A), but also to a significantly increased migratory speed: wt BMDC showed a mean migratory speed of 40µm/h and FHL2-/- BMDC 140µm/h (Fig 3.3 B, right panel). Furthermore, FHL2-/- BMDC showed a higher degree of directional persistence (Fig 3.3 A).

Thus, timelapse video-microscopy conclusively showed that FHL2 has an impact on DC migration, namely that FHL2 loss leads to increased migratory speed, and also increased persistence and directionality.

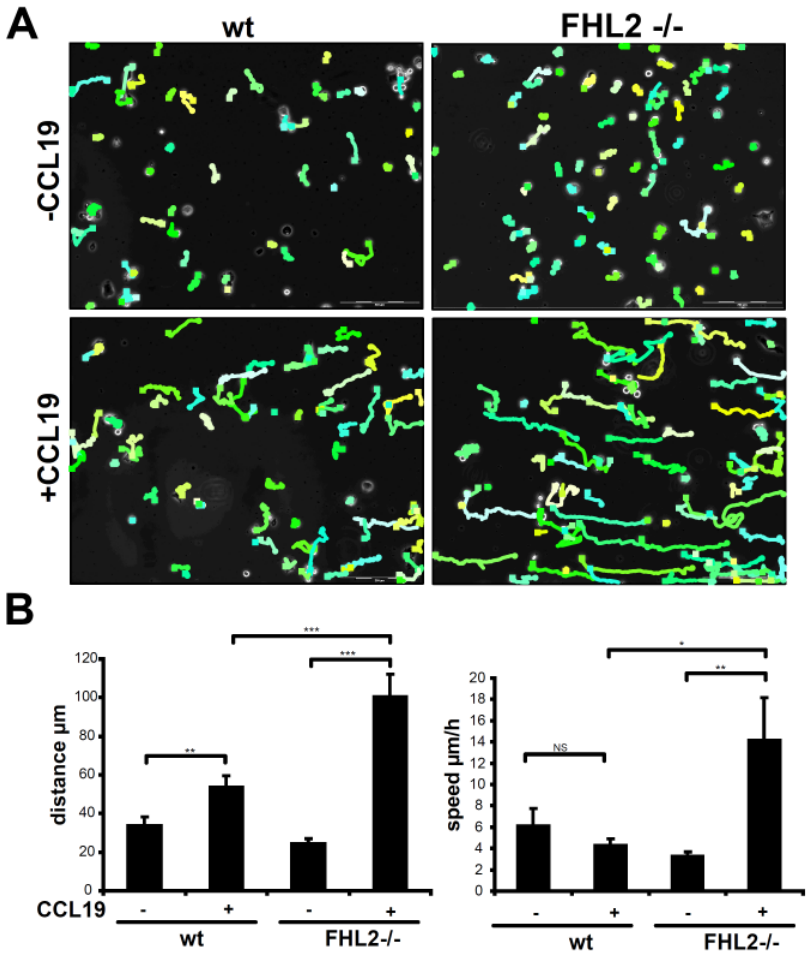


**Figure 3.3: Higher migratory speed and directionality towards a CCL19 gradient in FHL2-/- BMDC compared to wt BMDC.** Wt and FHL2-/- BMDC were generated as described. At day 7 immature BMDC were harvested and $10^5$ BMDC were left to adhere in collagen-coated IBIDI µ-slides for 45min at 37°C and filmed simultaneously. After 45min a CCL19 gradient was established and BMDC were filmed for an additional 60min. Time-lapse images were taken every 15s. **(A)** Single tracks of migrating BMDC analyzed using the Track-it software. **(B)** Mean distance and speed of migrating BMDC calculated by the Track-it software from Olympus. In each group the tracks of at least 70 BMDC were analyzed. Values are depicted as mean and error bars +/-SEM. Statistical significance was calculated using a Student's t-test: NS not significant, *p≤ 0.05, **p≤0.01, ***p≤0.001. The data shown here is representative of three or more independent experiments.

## 3.3 Enhanced *in vitro* and *in vivo* migration of FHL2-deficient BMDC

We wanted to confirm our results and to substantiate our conclusion gained from Time lapse microscopy by an additional methodology i.e. transwell. DCs were plated on an insert with a pore size of 5µm in transwells, which was placed in a well of a 24 well plate, making contact with the media filled in the bottom chamber. Here, the number of cells arrived in the bottom of the 24 well plate well which is quantified by flow cytometry correlates to their migratory capacity.

To examine the effect of FHL2 deficiency on CCL19-induced DC migration, immature wt or FHL2-/- BMDC were placed in the upper chamber of a transwell and left to migrate towards CCL19 or medium alone. When no CCL19 was present in the lower chamber, only a very low number of cells could be detected (Fig. 3.4 A). Both wt and FHL2-/- BMDC migrated in a CCL19 dependent manner as significantly more BMDC were counted when CCL19 was present in the lower well. Control experiments demonstrated when chemokine was added only to the upper or the upper and lower chamber no increased migration above basal levels was observed (Fig. 3.4 C). This was done to exclude that CCL19 by itself might influence of the morphology of BMDC so that they could pass through the membrane more easily. This would not have been a matter of active migration but rather dropping through the pores of the membrane. So, we can assume that this effect was specific to CCL19 attracting BMDC to the lower chamber, where they actively migrated to. Furthermore, significantly more FHL2-/- BMDC migrated into the lower chamber in the given time period than wt BMDC indicating that FHL2 deficiency significantly increases the CCL19-induced migration rate of BMDC (p value = 0.004). This difference was still significant when BMDC were matured either with LPS or TNF-α (Fig. 3.4 B). This difference between wt and FHL2-/- BMDC was even higher when matured with TNF-α when FHL2-/- BMDC showed approximately three fold increase in migration (Fig. 3.4 B, lower panel). Both demonstrated increased migratory speed after stimulation with TNF-α or LPS stimulated BMDC, but stimulated wt BMDC could never speed up to levels of immature FHL2-/- BMDC. Hence, we were able to confirm our results obtained from timelapse microscopy by transwell assays, i.e. FHL2-/- BMDC show increased migration towards CCL19.

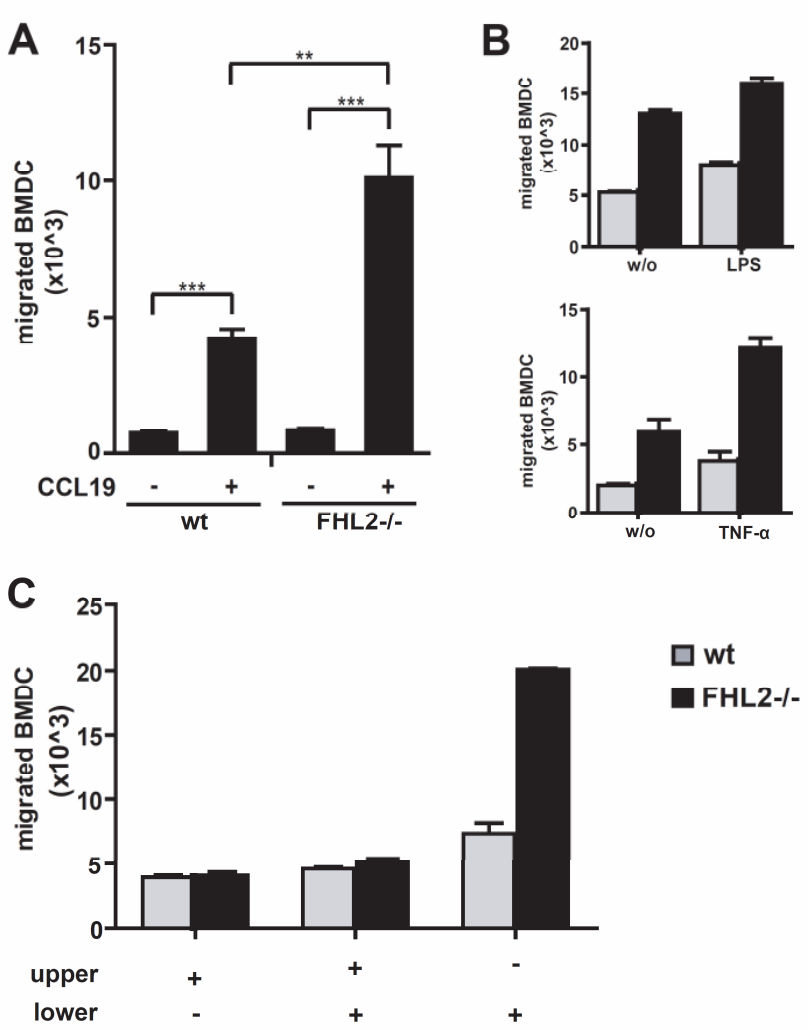


**Figure 3.4: FHL-/- BMDC show enhanced migration in a transwell assay towards CCL19, even after stimulation with LPS and TNF-α.** Wt and FHL2-/- BMDC were generated. **(A)** At day 7, immature BMDC **(A)**, LPS and TNF-α-matured **(B)** were harvested; and 2.5x10$^5$ BMDC were cultured in 100µl medium containing 0.5% BSA in the upper chamber of a 5µm pore transwell insert. The bottom chamber was filled with 600µl medium containing 0.5% BSA alone or supplemented with 10ng/ml CCL19. After 3h, migrated BMDC were harvested from the lower chamber and stained for CD11c. The amount of migrated CD11c+ BMDC was quantified by flow cytometry by addition of a set amount of calibration beads and calculated as follows: total migrated BMDC = (beads total * BMDC sample)/beads sample. Values are depicted as mean and error bars +/-SEM. Statistical significance was calculated using a Student's t-test: NS not significant, *p≤ 0.05, **p≤0.01, ***p≤0.001. The data shown here is representative of three or more independent experiments.

Directional migratory speed in DC is known to be regulated amongst others by CCR7 (Ohl et al., 2004). Since FHL2 can act as a transcriptional co-activator or –repressor (Johannessen et al., 2006; Lai et al., 2006; Muller et al., 2000; Muller et al., 2002) and thus might affect CCR7 expression, we investigated whether CCR7 expression was increased in FHL2-/- BMDC. However, staining of immature BMDC with CCL19-IgG fusion protein (Fig. 3.5 A) did not reveal differences in CCR7 expression levels between wt and FHL2-/- BMDC. This

indicates that the enhanced CCL19-induced migration of FHL2-/- BMDC was not due to altered CCR7 surface expression. Additionally, the expression levels of CCR7 remained the same between wt and FHL2-/- BMDC after incubation with LPS and TNF-α (Fig. 3.5 B). CCR7 was upregulated in both cell types, and with respect to TNF-α the expression of CCR7 in both cell types was slightly more in contrast to LPS matured.

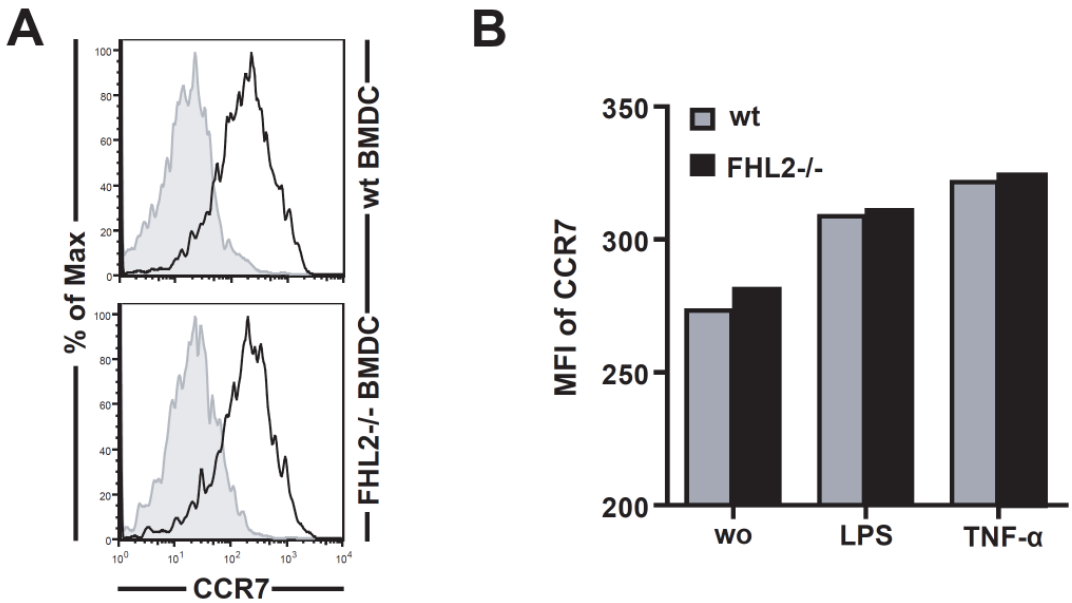


**Figure 3.5: CCR7 expression is the same between FHL2-/- and wt BMDC.** Day 7 immature **(A)**, matured with LPS and TNF-α **(B)** wt and FHL2-/- BMDC were stained with CCL19-Fc and anti-HuFc-PE or with anti-HuFc alone as a negative control and analyzed by flow cytometry. **(A)** CCR7 expression shown as a histogram. CCL19-Fc and anti-HuFc-PE (black lines) or anti-HuFc alone (grey filled). **(B)** Expression levels are shown as mean fluorescence intensity (MFI). The data shown here is representative of three or more independent experiments.

*In vitro* DC migration assays only partially resemble DC migration *in vivo* (Sixt et al., 2006). Therefore, we determined whether FHL2-/- BMDC also had altered migratory properties *in vivo*. To this end we injected equal amounts of immature or TNF-α matured (Cumberbatch et al., 1999; Cumberbatch and Kimber, 1992) wt and FHL2-/- BMDC that were fluorescently labeled with SNARF (FHL2-/-) and CFSE (wt) into the footpad of C57BL/6 recipient mice and quantified the number of CD11c positive BMDC that migrated into the draining popliteal LNs within 26h. *In vivo* studies suggest that the journey to the lymph node takes between 3–24 h (Kupiec-Weglinski et al., 1988; Roake et al., 1995) by which time DC express high levels of MHC complexes, and are functionally primed for

optimal interaction with T cells (Sallusto and Lanzavecchia, 1994). Both immature (Fig. 3.6 A, right panel) and TNF-α matured (Fig. 3.6 A, left panel) FHL2-/- and wt BMDC arrived in the draining LN in the given period of time, but the number of FHL2-/- BMDC was significantly higher. More interestingly, this effect was independent of the maturation status of the BMDC (Fig. 3.8) indicating that FHL2 deficiency also regulates migration of immature DC. We can also assume that this is not because of a better response to CCL19 or CCL21 because CCR7 is equally expressed on wt and FHL2-/- BMDC (Fig. 3.4, see Discussion). Dye swap experiments excluded possible dye specific effects, which can be seen in Figure 3.6 B: Representative dot plot depicting SNARF+ FHL2-/- and CFSE+ wt BMDC and the other way around within the recovered CD11c+ DC population. Regardless of which stain we used, SNARF or CFSE, FHL2-/- showed a higher migratory rate into the LN. To rule out that the loss of FHL2 had an effect on DC viability and therefore we could recover more FHL2-/- BMDC out of the draining LN, we examined cell survival with the help of an MTT assay *in vitro* over the same period of time, i.e. 26h (Fig. 3.6 C). Here, we could not see an advantage of FHL2-/- BMDC over wt BMDC with respect to survival. Thus, the increased number of FHL2-/- BMDC recovered from the popliteal LN was not due to a survival advantage over wt BMDC. Collectively, this indicates that FHL2-deficiency in BMDC leads to enhanced migratory activity both *in vitro* and *in vivo*.

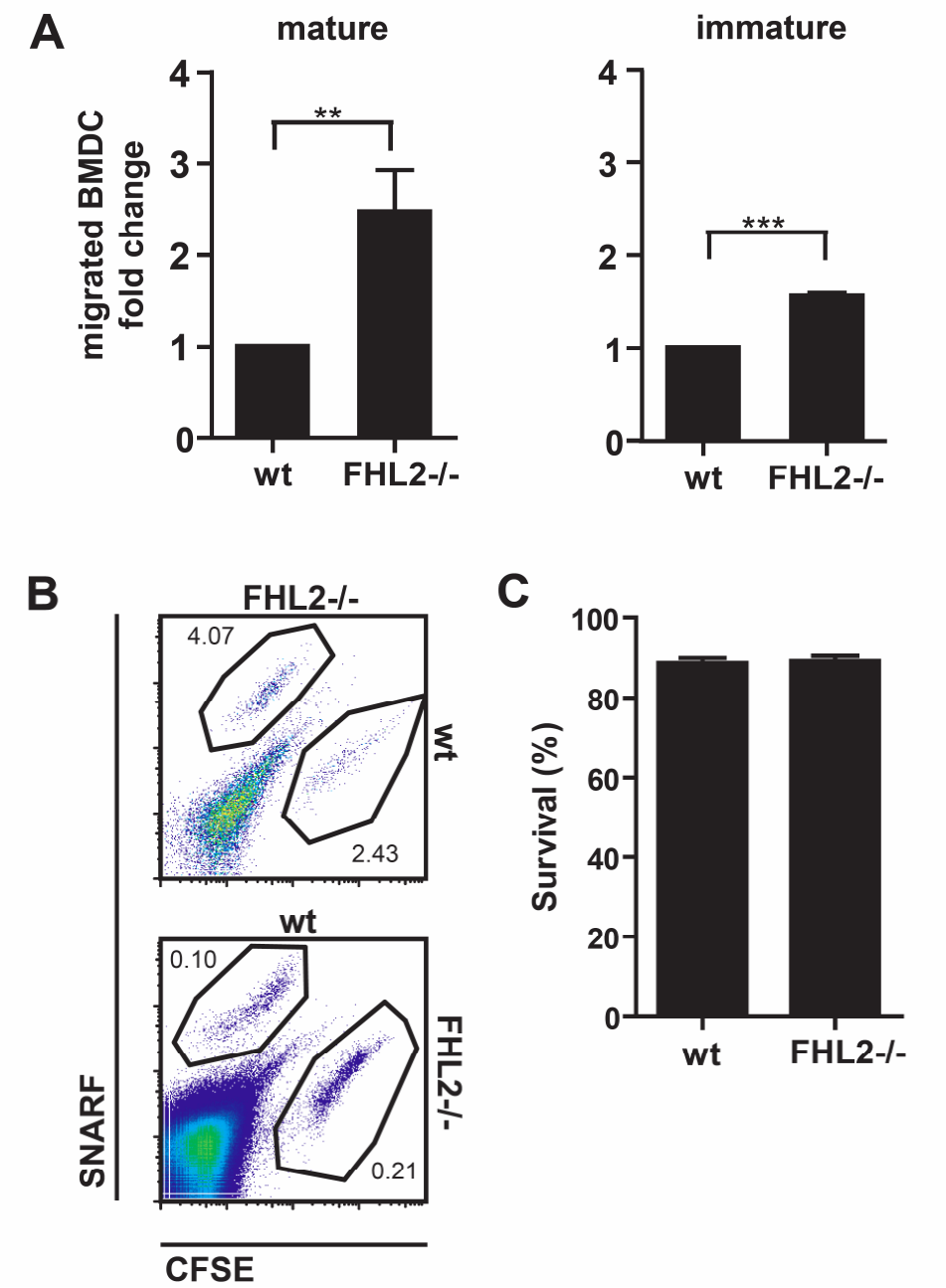


**Figure 3.6: Enhanced *in vivo* migration of FHL2-/- BMDC. (A)** Immature (left panel) or TNF-α matured (right panel) BMDC were harvested and wt and FHL2-/- BMDC were labeled with CFSE and SNARF, respectively. Wt and FHL2-/- BMDC were mixed at a ratio of 1:1 and injected into the footpad of wt recipient mice. After 26h single cell suspensions of the draining popliteal LNs were prepared, stained for CD11c and analyzed by flow cytometry. The total number of CD11c+ wt BMDC recovered from an individual popliteal LN was set to 1 and the number of FHL2-/- BMDC per wt BMDC is shown as fold increase. **(B)** Representative dot plot, gated on CD11c positive DC is shown. Numbers indicate the percentage of CFSE positive wt and SNARF positive FHL2-/- BMDC or the other way around within the DC population in the popliteal lymph node. **(C)** $2x10^5$ wt and FHL2-/- BMDC in six replicates were plated in a volume of 100µl in a 96 well plate. 24hrs later 10µl of MTT solution was added to each well. After 4hrs 100µl Solubilization Buffer was added and incubated overnight at 37°C. Survival was determined in a photometer at 570nm. Values are depicted as mean and error bars +/-SEM. Statistical significance was calculated using a Student's t-test: NS not significant, *p≤ 0.05, **p≤0.01, ***p≤0.001. The data shown here is representative of three or more independent experiments.

## 3.4 FHL2-/- BMDC express more lamellipodia than wt BMDC due to increased Rac1 activation

Cell locomotion depends on the protrusion of the leading edge, the traction of the cell body, and the retraction of the tail. For all these individual processes reorganization of the actin cytoskeleton is necessary (Keren et al., 2008; Le Clainche and Carlier, 2008). In detail, cells that are stationary and hardly moving express mostly stress fibers. In order to initiate cell migration slender cytoplasmic projections are formed that allow moderate migration. In very mobile cells like keratinocytes of fish and frog, also actin projections are called lamellipodia are formed with an underlying two-dimensional actin mesh. With respect to DC these projections are mostly seen in a mature DC after trigger of PRRs, when the DC needs to carry the antigen to the LN as fast as possible. We could also see a different conformation of the actin cytoskeleton after stimulation with LPS (Fig. 3.2 A, lower panel) and this lead most likely to enhanced cell migration (Fig 3.4, upper panel).

To answer the question, if there is a different reorganization of the actin cytoskeleton in FHL2-/- BMDC, the actin cytoskeletal conformation of immature FHL2-/- and wt BMDC was examined by immunofluorescent staining with phalloidin (Fig. 3.7 A). The morphology of FHL2-/- and wt BMDC differed significantly: While 90% of immature wt BMDC on collagen showed long protruding filopodia and only less than 10% of cells were small and veiled (Fig. 3.7 A, upper panels), up to 50% of the cells in an FHL2-/- BMDC culture showed this phenotype (Fig. 3.7 A, lower panels). The quantification is found in Fig 3.7 A, right panel. As mentioned before, the BMDC culture system yields a heterogeneous population of BMDC where a small proportion of DC matured spontaneously. This we could see in our own culture system, which is a very mixed population of different cell types and not a pure population, which is reflected by the numbers after counting the different morphologies. In this context it is interesting to note that authors from Bai et al. (2005) could also observe a difference in organization of the cytoskeleton of osteoclasts isolated out of wt and FHL2-/- mouse.

Fluorescent labeled phalloidin can be used to quantitative the amount of filamentous actin there is in a cell (Cooper, 1987; Koestler et al., 2009).

Phalloidin preferentially binds to polymerized F-actin, while lammellipodia are arranged of a more branched F-actin structure whereas in filopodia the structure of the actin cytoskeleton is more organized (Le Clainche and Carlier, 2008), therefore lamellipodia stain more strongly with phalloidin. The amount of F-actin was compared quantitatively by flow cytometry in serum starved immature and TNF-α matured wt and FHL2-/- BMDC (Fig 3.7 B). FHL2-/- BMDC showed significantly higher amounts of polymerized F-actin than wt BMDC. The difference between wt and FHL2-/- in polymerized F-actin was even more pronounced in TNF-α matured BMDC. So, by a different approach we could confirm our previous observation that the cytoskeleton in FHL2-/- exhibits differences to wt BMDC. This might explain why we could see elevated migration of FHL2-/- BMDC in timelapse Microscopy, transwell assay and *in vivo*.

The loss of filopodia and formation of veils or lamellipodia is associated with DC maturation and is thought to allow their rapid migration into secondary lymphoid organs (Burridge and Wennerberg, 2004; Calle et al., 2004b; Pollard and Borisy, 2003). The formation of protrusions at the leading edge of DC during migration is controlled by the small GTPases Rac and Cdc42 (Swetman et al., 2002). In detail, Cdc42 activity induces filopodia in immature DC, while Rac activity induces the loss of filopodia and formation of lamellipodia upon maturation (Burns et al., 2004). Generally small GTPases cycle between a GTP-bound active form and a GDP-bound inactive form. When bound to GTP they interact with their downstream targets, which include protein kinases, activators of actin polymerization as well as adaptor proteins. To analyze whether the observed increased migration of FHL2-/- BMDC was due to increased Rac1 activation, we determined the amount of Rac-GTP in immature wt and FHL2-/- BMDC by an ELISA based Rac1 activation assay. We found a significantly higher amount of active Rac1 in FHL2-/- BMDC compared to wt BMDC (Fig. 3.7 C), indicating that in FHL2-/- BMDC deregulated control of the Rac GTPase is responsible for the lamellipodia formation observed leading to migratory changes.

Rho-kinase, an effector of the small GTP-binding protein Rho, plays an important role in various cellular functions including vascular smooth muscle contraction, proliferation, and migration as well as inflammatory cell mobility (Oka et al., 2007). In addition, FHL2 is known to translocate into the nucleus in RhoA-dependent manner (Muller et al., 2002). Therefore we wanted to know whether Rho is involved in the accelerated migration of FHL2-/- BMDC. To address this question, we blocked Rho with several inhibitors. Y27632 is a potent, ATP-competitive inhibitor of Rho-associated protein kinases including p160ROCK and ROCK-II (Darenfed et al., 2007; Ishizaki et al., 2000). Fasudil is a potent inhibitor of Rho-associated kinase II and additionally inhibits protein kinase C-related kinase 2, mitogen- and stress-activated protein kinase, and mitogen activated protein kinase-activated protein kinase 1b (Huentelman et al., 2009). CCG-1423 is a specific inhibitor of Rho pathway-mediated signaling and activation of serum response factor (SRF) transcription (Evelyn et al., 2007).

Wt and FHL2-/- BMDC were incubated together with these inhibitors during the migration towards CCL19 in a Transwell. Y27632 did not change migratory behavior of wt and FHL2-/- BMDC (Fig. 3.8 A). Fasudil and CCG-1423 seem to have a slight effect on the migration speed of wt and FHL2-/- (Fig. 3.8 B), but diminished migration level to the same extent. Also another group concluded that the Rho family GTPases Rac1 and Rac2 but not Rho itself control the formation of dendrites in mature DCs, their polarized short-range migration toward T cells, and T cell priming (Benvenuti et al., 2004).

So, we can assume FHL2 exhibits its function in BMDC independent of Rho signaling, but show higher amounts of activated Rac1, which is known to induce lammellipodia which is formed to a higher number in FHL-/- BMDC culture.

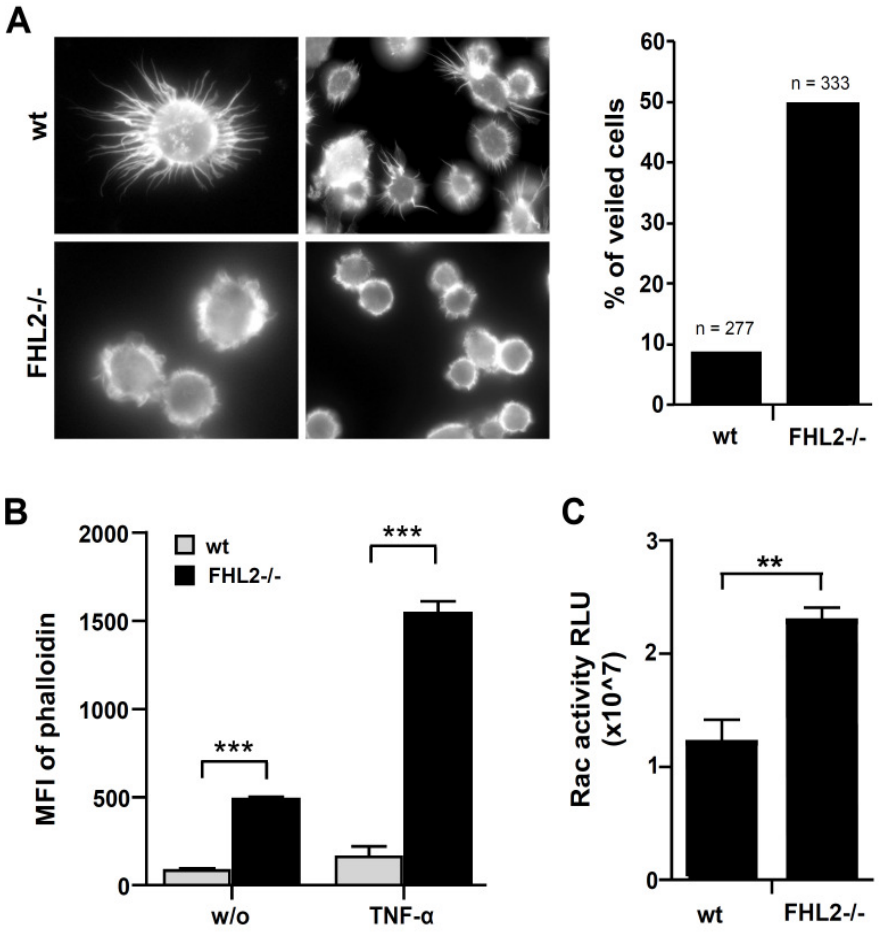


**Figure 3.7: FHL2-/- BMDC form more lamellipodia and have higher levels of Rac activation. (A)** At day 7 immature BMDC were left to adhere on a collagen-coated cover glass for 2h. Then cells were fixed, permeabilized and stained with phalloidin. Left panel: Pictures of wt and FHL2-/- BMDC (40x). Right panel: Percentage of small, veiled BMDC, lacking filopodia within the immature wt BMDC population compared to immature FHL2-/- BMDC. n = the amount of BMDC analyzed in each group. **(B)** On day 7, BMDC were cultured for further two days in medium containing 0.5% FCS. At the same time maturation was induced by 30ng/ml TNF-α. BMDC were stained intracellularly with Phalloidin$^{Alexa647}$ for 30min on ice. Here, the mean fluorescence intensity of Phalloidin gated on CD11c+ cells is depicted. **(C)** Day 7 immature BMDC were cultured in medium containing 0.5% FCS. On day 9 BMDC were completely serum starved for at least 4h and then lysed. The protein lysate was investigated for Rac activity in an ELISA coated with Rac-GTP-binding protein. Signal intensity was measured with a luminometer at 600nm, and Rac activity is shown as relative luminometric units (RLU). Values are depicted as mean and error bars +/-SEM. Statistical significance was calculated using a Student's t-test: NS not significant, *p≤ 0.05, **p≤0.01, ***p≤0.001. The data shown here is representative of three or more independent experiments.

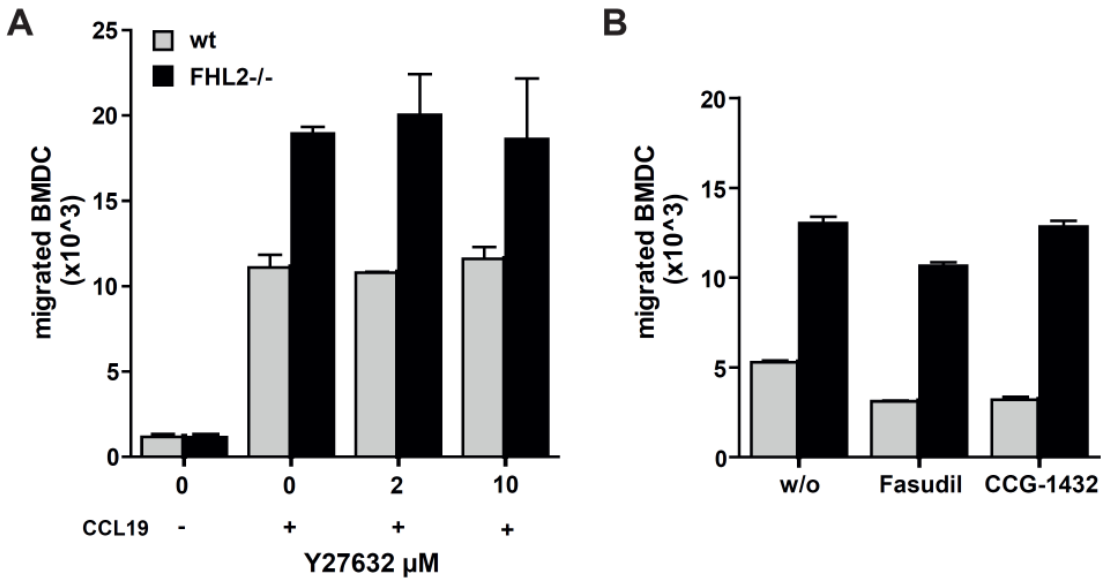


**Figure 3.8:** FHL-/- DC migration is independent of Rho signaling. **(A,B)** Wt and FHL2-/- BMDC were pre incubated with 2µM and 10µM Y27632 **(A),** 2.5µM Fasudil and 2mM CCG-1432 **(B)** for one hour in the insert and then transferred on a transwell. In the lower well 200ng/ml CCL19 was present as well as the previously mentioned inhibitors with the corresponding concentration.

### 3.5 FHL2 deficiency does not lead to spontaneous BMDC maturation

Both increased migration and the formation of lamellipodia are associated with DC maturation (Burns et al., 2004). FHL2 known to be a co-activator or –repressor of several transcription factors e.g. NF-kB it could govern maturation of BMDC. To determine whether in the absence of FHL2, leads to spontaneously maturation, the expression of costimulatory molecules and MHC class molecules as well as the production of pro-inflammatory cytokines by immature wt and FHL2-/- BMDC was examined. However, the expression levels of CD40, CD80, CD86, MHC class I and II (Fig. 3.9 A, upper two rows) did not differ between immature wt and FHL2-/- BMDC. Furthermore, these markers were upregulated to the same extent on both wt and FHL2-/- BMDC by incubation with LPS or TNF-α (Fig. 3.9 A, four lower two rows). BMDC treated with TNF-α showed overall higher expression levels compared to LPS stimulation, which have been observed by other groups (Landi et al., 2010).

Also the ability to produce IL-12 and TNF-α at basal levels did not differ between wt and FHL2-/- BMDC (Fig. 3.9 B), indicating that FHL2-/-BMDC did not exist in a more mature state. As a positive control, we incubated BMDC with LPS, because it is known that LPS is a potent stimulator of IL-12 and TNF-α

production via TLR (Brightbill et al., 1999; Dumitru et al., 2000). Here, incubation with LPS induced the production of IL-12 and TNF-α to about 35% in wt and FHL2-/- BMDC. But also there we could not see a difference in cytokine production after LPS stimulation between wt and FHL2-/- BMDC. Incubation of BMDC with TNF-α did not have an effect on cytokine secretion. Together, these data show that the enhanced migratory capacity towards CCL19 of FHL2-/- BMDC is associated with the formation of lamellipodia, but does not correlate to their maturation status.

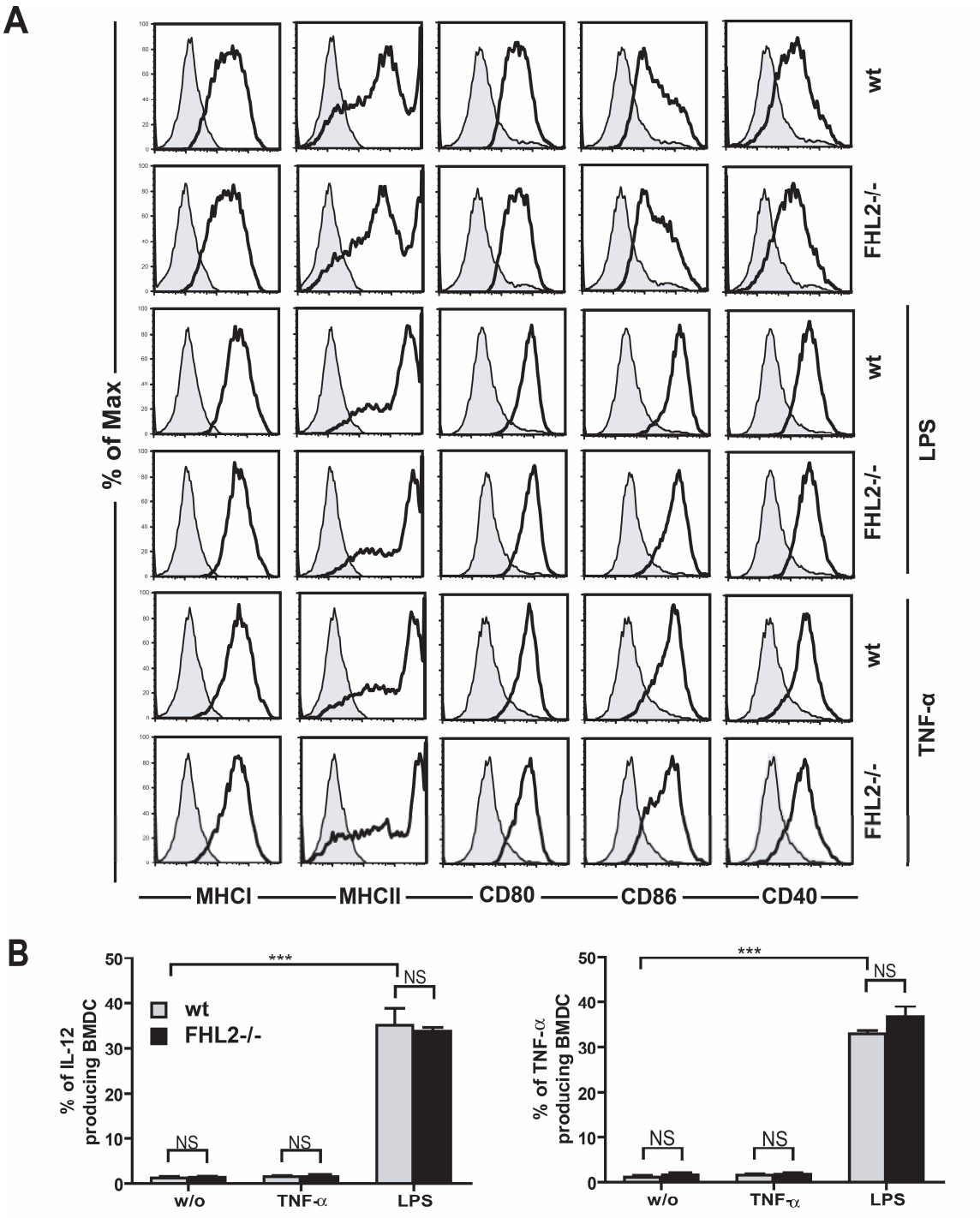


**Figure 3.9: FHL2-/- BMDC are not constitutively mature. (A)** Immature and mature wt and FHL2-/- day 7 BMDC were stained for the maturation markers CD40, CD80, CD86, MHC class I and II. Black open histograms: specific Ab staining, grey filled histograms: isotype control. **(B)** Untreated and LPS matured wt and FHL2-/- day 7 BMDC were incubated for 5h with Monensin and Brefeldin A, and stained intracellularly with Abs against IL-12 and TNF-α, gated on CD11c+ cells. The percentage of BMDC producing IL-12 and TNF-α is shown. Values are depicted as mean and error bars +/-SEM. Statistical significance was calculated using a Student's t-test: NS not significant, *p≤ 0.05, **p≤0.01, ***p≤0.001. The data shown here is representative of three or more independent experiments.

## 3.6 Antigen uptake and presentation in BMDC are not influenced by FHL2

Antigen uptake by DCs is essential for the presentation of antigens by MHC molecules to T cells in the LN in order to evoke an efficient immune response. Immature DCs endocytose avidly through a variety of mechanisms, including 'nonspecific' uptake by constitutive macropinocytosis and 'specific' uptake via receptor-mediated endocytosis and phagocytosis (Trombetta and Mellman, 2005). The exact mechanism of antigen uptake is not completely understood, but it is known that actin and its regulation by Rho family GTPases play important roles in mediating phagocytosis and macropinocytosis. For example, macropinocytosis involves the extension of membrane ruffles, which requires polymerization and reorganization of actin (Caron and Hall, 1998). Rac has an important role in the constitutive formation of macropinosomes in DCs but may be required downstream of membrane ruffling (Nobes and Marsh, 2000; West et al., 2000). DCs developmentally regulate endocytosis at least in part by controlling levels of activated Cdc42 (Garrett et al., 2000). We know from our own observations that loss of FHL2 in BMDC leads to increased migration probably due to higher amounts of activated Rac which causes differential organization of actin cytoskeleton. Thus, we thought that also loss of FHL2 might affect antigen uptake in BMDC.

We, therefore, compared antigen uptake by immature wt and FHL2-/- BMDC, and as model antigens we used OVA and Dextran. Both are endocytosed by two different ways: OVA is endocytosed receptor mediated (Kindberg et al., 1990), and Dextran is internalized by macropinocytosis (West et al., 1999). To this end, BMDC were incubated with fluorescently labeled Dextran or OVA for 30min at 37°C or as a negative control 4°C, and fluorescence intensity was analyzed in flow cytometry (Fig. 3.10 A). When BMDC were incubated with $OVA^{Alexa647}$ at 4°C (dashed lines) the histogram overlapped with unstained control (grey filled) which means they were not able to take up antigen. This changed dramatically when the BMDC were incubated with $OVA^{Alexa647}$ at 37°C, where a big shift to the right could be seen. When incubated with $Dextran^{FITC}$ at 4°C, there was a small shift compared to unstained control, meaning that they still endocytose antigen unspecifically. This shift was amplified when BMDC were incubated at 37°C. However, we did not observe any significant

differences in case of incubation with OVA and Dextran between wt and FHL2-/- BMDC, indicating that FHL2 does not influence antigen uptake in BMDC.

After engulfment of antigen by DC, it undergoes through a lot of changes to efficiently equip them as an APC. When the DC arrived in the LN and comes into contact with a lymphocyte, a so called immunological synapse is formed. It consists of a central cluster of T cell receptors (TCRs) interacting with MHC molecules on DC surrounded by a ring of adhesion molecules. There are active changes taking place in the T cell cytoskeleton i.e. accumulation of F-actin and other cytoskeletal proteins in the T cell at the contact point, which result in the dynamic clustering of T cell surface receptors and signaling molecules at the interface with the APC (Grakoui et al., 1999; Pardi et al., 1992). But also DC actin cytoskeletal rearrangement is critical for the clustering and activation of resting T cells, indicating an important role for the DC cytoskeleton in the establishment of the immunological synapse (Al-Alwan et al., 2003; Al-Alwan et al., 2001). Actin reorganization is usually conducted by members of the small Rho GTPases. Constitutive activation of Rho GTPases in DC differentially modifies a lot of DC functions like adherence, chemotaxis, endocytosis, and also antigen presentation (Ladwein and Rottner, 2008; Shurin et al., 2005). Although we know that loss of FHL2 has an impact on the composition of the cytoskeleton and migration, but not on other processes like maturation and antigen uptake as discussed in the previous sections. Still we were very interesting to find out if this holds true for antigen presentation. We already know that wt and FHL2-/- BMDC provide the same amount and kind of signals with respect to cytokine production, co-stimulatory molecules and antigen dose, so a difference could only because of a differential organized cytoskeleton.
To test whether the loss of FHL2 affects antigen presentation by DC, we performed co-culture assays with BMDCs and T cells. We isolated T cells out of the spleen of OT-I and OT-II transgenic mice, which can specifically recognize the OVA peptide in the context of an MHC I and MHC II molecule, respectively. If a T cell has recognized its specific antigen on an APC, it undergoes a huge transition and amongst enters the mitotic cycle to augment its number for effective fight against the invading organism. This behavior by T cells serves as a helpful measure to check for efficient antigen presentation by BMDC.

Therefore, they were stained with CFSE and added to FHL2-/- and wt BMDC, which have been pulsed before with whole OVA protein for 2hrs (Fig. 3.10 B). CFSE can be used to monitor lymphocyte proliferation due to the progressive halving of CFSE fluorescence within daughter cells following each cell division as seen in flow cytometer (Lyons and Parish, 1994). When there was no OVA present, both OT-I and OT-II T cells did not respond to the DC as seen by a single and very bright population (grey filled). There was no difference in the proliferation profile of both OT-I and OT-II T cells stimulated by FHL2-/- or wt BMDC, but in both cases a higher proliferation index of OT-II could be observed.

Antigen binding to the TCR stimulates the secretion of IL-2, and the expression of IL-2 receptors (IL-2R). The IL-2/IL-2R interaction then stimulates the growth, differentiation and survival of antigen selected T cells via the activation of the expression of specific genes. They produce high amounts of IL-2, which works in an autocrine loop to drive them into mitosis (Malek and Castro, 2010). Wt and FHL2-/- BMDC were incubated with various concentrations of OVA, OT-I and OT-II T cells were then added and as a read out for efficient antigen recognition by T cells IL-2 release in the supernatant was assessed after 24h by ELISA (Fig. 3.10 C and D). BMDCs do not tend to produce IL-2 by themselves as seen when no OVA was present, therefore the IL-2 originated exclusively from T cells. At lower OVA concentrations FHL2-/- BMDC induced slightly higher IL-2 production by OT-I and OT-II T-cells, however these differences were not statistically significant. Also, at higher OVA concentration, there was no difference in the production of IL-2 induced by wt and FHL2-/- BMDC. Together, based on these data we concluded that although FHL2 influences the conformation of the cytoskeleton and subsequently the migratory behavior of DC it does not influence antigen uptake or presentation or T cell activation.

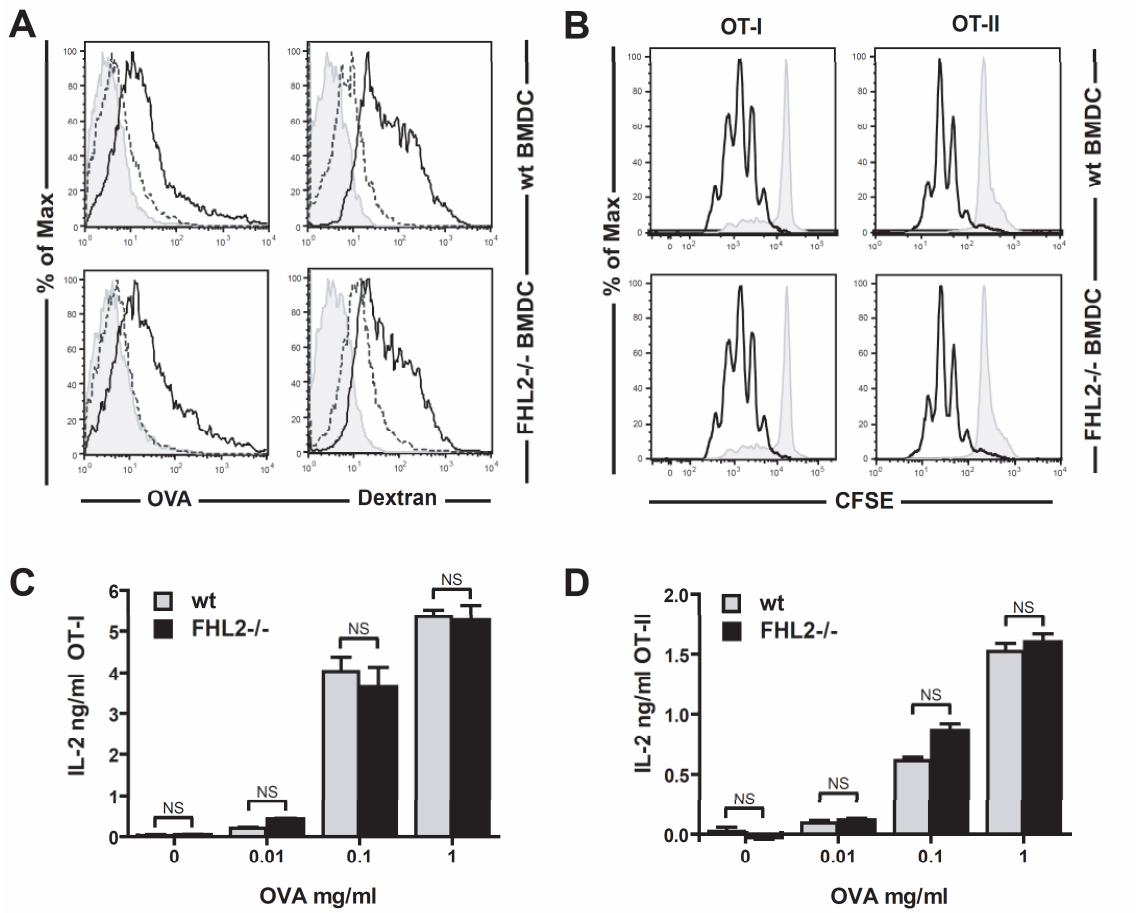


**Figure 3.10: Antigen uptake and presentation via MHCI and MHCII is not altered in FHL2-/- BMDC. (A)** Day 7 Wt and FHL2-/- BMDC were harvested and $2x10^5$ BMDC were left to adhere for 1h. BMDC were incubated with 200µg/ml $Dextran^{FITC}$, 2µg/ml OVA or medium only at 37°C or as a negative control at 4°C. After 30min cells were harvested and analyzed by flow cytometry. Histograms depict cells gated on CD11c. Black lines: incubation with $Dextran^{FITC}$ or $OVA^{Alexa647}$ at 37°C, dashed lines: 4°C control, grey filled: medium only. **(B-D)** Day 7 wt and FHL2-/- CD11c+ BMDC were either loaded with OVA or left untreated and were then co-cultured with CFSE-labeled (**B**) or unlabeled (**C,D**) CD8+ OT-I T cells or CD4+ OT-II T cells. **(B)** $4x10^5$ BMDC were incubated for two hours with 1mg/ml OVA or medium alone. Proliferation of CFSE labeled CD8+ as well as CD4+ OVA-specific T cells were checked 72h later by flow cytometry by gating on CD8+ or CD4+ cells. Black open histograms: T cells co-cultured on BMDC incubated with OVA. Grey filled histograms: T cells co-cultured on BMDC without OVA. **(C,D)** After 24h of co-culture the supernatant was assayed by ELISA for IL-2. Grey bars: IL-2 production after incubation with wt BMDC, black bars: FHL2-/- BMDC. Values are depicted as mean and error bars +/-SEM. Statistical significance was calculated using a Student's T-test: NS not significant, *p≤ 0.05, **p≤0.01, ***p≤0.001. The data shown here is representative of three or more independent experiments.

## 3.7 Sphingosine-1-phosphate receptor 1 is upregulated in FHL2-/- BMDC

Besides the CCR7 ligands CCL19 and CCL21, the lysophospholipid S1P also plays an important role in DC migration and positioning in the LN (Czeloth et al., 2007). The S1P receptors S1PR1-4 are differentially expressed depending on the maturation status of DC (Czeloth et al., 2005) and this influences their migratory behavior. We therefore analyzed the expression pattern of the S1PR1-4 in immature and mature wt BMDC and FHL2-/- BMDC by qRT-PCR. Consistent with previous reports (Czeloth et al., 2005), we found that after maturation with TNF-α S1PR1 and S1PR3 mRNA levels were upregulated in wt BMDC, whereas S1PR4 mRNA levels were diminished and S1PR2 mRNA levels were unchanged (Fig. 3.11). Interestingly, in both immature and mature FHL2-/- BMDC we found significantly higher levels of S1PR1 mRNA (Fig. 3.11, upper left panel), whereas S1PR2-4 mRNA levels did not differ significantly from the levels in the wild type BMDC. As ligation of the S1PR1 by S1P in DC is associated with migration initiation or enhancement (Czeloth et al., 2005), these data suggest that FHL2 regulates DC migration via inhibiting the expression of S1PR1.

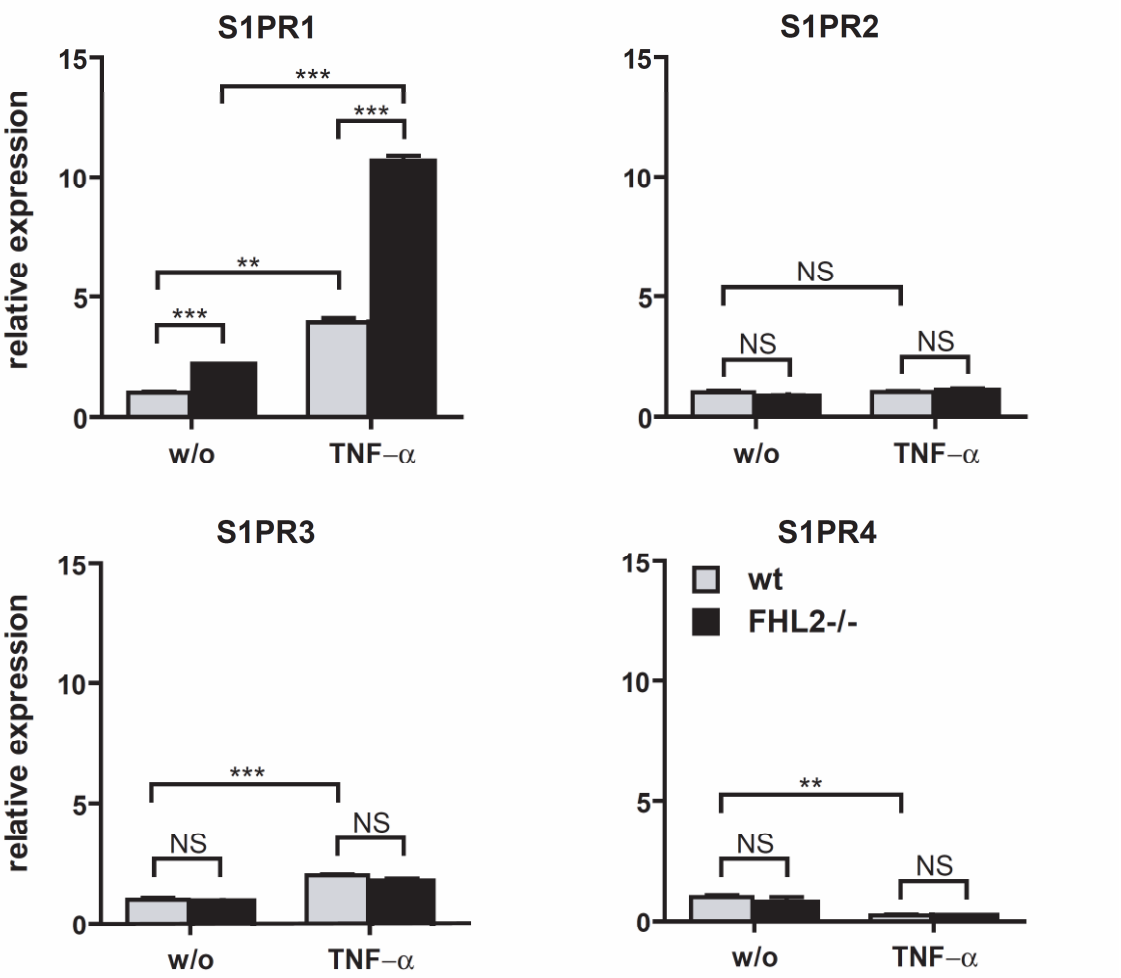


**Figure 3.11: FHL2-/- BMDC show high expression levels of S1PR1.** mRNA was isolated from day 7 immature or day 9 TNF-α-matured wt and FHL2-/- BMDC. The expression of S1PR1-4 was determined by quantitative RT-PCR. For calculation the ΔΔCT method was applied by normalizing to the constitutively expressed housekeeper 18s RNA. Grey bars: wt BMDC, black bars: FHL2-/- BMDC. Values are depicted as mean and error bars +/-SEM. Statistical significance was calculated using a Student's t-test: NS not significant, *p≤ 0.05, **p≤0.01, ***p≤0.001. The data shown here is representative of three or more independent experiments.

## 3.8 Downregulation of S1PR1 using siRNA and antagonist abrogates the increased migratory speed of FHL2-/- BMDC

To investigate whether upregulation of S1PR1 in FHL2-/- BMDC functions as an accelerating receptor (Sugimoto et al., 2003), leading to the observed increased migration of FHL2-/- BMDC, we suppressed expression of S1PR1 by transfecting both immature wt and FHL2-/- BMDC with S1PR1-specific or unspecific control siRNA (scrambled). As expected, in FHL2-/- BMDC transfected with control siRNA, S1PR1 mRNA levels were significantly higher

compared to wt BMDC transfected with control siRNA (Fig. 3.12 A). Furthermore, in both wt and FHL2-/- BMDC we could successfully knock-down S1PR1 mRNA levels by transfection with S1PR1-specific siRNA. In wt BMDC this led to 72 % and in FHL2-/- BMDC to 75% knock-down (Fig. 3.12 B). Now wt and FHL2-/- showed similar expression levels of S1PR1. Knock-down of S1PR1 in FHL2-/- BMDC significantly reduced their migratory rate to about half of the FHL2-/- BMDC transfected with control siRNA, which equaled the migratory rate of wt BMDC (Fig 3.12 B). Interestingly, although some S1PR1 knock-down was achieved in wt BMDC, this did not influence their migratory rate.

In a second approach, we used the selective S1PR1 antagonist SEW2871 (Sanna et al., 2004) in various concentration, which leads to receptor internalization, to inhibit S1PR1 function in FHL2-/- BMDC (Fig. 3.12 C, upper panel). Again, the increased migratory rate in FHL2-/- BMDC was significantly reduced by S1PR1 inhibition at already low concentrations (0.1µM). At very high concentrations (1µM), it seemed that also migration of wt BMDC was slightly reduced, but not as much as in FHL2-/- BMDC. Importantly, migratory speed of FHL2-/- BMDC was suppressed to levels of wt BMDC.

In addition, we stained the BMDC incubated with SEW8271 with CD86 and MHCII (Fig. 3.12 C, lower panel) to be sure that SEW2871 does not influence the maturation of BMDC and this might change their migratory behavior. Indeed, in this experiment the fraction of the CD86 and MHCII highly positive cells ranged only between 12.51 and 15.10% in all treatments, which was not enough to influence their migratory behavior.

In summary, these data indicate that in FHL2-/- BMDC, repression of S1PR1 is lost leading to its overexpression, and that signaling via S1PR1 is responsible for the increased migratory phenotype of FHL2-/- BMDC.

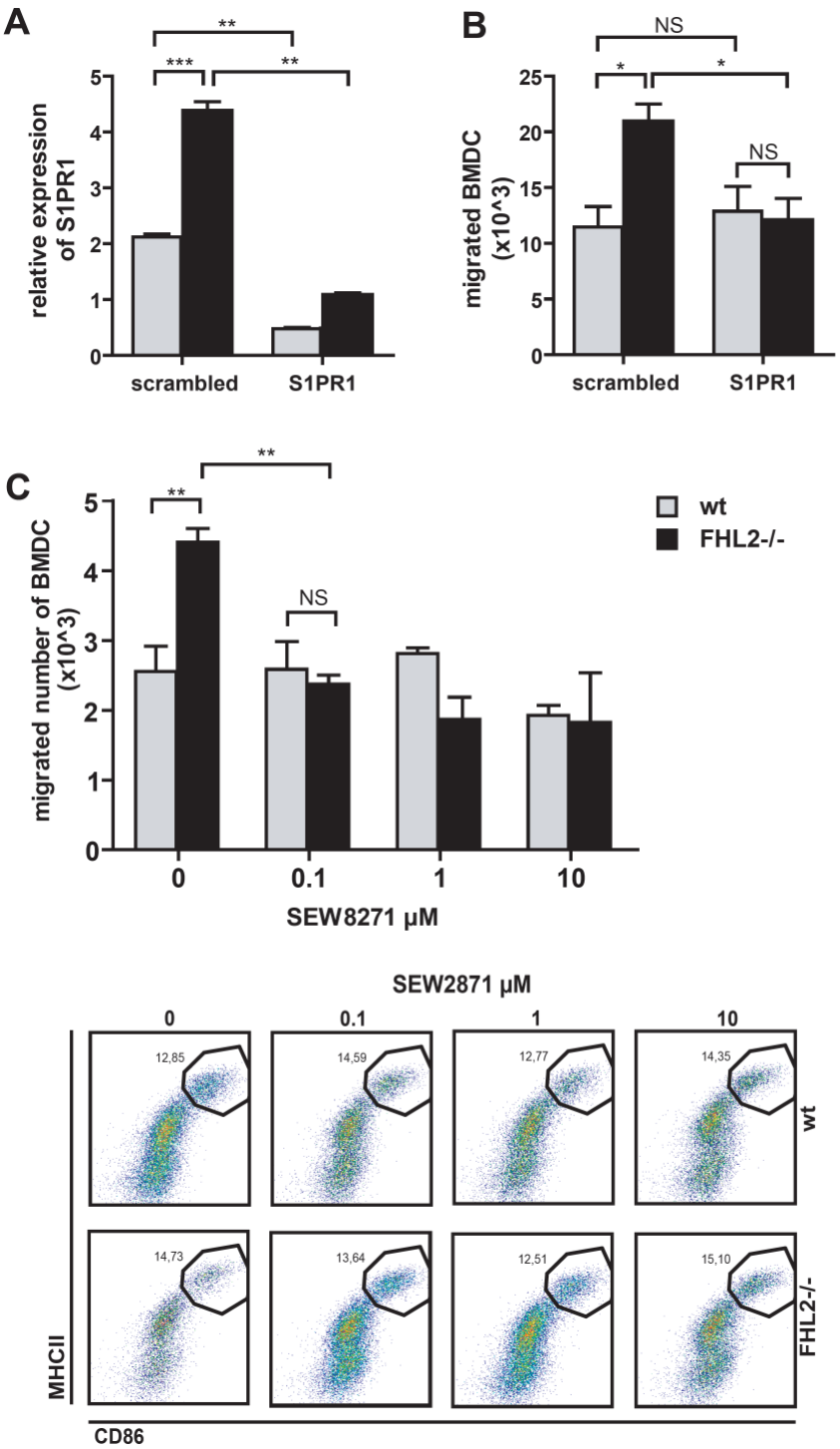


**Figure 3.12: Enhanced migration of FHL2-/- BMDC is due to higher levels of S1PR1. (A,B)** $4x10^6$ day 7 wt and FHL2-/- BMDC were electroporated with either siRNA targeted against S1PR1 or non targeting siRNA. **(A)** Two days later, RNA was isolated from electroporated BMDC and converted to cDNA. The knock down of S1PR1 was quantified by RT-PCR. **(B)** In parallel, the electroporated BMDC were analyzed for their migratory behavior in a Transwell assay. **(C,D)** Day 7 wt and FHL2-/- BMDC were incubated for 16 h with 0, 0.1, 1 and 10µM SEW2871, harvested, analyzed for their migratory behavior in a Transwell assay **(C)**, and in parallel for CD86 and MHCII expression by flow cytometry **(D)**. Values are depicted as mean and error bars +/-SEM. Statistical significance was calculated using a Student's t-test: NS not significant, *p≤ 0.05, **p≤0.01, ***p≤0.001. The data shown here is representative of three or more independent experiments.

## 3.9 External addition of S1P does not influence antigen uptake and migration of wt BMDC

Knowing that S1PR1 is increased in FHL2-/- BMDC, which most likely leads to enhanced chemotaxis of FHL2-/- BMDC. We were interested in what way the ligand for the receptor namely S1P might have an influence on other DC function like antigen uptake and migration. Ligation of S1PR1 by S1P induces BMDC migration towards CCL19 to a small extent in a transwell assay. This small increase is probably due to the fact that even without the external addition of S1P to the culture medium, there is already S1P in the medium.

Wt BMDCs were preincubated with S1P and then their migration was analyzed in a transwell assay, while S1P was still present during the migration (Fig. 3.13 B). External addition of S1P did not change their migratory behavior. In addition to migration, we also wanted to check, whether S1P might impact BMDC in a functional assay, i.e. antigen uptake. Therefore, wt and FHL2-/- BMDC were preincubated with S1P. The ability to take up antigen was assayed as explained in section 3.6. We could not observe a difference between wt and FHL2-/- BMDC in their ability to take up antigen, if incubated with S1P or not (Fig. 3.13 A). Since we could not observe any difference regarding their capability to take up antigen, we assume that wt and FHL2-/- BMDC after incubation with S1P would consequently do not show a difference in presenting antigen. This is the reason why we did not test, whether addition of S1P has an effect on antigen presentation.

Thus, external addition of S1P did not change the phenotypes or functions of wt and FHL2-/- BMDC.

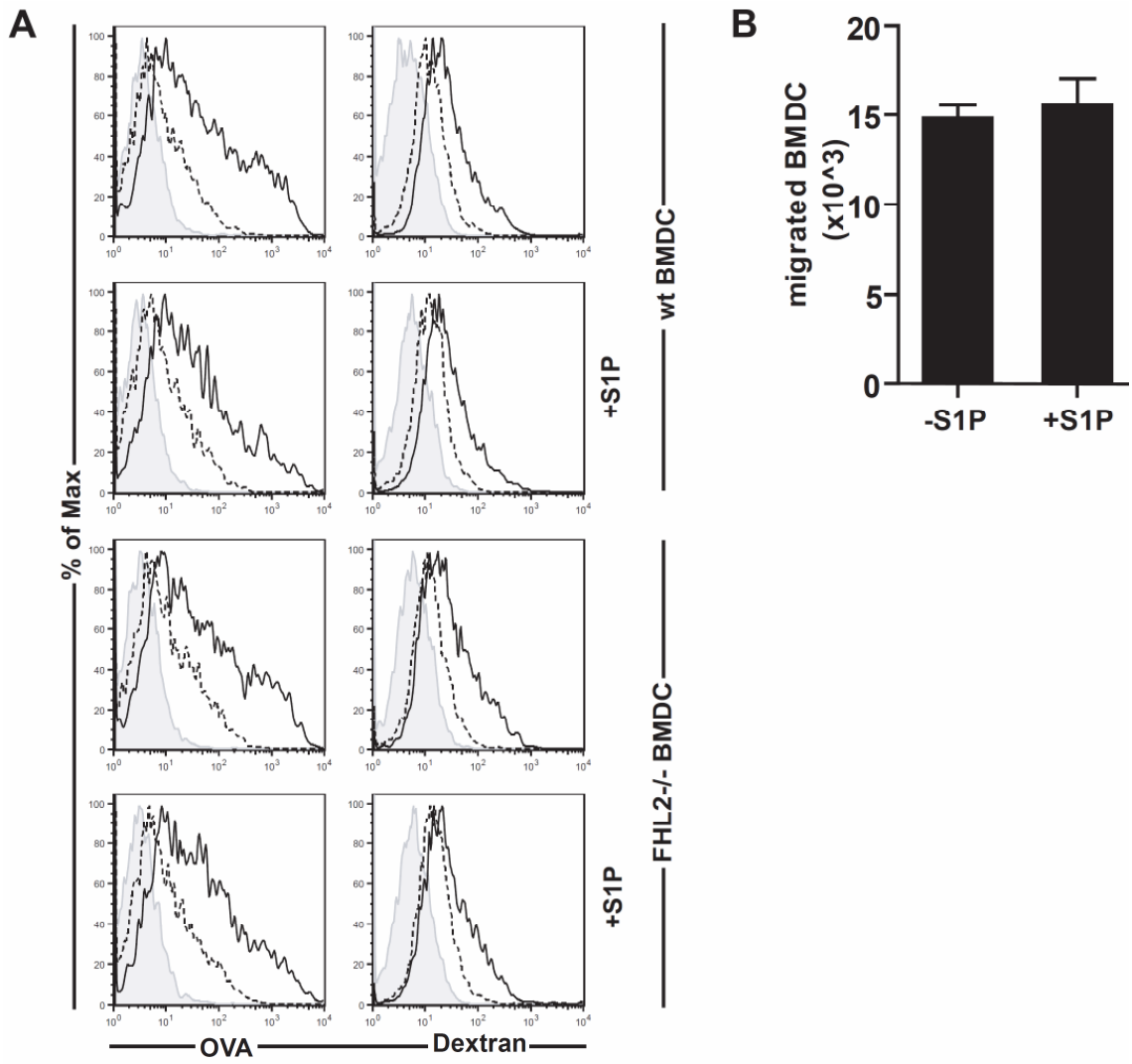


**Figure 3.13: Migration and antigen uptake is not changed after incubation with S1P. (A,B)** Day 7 BMDCs were incubated for 1h with 100nM S1P. Antigen uptake **(A)** and migration **(B)** was determined as described before, respectively. Values are depicted as mean and error bars +/-SEM. Statistical significance was calculated using a Student's t-test: NS not significant, *p≤ 0.05, **p≤0.01, ***p≤0.001. The data shown here is representative of three or more independent experiments.

# 4. Discussion

DC reside in the periphery, where they continuously sample their environment for antigen, which they take up, process and display as peptides in the context of MHC class molecules and present to T cells in the LN. During an infection, DC encounter danger signals in the form of a distinct and highly conserved structure of a pathogen that will trigger PRRs to undergo a drastic change of their phenotype which ultimately will equip them as efficient APCs. They upregulate costimulatory and MHC molecules and increase production of inflammatory cytokines, which are very important for T cells to turn into activated effector T cells. They also change their chemokine receptor profile, i.e. they highly upregulate CCR7 receptor and concomitantly downregulate all other chemokine receptors, which aid the DC to find its way to the draining LN where T and B cell home, which in turn secrete the ligand for CCR7, CCL19 and CCL21. These chemokines are expressed by peripheral lymphatic endothelial cells as well as LN stroma cells and guide DCs to downstream LNs (MartIn-Fontecha et al., 2003). This transition is accompanied by a huge change of their morphology of the actin cytoskeleton, which enable them to migrate very efficiently to the LN to interact with T cells. Given this complex life cycle, the ability of DCs and their progenitors to migrate throughout the body is a critical aspect of their immunological function. Thus, migration is a very important and critical part of DC function in order to exert their function as a professional APC and any misbalance might result in a different outcome of the immune response which might be detrimental for the organism (Alvarez et al., 2008).

FHL2-/- mice display wound healing disturbance due to defective migration of fibroblasts (Wixler et al., 2007) and collagen metabolism (Kirfel et al., 2008). Nuclear expression of FHL2, high Gleason score and grade correlate with relapse during follow-up in prostate cancer (Kahl et al., 2006), and it is highly expressed in primary and metastatic colon cancer but not in normal tissues (Zhang et al., 2010). Furthermore, FHL2 is known to associate with actin cytoskeleton components (Li et al., 2001), and might influence the morphology of the cell (Bai et al., 2005).

These observations made it worth to study the role of FHL2 as a regulator of DC migration. Migration of DC is very important to fulfill their function as an APC to elicit a successful immune response during the crosstalk of T cell. For example, in a different mouse model, deficient of RBP-J (Feng et al., 2010), authors could observe the detrimental effect on tumor formation, when DCs show inefficient migration. The RBP-J deficient DCs expressed lower MHCII, CD80, CD86, and CCR7 resulting in inefficient DC migration and T cell activation *in vitro* and *in vivo*, so T cells did not possess efficient cytotoxicity against tumor cells.

## 4.1 FHL2 is expressed in wt BMDC and localized at the membrane in mature DC after stimulation with CCL19

First of all, we were interested in the localization of FHL2 within wt BMDC (Fig. 3.2 A), because depending on the position of FHL2 within a cell it can exert two different mechanistically effects. In addition, we treated BMDC with LPS and CCL19, because both can influence the morphology and migration of DC which might be controlled by FHL2. In the immature culture, DCs showing an immature morphology characterized by filopodia formation FHL2 is located in the nucleus. Their large cytoplasm has filopodia structure and long dendrites, which are very helpful in capturing antigen (Svitkina et al., 2003). Stimulation of DC with LPS leads via TLR4 signaling to maturation of DC with a change in morphology to a smaller, veiled phenotype expressing lamellipodia, but still in these cells FHL2 remained in the nucleus. In addition to locomotion, CCR7 controls several other factors of DC function: CCL19 induces the apparition of dendritic protrusions in DC (Yanagawa and Onoe, 2002), indicating that CCR7 can regulate the cytoarchitecture probably by controlling the actin cytoskeleton. The same authors reported that the stimulation of CCR7 with ligands CCL19 and CCL21 positively regulates the rate of endocytosis of the mature DCs with concomitant up-regulation of Cdc42 and Rac activities (Yanagawa and Onoe, 2003). The same observation holds true for CCL19 treatment in our BMDC culture in combination with LPS treatment, where also the cytoarchitecture and localization of FHL2 changed dramatically. Now, FHL2 cannot be seen in the nucleus anymore, instead can be found at the membrane. FHL2 is known to be

associated with focal adhesions which are at the cell membrane making attachment to ECM, but since DC are devoid of focal adhesion, we would surmise these are podosomes that FHL2 rather associates to in DC. In the mature fraction of BMDC, FHL2 seems to move after CCL19 ligand binding out of the nucleus to the cell membrane, where it plays a different function, necessary for a DC to migrate to the LN after antigen uptake.

Before we focus on our main issue the loss of FHL2 in DC migration in FHL2 deficient mice to better answer our question how FHL2 impacts DC migration, we checked how FHL2 was expressed in wt BMDC and wanted to be sure that FHL2 is missing in FHL2 deficient BMDC. By RT-PCR (Fig. 3.2 B) as well as Western Blot (Fig. 3.2 C) we could show that FHL2 is lost in the KO mouse. FHL2 is completely lost in several organs like heart, colon, lung, muscle tissue and BMDC from KO mice shown by RT-PCR. Low levels expression of FHL2 in wt BMDC and lung compared to heart, colon and muscle can be observed on mRNA level.

Western Blot analysis showed expression of FHL2 in heart tissue of wt mouse and absence of FHL2 in KO mouse proving that FHL2 is not present in the KO mouse. However, Western Blot failed to detect FHL2 in wt BMDC. There are possible explanations: First of all, FHL2 is highly expressed in heart tissue (Chan et al., 1998; Genini et al., 1997) and FHL2 is expressed in BMDC at lower levels compared to other organs as shown by RT-PCR which makes detection difficult. Wixler et al. (2000) were not able to detect FHL2 reliably in various other cell types or tissues other than heart. They reasoned that FHL2 exhibits a different conformational state under experimental conditions so that the antibody cannot bind. They also stated that binding of FHL2 to integrins which are incorporated in the cell membrane is very tight. After lysis of BMDC to get access to the proteins, the whole sample is centrifuged to remove cell debris. So, FHL2 could still be bound to the cell membrane, which is not loaded on SDS-PAGE. For these reasons we concentrated FHL2 by IP with a polyclonal antibody in wt and FHL2-/- lysate of BMDC (Fig. 3.2 D) and loaded the enriched FHL2 on SDS-PAGE gel. Here we could detect FHL2 on protein level in wt BMDC, which was lost in FHL2-/- DC. So, FHL2 is expressed in wt

DC, but only in very small amounts, which is still sufficient leading to a different phenotype.

## 4.2 Increased migration of FHL2-/- is not due to different expression levels of CCR7

We answered the migration issue in a first experiment by timelapse microscopy. We observed that FHL2-/- deficient BMDC exhibited significant higher migratory speed on collagen coated surface than wt BMDC towards a CCL19 chemokine gradient (Fig. 3.3 A). Moreover, we could demonstrate that FHL2-/- BMDC travel with enhanced directionality and persistence (Fig.3.3 B) compared to wt BMDC. The difference in migratory speed between FHL2-/- and wt BMDC shown by timelapse microscopy could be confirmed by transwell assay towards CCL19 (Fig. 3.4 A).

On possible explanation for observed enhanced migratory phenotype of BMDC lacking FHL2 is the upregulation of the CCR7 receptor, which is highly expressed in mature and fast migrating cells. Furthermore in mature DC ligand binding of CCL19 made FHL2 translocate from the nucleus to occur at the cell membrane (Fig. 3.2 A). CCR7 is not only the guide for the DC, it is also the accelerator for DC migration (Dieu et al., 1998; Sozzani et al., 1998). CCR7 regulates in DC two signaling modules, one formed by $G_i$ and a specific hierarchy of MAPK family members that regulates chemotaxis and another formed by Rho/Pyk2/cofilin that regulates the migratory speed of DCs. Therefore, the stimulation of CCR7 by its ligand leads to an increase in the activity of these signaling molecules and consequently to an increase in the migratory speed of the cells. The stimulation by CCR7 ligands of the intrinsic migratory speed axis behaves as an accelerator system that increases the speed at which DCs move toward the maximum concentrations of CCL19 and CCL21. In the *in vivo* context, this regulatory process would have the obvious advantage of more rapidly directing DCs to LN regions. FHL2 could be involved in this process acting as a co-activator of transcription factor of CCR7. Since we could not see any differences in CCR7 expression levels (Fig. 3.5 A), it does not seem that FHL2 acting as transcriptional co-activator has an influence on the expression levels of CCR7. So, all the previously described potential roles of

CCR7 increasing DC migration does not take place in our FHL2-/- model. So, another mechanism must be responsible for it. Even treatment with LPS and TNF-α (Fig. 3.5 B) could not change expression levels of CCR7 between wt and FHL2-/- BMDC, although the overall expression level was increased compared to immature DC.

The passage of leukocytes through basement membranes involves proteolytic degradation of extracellular matrix (ECM) components executed by focalized proteolysis where matrix metalloproteinases (MMPs) are engaged. They were demonstrated to degrade and remodel numerous ECM components (Abecassis et al., 2003; Park et al., 2008), and thereby being important for the regulation of cellular functions, e.g. migration (Di Girolamo et al., 2006; Ratzinger et al., 2002). ADAM-17 and FHL2 colocalize with the actin-based cytoskeleton that suggests that FHL2 might have a role in the regulation of ADAM-17 (Canault et al., 2006); and FHL2-/- mesenchymal stem cells show perturbed organization of ECM (Park et al., 2008). Maybe this would change the outcome for the migration of FHL2-/- BMDC *in vivo* compared to the *in vitro* situation, where we could see enhanced migration of FHL-/- BMDC. We could verify increased migratory speed of BMDC deficient of FHL2 *in vivo* by injection of unstimulated or TNF-α stimulated FHL2-/- and wt BMDC into the footpad of wt mice (Fig. 3.6 A). So, in our mouse model, *in vivo* migration showed the same result as *in vitro*, i.e. FHL2-/- BMDC migrate faster than wt BMDC. It seems like that FHL2-/- BMDCs do not alter their *in vivo* environment by e.g. ECM remodeling as proposed before in such a way that FHL2-/- BMDC behave complete differently with respect to migration: They were not slower or showed similar migration level. Maybe it had an effect *in vivo*, so that migration was amplified, but it is really hard to compare. Interestingly, the difference between wt and FHL2-/- BMDC was bigger when treated with TNF-α than not stimulated. Somehow, TNF-α amplified the phenotypical effects on FHL-/- BMDC. ADAM-17 mediates release of TNF from the cell surface (Black et al., 1997). Less ADAM-17 was detected at the surface of wt mouse macrophages compared to FHL2 deficient macrophages. Maybe, there is a connection between TNF-α signaling and FHL2 via ADAM-17. Although we never directly in one single experiment compared migratory velocities of immature and mature DCs *in vivo*, we would

expect that also here TNF-α matured DCs showed higher migration levels compared to immature DCs as determined by other groups (De Vries et al., 2003).

But maybe we were able to obtain more FHL2-/- BMDC from the LN, because FHL2 has an anti-apoptotic effect, which prevents BMDC deficient of FHL2 to die in contrast to wt BMDC. FHL2 is known to regulate the cell cycle (Martin et al., 2007), so it can trigger apoptosis (Scholl et al., 2000). In several different cell lines FHL2 inhibited growth *in vitro* (Amann et al., 2010; Ding et al., 2009), and in colon cancer cells it Inhibited tumorigenesis in nude mice (Wang et al., 2007). One other group (Labalette et al., 2008a; Labalette et al., 2008b) could even see the opposite effect: FHL2 deficiency triggers a broad change of the cell cycle program that is associated with down-regulation of several G(1)/S and G(2)/M cyclins, and DNA replication machinery, thus correlating with reduced cell proliferation. Nevertheless, we could neither see a beneficial or detrimental effect on cell viability, i.e. we could not see that FHL2 regulate these processes in DCs by determining the survival of wt and FHL2-/- *in vitro* by a MTT (Fig. 3.6 C). Overall, all these data indicate that FHL2-/- BMDC migrate faster than wt BMDC *in vivo*.

This is in contrast to observations made by several other groups, where loss of FHL2 leads to a defect in migration. In human glioblastoma cells FHL2 knockdown by short hairpin RNA inhibited cell proliferation and migration. Conversely, overexpression of FHL2 stimulated the proliferation, anchorage-independent growth, and migration of glioblastoma cells (Li et al., 2008). Also, FHL2 overexpression markedly accelerated cell migration, whereas FHL2 siRNA decreased SW480 cell invasion (Zhang et al., 2010). In these studies loss of FHL2 lead to impaired migration (Wixler et al., 2007), whereas our experiments or other groups (Labalette et al., 2010) observed accelerated cell migration. This can be explained by the fact that FHL2 associated cell migration is cell type specific due to intrinsic or external factors which varies in every environment. But there is a difference of leukocytes or DCs from other cell types with respect to the mode of migration. The most primitive and effective form of cell migration is amoeboid movement, which mimics features of the single-cell behavior of the amoeba. These cells use a fast ‘crawling’ type of movement that

is driven by short-lived and relatively weak interactions with the substrate, which ends up to move at high velocities (2–30 µm/min; Friedl et al., 1998). Amoeboid movement is carried out by hematopoietic stem cells, leukocytes and certain tumor cells. In contrast to cells that use amoeboid migration, mesenchymal cells accomplish the complete four-step migration sequence. In 3D tissues, mesenchymal cells adopt a spindle-shaped, fibroblast-like morphology, as characteristic for fibroblasts, myoblasts, single endothelial cells or sarcoma cells. The elongated morphology is dependent on integrin-mediated adhesion dynamics and the presence of high traction forces on both cell poles (Friedl, 2004).

Integrin adhesion receptors are heterodimeric glycoproteins which are composed of noncovalently associated α and β transmembrane subunits (Lad et al., 2007). Integrins play a very important role for cell migration, since ligand binding to integrins leads to integrin clustering and recruitment of actin filaments and signalling proteins to the cytoplasmic domain of integrins (Brakebusch and Fassler, 2003). FHL2 also interacts with several integrins (Samson et al., 2004; Wixler et al., 2000). It was demonstrated integrins are involved in DC migration (van Helden et al., 2006). This contradicts to murine leukocytes, where all integrins heterodimers were ablated and that functional integrins do not contribute to migration in three-dimensional environments (Lammermann et al., 2008). Instead, these cells migrate by the sole force of actin-network expansion, which promotes protrusive flowing of the leading edge. Therefore we did not check, if integrin signaling is involved in FHL2-/- BMDC migration. Although as determined in later conducted experiments: DCs without integrins could switch to a different migration mode (Quast et al., 2009; Renkawitz et al., 2009), and chemotactic DCs mechanically adapt to the adhesive properties of their substrate by switching between integrin-mediated and integrin-independent locomotion (Renkawitz et al., 2009).

## 4.3 FHL2-/- BMDC have more lamellipodia due to elevated levels of Rac1

After taking up antigen and PRR signaling has been triggered, DC go through a lot of changes converting them from a drinking cell to an highly efficient antigen presenting cell (Norbury, 2006). To fulfill this task they have to transport the antigen to the LN swiftly, therefore also the actin cytoskeleton will change dramatically. Since reorganization of the actin cytoskeleton is the basis for cellular migration (Mitchison and Cramer, 1996), the cytoskeletal actin conformation of FHL2-/- and wt BMDC was examined by immunofluorescent staining with phalloidin (Fig. 3.7 A). As discussed before in section 3.1 in a seven day DC culture there are already a number of DCs that have matured spontaneously. The number of DC showing a typical more mature phenotype with expanding veils and lamellipodia was significant higher in the DC culture derived from FHL2-/- mouse than wt DC. Thus, FHL2 has an impact of the reorganization of the actin cytoskeleton, which probably contributes to the enhanced migration speed of FHL2-/- BMDC. Binding of phalloidin to F-actin mirrors the amount of filamentous actin which is higher in fast migrating cells (Fukui et al., 2001). This was quantified by intracellular staining of phalloidin in flow cytometry where significant higher amounts of F-actin were present in FHL2-/- BMDC (Fig. 3.7 B). This difference was more distinctive after stimulation with TNF-α, which is reflected by the *in vivo* migration of wt and FHL2-/- BMDC to popliteal LN, where the difference was higher when stimulated with TNF-α. It seems that TNF-α does not lead to enhanced maturation of FHL2-/- but is able to enhance the migratory capacity of FHL2-/- DC and levels of filamentous actin. Thus TNF-α seems to turn on two independent pathways in DC maturation: It stimulates properties necessary for migration, but does not induce maturation as compared e.g. LPS. Lamellipodia formation is caused mainly by activated Rac1, which we find higher amounts in FHL2-/- DC compared to wt DC.

## 4.4 FHL2-/- BMDC do not show a more mature phenotype and differences in antigen uptake and presentation

To present antigens or pathogens to naive T cells, DC must mature after capturing and processing exogenous antigens and also provide three essential signals: An antigen presentation signal via an MHC-peptide complex to TCR, costimulatory signals e.g., CD40, CD80, and CD86, and proinflammatory cytokines e.g., IL-6, IL-12, and TNF-α (Lutz and Schuler, 2002). The expression of cell surface molecules and production of proinflammatory cytokines in DC are primarily regulated by NF-κB (Ouaaz et al., 2002; Rescigno et al., 1998). Thus, regulating NF-κB activation is of critical importance for immunoregulation and prevention of allograft rejection (Shinoda et al., 2010). Deficiency of FHL2 could influence the expression levels of costimulatory molecules by regulating NF-κB transcription, since nuclear translocation of the p65 subunit of NF-κB is enhanced in FHL2-deficient osteoclast precursors (Bai et al., 2005) and expression of FHL2 results in enhancement of NF-κB activation (Stilo et al., 2002). After antigen uptake and processing, peptide is loaded on MHC and transported to the surface of the cell ready to communicate with T cells. Shuttling of MHC to cell surface also depends on the dynamics of the actin cytoskeleton and activation of small Rho GTPases like Rac1, and both incidents are different in FHL2-/- DC (Erickson et al., 1996; Turley et al., 2000; Luna et al., 2002).

Maybe all the processes are changed in FHL2-/-BMDC and influence the maturation state. We found that the maturation markers such as MHCI, MHCII, CD80, CD86 and CD40 are expressed to similar level between FHL2-/- and wt BMDC (Fig. 3.8 A). After incubation with TNF-α, these markers were elevated to similar degree in FHL2-/- and wt BMDC. Even a higher expression was observed when BMDC were stimulated with LPS (Efron et al., 2005; Granucci et al., 2001). Thus, it seems that NF-κB signaling is not altered in FHL2-/- BMDC, which could have influenced the expression levels of costimulatory molecules. In order to determine, if NF-κB signaling is different in FHL2-/- BMDC, a further number of experiment, e.g. by Western Blot is required. Also Qiao et al., 2009 failed to show a direct association of FHL2 with nuclear NF-κB in gastrointestinal cancer. Although the actin cytoskeleton is differentially arranged

in FHL2-/- BMDC this did not seem to affect transport of MHC class molecules to the surface.

As a third signal DC provide soluble molecules to the T cell like IL-12 and TNF-α to turn them into effector T cells. Differential production of IL-12 would rather lead to a Th1 phenotype during the crosstalk of DC and T cell (Macatonia et al., 1995), and this effect is even enhanced by administration of LPS (Mellman and Steinman, 2001). Induction of IL-12 occurs in response to signals that require either p50 or cRel NF-κB family members (Murphy et al., 1995; Zhang et al., 2000). DC-derived TNF-α is responsible for the development of IL-10-producing $CD4^+$ regulatory T cells by immature DCs (Hirata et al., 2010). Another study confirmed this *in vivo*, where stimulation by TNF-α results in incompletely matured DCs (semi-mature DCs) which induce peptide-specific IL-10-producing T cells *in vivo* and prevent experimental autoimmune encephalomyelitis (Menges et al., 2002). But also here we could not observe any difference between wt and FHL2-/- DC with respect to production of IL-12 and TNF-α and also not after additional stimulation with LPS (Fig. 3.9 B). Incubation of BMDC with TNF-α did not induce secretion of IL-12 and TNF-α, which was speculated to be the reason that TNFα- matured DC rather induce tolerance (Menges et al., 2002). Hence, we assume that increased migration in FHL2-/- is not due to a constitutive maturation of BMDC. FHL2 does not influence the maturation status of DC, but according to our until now conducted experiments migration of BMDC.

The main task of DC is to present antigen to T cells after they have taken it up in the periphery, which will lead to an efficient immune response or tolerance depending on the signals provided by DC. Although we know that these signals i.e. maturation markers and cytokine production are not different, there still can be a difference regarding antigen uptake and presentation between wt and FHL2-/- DC, because also organization of the cytoskeleton influences the process of antigen uptake and presentation. Macropinocytosis and endocytosis are related processes, both depending on regulated actin assembly and thus the activity of the Rho family GTPases Cdc42 and Rac (Garrett et al., 2000; West et al., 2000). DCs have many routes to take up antigen either by macropinocytosis e.g dextran or receptor mediated like OVA. When feeding

both types of DC with OVA or dextran, we could not observe any difference in uptake (Fig. 3.10 A). Although FHL2 contributes to the organization of the cytoskeleton, this change does not seem relevant in the process of antigen uptake. We know that FHL2 has an influence on cell morphology and organization of the cytoskeleton, which is crucial in taking up antigen and in the crosstalk between DC and T cell. Selective Rac1 inhibition in DCs diminishes apoptotic cell uptake and cross-presentation *in vivo* (Benvenuti et al., 2004). Inhibition of the Rac-Cdc42-Ral pathway markedly reduces dendritic probings as well as short and long-term contacts with T cells *in vitro* (Swetman et al., 2002). Rac1 signaling, which is enhanced in FHL2-/- BMDC, did not seem to play a role regarding antigen presentation in FHL2-/- BMDC. This we could observe for presenting the model antigen OVA to OVA specific T cells in a co-culture, when we looked for proliferation of T cells by CFSE dilution and IL-2 production (Fig. 3.10 B, C and D).

### 4.5 S1PR1 expression is increased in FHL2-/- BMDC

Ligand binding by S1P plays a role in FHL2 signaling in several cell lines leading to a translocation of FHL2 in the nucleus (Muller et al., 2002). Additionally, S1PR are differentially expressed in mature DC, which also have faster migrating abilities than immature DC, showing high expression levels of S1PR1 and 3 and diminished or steady expression of S1PR2 and 4 (Czeloth et al., 2005). Furthermore, CHO cells overexpressing S1PR1 and 3 show higher migration levels than their controls (Okamoto et al., 2000). All this made us elucidate the expression levels of S1PR further, because this might explain the increased migration behavior noticed in FHL2-/- DC. Indeed, we could detect higher expression levels of S1PR1 in FHL2-/- DC determined by qRT-PCR, and this effect was even more pronounced after stimulation with TNF-α (Fig. 3.10). The expression of S1PR2-4 does not seem to be different between wt and FHL2-/- BMDC and show differential expression levels to the same extent after incubation with TNF-α compared to non-treated, which is in accordance to the observations of other groups (Maeda et al., 2007; Rathinasamy et al., 2010).
We could confirm this observation more functionally in a migration assay after knockdown of S1PR1 by electroporation with S1PR1 specific siRNA: S1PR1

loss reversed the phenotype of FHL2-/- BMDC (Fig. 3.13 A and B). We wanted to explore this further with the help of a specific small molecular inhibitor against S1PR1 SEW2871, which can have an agonistic or antagonistic effect on S1PR1. On the one hand cells including DC tend to migrate towards SEW2871, but on the other hand incubation of cells with it leads to internalization of S1PR1 which is not fully functional anymore (Sanna et al., 2004). This happened when incubating SEW2871 with FHL2-/- DC which lead to slower migration compared to control and approaching the migration levels of wt DC (Fig. 3.12 C). We could exclude that SEW2871 itself might have an effect on the maturation status of BMDC, which could also cause differential migration capabilities of BMDC. Thus, S1PR1 must play a role in FHL2 signaling causing accelerated DC migration ability, but does not have an impact on several other DC functions like antigen uptake and presentation. But these processes seem to be regulated by other S1PRs like 3 rather than S1PR1 (Maeda et al., 2007), and endocytosis seems mainly to be controlled by Cdc42, which we did not look for. S1P by itself did not change antigen uptake ability (Fig. 3.13 A) or migration status (Fig. 3.13 B) by immature DC, which fits to the observations made by (Maeda et al., 2007), who did not observe that S1P affected mature DC regarding these processes.

## 4.6 Summary

Our observation suggests the following mechanism in FHL2-/- BMDC. We think that in FHL2-/- BMDC the following chain of events are occurring based on a combination of our findings and literature: Immature DC show high expression levels of S1PR2 (Czeloth et al., 2005) and signaling via S1PR2 by S1P, which is present in the serum supplemented to the media, leads to RhoA mediated FHL2 translocation into the nucleus (Muller et al., 2002). Being able to bind to proteins it will bind to an unknown transcription factor acting in this setting as a co-repressor of transcription of S1PR1 which we know is quite low in immature DC. This is supported by the fact that we mainly find FHL2 in the nucleus in immature BMDC. At the same time, residing in the periphery with slight expression of CCR7 it cannot respond to CCL19, therefore not being able to migrate quickly (Fig. 4.1 A).

We propose that in the KO setting the same scenario is taking place after a DC has matured after PRR stimulation (Fig. 4.1 B). In a mature DC signaling via S1PR2 by S1P declines, so no FHL2 is present in the nucleus inhibiting the transcription of S1PR1, which is increased in mature DC. We know that in mature DCs after ligand binding with CCL19 FHL2 is not present in the nucleus anymore, but can be found at the cell membrane. The same is true for KO DC where no FHL2 is present in the nucleus. S1PR1 lead via $G_i$ receptor to higher amounts of Rac1 which entail lamellipodia formation and in the end increased migration (Takuwa, 2002).

Literature hints that it is most likely S1PR2 working upstream of FHL2, but this theory has to be confirmed by e.g. knock down of S1PR2 and as a read out followed by a migration assay. In order to fortify the underlying mechanism it would be sufficient finding the missing link in the regulation of S1PR1 transcription by FHL2. There is a pile of literature hinting to Forkhead Box O1 (Foxo1) being the transcription factor for S1PR1. FHL2 inhibits Foxo4 (Shi et al., 2010) and Foxo1 transcriptional activity in prostate cancer cells by promoting the deacetylation of Foxo1 by Sirtuin1 (SIRT1; Yang et al., 2005). In quiescent T cells, nonphosphorylated active Foxos maintain expression of Kruppel-like factor 2 (KLF2), that regulates expression CCR7 and S1PR1 (Finlay and Cantrell, 2010). Taken together, these results suggested that Foxo3 may control expression of S1PR1. Indeed, there was a small, but consistent, reduction in S1PR1 mRNA in Foxo3−/− B cells to 75% of wt levels (Hinman et al., 2009). They demonstrate using transcriptional profiling that Foxo1 also increases transcripts of S1PR1 and 4 (Fabre et al., 2008).

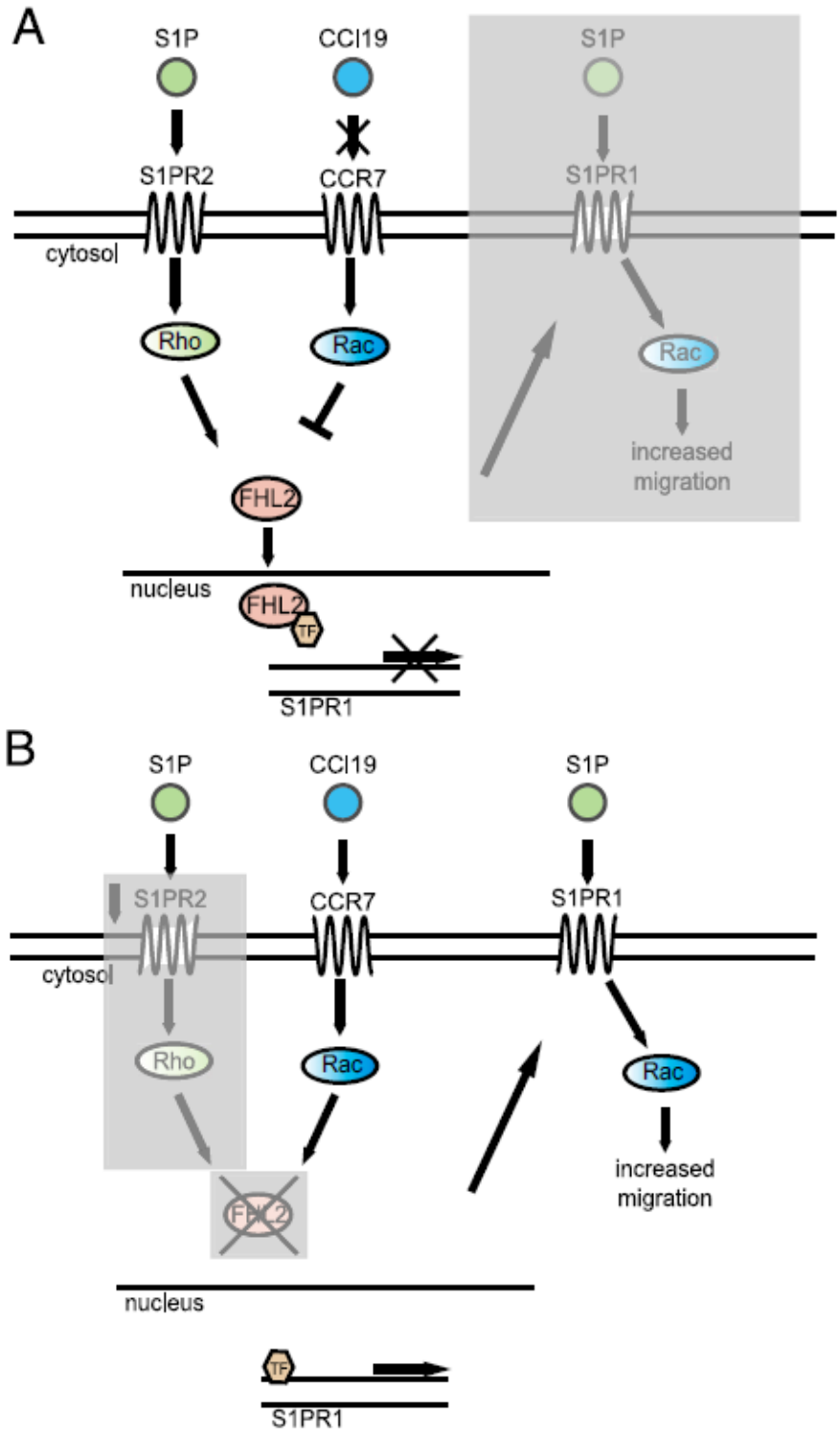


**Figure 4.1: Model of FHL2-mediated repression of S1PR1 expression and regulation of DC migration. (A)** In immature wt DCs, signaling via S1PR2 leads to Rho activation, causing translocation of FHL2 into the nucleus, where FHL2 represses transcription of S1PR1 by binding to the transcription factor of the promoter region. Additionally, low expression levels of CCR7 blocks Rac activity. **(B)** Maturation of DCs leads to downregulation of S1PR2. Subsequent diminished Rho activation inhibits nuclear translocation of FHL2 into the nucleus, which has the same effect as FHL2 deficiency (i.e. reduced repression of S1PR1 transcription). S1P signaling via greater S1PR1 levels increases Rac activation, which leads to an increased migratory rate of mature or FHL2-/- DCs.

## 4.7 Conclusion

The interaction of DC with naive T cells can lead to different forms of immune responses ranging from immunity or to T-cell tolerance, depending on the type of DC and its activation state (Shortman and Naik, 2007). The common view supposes that immature DC induce tolerance, whereas mature DC induce immunity to antigens (Sousa, 2006). The question is what the outcome would be in FHL2-/- BMDC or in FHL2-/- mice or would it be any different compared to wt DC? And how can we you use this information? Fainaru et al. (2005) reported that in Runx3 KO mice, expression of CCR7 is enhanced, resulting in increased migration of alveolar DC to the lung-draining LN. This increased DC migration and the consequent accumulation of activated DC in draining LN is associated with the development of asthma-like features. But they also showed higher expression levels of CD86 and MHCII what drove the T cells to a more activated state. However wt and FHL2-/- BMDC are equally mature. On the other hand disordered migratory DC cannot mount an effective T cell mediated specific immune response as seen in PI3K–/– DCs, which migrate poorly towards chemotactic factors *in vitro* and *in vivo*, leading to defective cutaneous hypersensitivity responses (Del Prete et al., 2004). FHL2-/- BMDCs are a very helpful model to study how migration influences T cell activation based on their migration on not what additional factors like maturation status or antigen presentation capabilities they are providing during the crosstalk of T cells. We postulate that FHL2-/- DC are able to induce tolerance to antigens, because immature FHL2-/- DC reach the LN earlier than wt DC and most likely cannot deliver an activation signal to antigen-specific T cells because of a lack of costimulatory molecules. FHL2-/- BMDC could serve as a convenient model to investigate the induction of tolerance to T cells. The role of migration of DC in a lot of diseases and tumor models can be studied on the basis of FHL2-/- BMDC, and the effect seen is only due to the enhanced migration of DC. If this is the case inhibition of FHL2 could be used as a therapeutic target

Testing this hypothesis needs more complex *in vivo* experiments, and therefore it is necessary to look for altered ability in antigen uptake and presentation in FHL2-/- BMDC in contrast to wt BMDC *in vivo*. Because it is important to know that the effect seen in these kinds of experiments is only due the enhanced

migration of FHL2-/- BMDC. The current model of FHL2 signaling is recommended in Fig. 4.1.

# References

Abecassis, I., Olofsson, B., Schmid, M., Zalcman, G., and Karniguian, A. (2003). RhoA induces MMP-9 expression at CD44 lamellipodial focal complexes and promotes HMEC-1 cell invasion. Exp Cell Res 291, 363-376.

Adams, J.C. (2002). Regulation of protrusive and contractile cell-matrix contacts. J Cell Sci 115, 257-265.

Akira, S., Takeda, K., and Kaisho, T. (2001). Toll-like receptors: critical proteins linking innate and acquired immunity. Nat Immunol 2, 675-680.

Akira, S., Uematsu, S., and Takeuchi, O. (2006). Pathogen recognition and innate immunity. Cell 124, 783-801.

Al-Alwan, M.M., Liwski, R.S., Haeryfar, S.M., Baldridge, W.H., Hoskin, D.W., Rowden, G., and West, K.A. (2003). Cutting edge: dendritic cell actin cytoskeletal polarization during immunological synapse formation is highly antigen-dependent. J Immunol 171, 4479-4483.

Al-Alwan, M.M., Rowden, G., Lee, T.D., and West, K.A. (2001). The dendritic cell cytoskeleton is critical for the formation of the immunological synapse. J Immunol 166, 1452-1456.

Alvarez, D., Vollmann, E.H., and von Andrian, U.H. (2008). Mechanisms and consequences of dendritic cell migration. Immunity 29, 325-342.

Amann, K.J., and Pollard, T.D. (2001). The Arp2/3 complex nucleates actin filament branches from the sides of pre-existing filaments. Nat Cell Biol 3, 306-310.

Amann, T., Egle, Y., Bosserhoff, A.K., and Hellerbrand, C. (2010). FHL2 suppresses growth and differentiation of the colon cancer cell line HT-29. Oncol Rep 23, 1669-1674.

Ananthakrishnan, R., and Ehrlicher, A. (2007). The forces behind cell movement. Int J Biol Sci 3, 303-317.

Arikawa, K., Takuwa, N., Yamaguchi, H., Sugimoto, N., Kitayama, J., Nagawa, H., Takehara, K., and Takuwa, Y. (2003). Ligand-dependent inhibition of B16 melanoma cell migration and invasion via endogenous S1P2 G protein-coupled receptor. Requirement of inhibition of cellular RAC activity. J Biol Chem 278, 32841-32851.

Bai, S., Kitaura, H., Zhao, H., Chen, J., Muller, J.M., Schule, R., Darnay, B., Novack, D.V., Ross, F.P., and Teitelbaum, S.L. (2005). FHL2 inhibits the activated osteoclast in a TRAF6-dependent manner. J Clin Invest 115, 2742-2751.

Banchereau, J., and Steinman, R.M. (1998). Dendritic cells and the control of immunity. Nature 392, 245-252.

Becker, S., von Otte, S., Robenek, H., Diedrich, K., and Nofer, J.R. (2010). Follicular Fluid High-Density Lipoprotein (FF-HDL)-Associated Sphingosine 1-Phosphate (S1P) Promotes Human Granulosa Lutein Cell Migration via S1P Receptor Type 3 (S1PR3) and Small G Protein RAC1. Biol Reprod.

Benvenuti, F., Hugues, S., Walmsley, M., Ruf, S., Fetler, L., Popoff, M., Tybulewicz, V.L., and Amigorena, S. (2004). Requirement of Rac1 and Rac2 expression by mature dendritic cells for T cell priming. Science 305, 1150-1153.

Black, R.A., Rauch, C.T., Kozlosky, C.J., Peschon, J.J., Slack, J.L., Wolfson, M.F., Castner, B.J., Stocking, K.L., Reddy, P., Srinivasan, S., et al. (1997). A metalloproteinase disintegrin that releases tumour-necrosis factor-alpha from cells. Nature 385, 729-733.

Bowie, A.G., and Unterholzner, L. (2008). Viral evasion and subversion of pattern-recognition receptor signalling. Nat Rev Immunol 8, 911-922.

Brakebusch, C., and Fassler, R. (2003). The integrin-actin connection, an eternal love affair. EMBO J 22, 2324-2333.

Brightbill, H.D., Libraty, D.H., Krutzik, S.R., Yang, R.B., Belisle, J.T., Bleharski, J.R., Maitland, M., Norgard, M.V., Plevy, S.E., Smale, S.T., et al. (1999). Host defense mechanisms triggered by microbial lipoproteins through toll-like receptors. Science 285, 732-736.

Burns, S., Hardy, S.J., Buddle, J., Yong, K.L., Jones, G.E., and Thrasher, A.J. (2004). Maturation of DC is associated with changes in motile characteristics and adherence. Cell Motil Cytoskeleton 57, 118-132..

Burridge, K., and Wennerberg, K. (2004). Rho and Rac take center stage. Cell 116, 167-179.

Calle, Y., Chou, H., Thrasher, A.J., and Jones, G.E. (2004). Wiskott-Aldrich syndrome protein and the cytoskeletal dynamics of dendritic cells. J Pathol 204 460–469.

Canault, M., Tellier, E., Bonardo, B., Mas, E., Aumailley, M., Juhan-Vague, I., Nalbone, G., and Peiretti, F. (2006). FHL2 interacts with both ADAM-17 and the cytoskeleton and regulates ADAM-17 localization and activity. J Cell Physiol 208, 363-372.

Caron, E., and Hall, A. (1998). Identification of two distinct mechanisms of phagocytosis controlled by different Rho GTPases. Science 282, 1717-1721.

Chan, K., Tsui, S., Lee, S., Luk, S., Liew, C., Fung, K., Waye, M., and Lee, C. (1998). Molecular cloning and characterization of FHL2, a novel LIM domain protein preferentially expressed in human heart. Gene 210(2), 345-350.

Chan, K.T., Cortesio, C.L., and Huttenlocher, A. (2007). Integrins in cell migration. Methods Enzymol 426, 47-67.

Charest, P.G., and Firtel, R.A. (2007). Big roles for small GTPases in the control of directed cell movement. Biochem J 401, 377-390.

Chen, D., Xu, W., Bales, E., Colmenares, C., Conacci-Sorrell, M., Ishii, S., Stavnezer, E., Campisi, J., Fisher, D.E., Ben-Ze'ev, A., et al. (2003). SKI activates Wnt/beta-catenin signaling in human melanoma. Cancer Res 63, 6626-6634.

Chu, P.-H., Ruiz-Lozanoa, P., Zhoua, Q., Caia, C., and Chena, J. (2000a). Expression patterns of FHL/SLIM family members suggest important functional roles in skeletal muscle and cardiovascular system. Mechanisms of Development 95, 259-265.

Chu, P., Bardwell, W., Gu, Y., Ross, J.J., and Chen, J. (2000b). FHL2 (SLIM3) Is Not Essential for Cardiac Development and Function. Mol Cell Biol 20, 7460–7462.

Cinamon, G., Matloubian, M., Lesneski, M.J., Xu, Y., Low, C., Lu, T., Proia, R.L., and Cyster, J.G. (2004). Sphingosine 1-phosphate receptor 1 promotes B cell localization in the splenic marginal zone. Nat Immunol 5, 713-720.

Cooper, J.A. (1987). Effects of cytochalasin and phalloidin on actin. J Cell Biol 105, 1473-1478.

Cory, G.O., and Ridley, A.J. (2002). Cell motility: braking WAVEs. Nature 418, 732-733.

Cumberbatch, M., Griffiths, C.E., Tucker, S.C., Dearman, R.J., and Kimber, I. (1999). Tumour necrosis factor-alpha induces Langerhans cell migration in humans. Br J Dermatol 141, 192-200.

Cumberbatch, M., and Kimber, I. (1992). Dermal tumour necrosis factor-alpha induces dendritic cell migration to draining lymph nodes, and possibly provides one stimulus for Langerhans' cell migration. Immunology 75, 257-263.

Czeloth, N., Bernhardt, G., Hofmann, F., Genth, H., and Forster, R. (2005). Sphingosine-1-phosphate mediates migration of mature dendritic cells. J Immunol 175, 2960-2967.

Czeloth, N., Schippers, A., Wagner, N., Muller, W., Kuster, B., Bernhardt, G., and Forster, R. (2007). Sphingosine-1 phosphate signaling regulates positioning of dendritic cells within the spleen. J Immunol 179, 5855-5863.

Darenfed, H., Dayanandan, B., Zhang, T., Hsieh, S.H., Fournier, A.E., and Mandato, C.A. (2007). Molecular characterization of the effects of Y-27632. Cell Motil Cytoskeleton 64, 97-109.

De Vries, I.J., Krooshoop, D.J., Scharenborg, N.M., Lesterhuis, W.J., Diepstra, J.H., Van Muijen, G.N., Strijk, S.P., Ruers, T.J., Boerman, O.C., Oyen, W.J., et al. (2003). Effective migration of antigen-pulsed dendritic cells to lymph nodes in

melanoma patients is determined by their maturation state. Cancer Res 63, 12-17.

Di Girolamo, N., Indoh, I., Jackson, N., Wakefield, D., McNeil, H.P., Yan, W., Geczy, C., Arm, J.P., and Tedla, N. (2006). Human mast cell-derived gelatinase B (matrix metalloproteinase-9) is regulated by inflammatory cytokines: role in cell migration. J Immunol 177, 2638-2650.

Dieu, M.C., Vanbervliet, B., Vicari, A., Bridon, J.M., Oldham, E., Ait-Yahia, S., Briere, F., Zlotnik, A., Lebecque, S., and Caux, C. (1998). Selective recruitment of immature and mature dendritic cells by distinct chemokines expressed in different anatomic sites. J Exp Med 188, 373-386.

Ding, L., Wang, Z., Yan, J., Yang, X., Liu, A., Qiu, W., Zhu, J., Han, J., Zhang, H., Lin, J., et al. (2009). Human four-and-a-half LIM family members suppress tumor cell growth through a TGF-beta-like signaling pathway. J Clin Invest 119, 349-361.

Dogterom, M., Kerssemakers, J.W., Romet-Lemonne, G., and Janson, M.E. (2005). Force generation by dynamic microtubules. Curr Opin Cell Biol 17, 67-74.

Dumitru, C.D., Ceci, J.D., Tsatsanis, C., Kontoyiannis, D., Stamatakis, K., Lin, J.H., Patriotis, C., Jenkins, N.A., Copeland, N.G., Kollias, G., et al. (2000). TNF-alpha induction by LPS is regulated posttranscriptionally via a Tpl2/ERK-dependent pathway. Cell 103, 1071-1083.

Efron, P., Tsujimoto, H., Bahjat, F., Ungaro, R., Debernardis, J., Tannahill, C., Baker, H., Edwards, C., and Moldawer, L. (2005). Differential maturation of murine bone-marrow derived dendritic cells with lipopolysaccharide and tumor necrosis factor-alpha. J Endotoxin Res 11(3), 145-160.

El Mourabit, H., Muller, S., Tunggal, L., Paulsson, M., and Aumailley, M. (2003). Characterization of recombinant and natural forms of the human LIM domain-containing protein FHL2. Protein Expr Purif 32, 95-103.

El Mourabit, H., Muller, S., Tunggal, L., Paulsson, M., and Aumailley, M. (2004). Analysis of the adaptor function of the LIM domain-containing protein FHL2 using an affinity chromatography approach. J Cell Biochem 92, 612-625.

Erickson, J.W., Zhang, C., Kahn, R.A., Evans, T., and Cerione, R.A. (1996). Mammalian Cdc42 is a brefeldin A-sensitive component of the Golgi apparatus. J Biol Chem 271, 26850-26854.

Evelyn, C.R., Wade, S.M., Wang, Q., Wu, M., Iniguez-Lluhi, J.A., Merajver, S.D., and Neubig, R.R. (2007). CCG-1423: a small-molecule inhibitor of RhoA transcriptional signaling. Mol Cancer Ther 6, 2249-2260.

Fabre, S., Carrette, F., Chen, J., Lang, V., Semichon, M., Denoyelle, C., Lazar, V., Cagnard, N., Dubart-Kupperschmitt, A., Mangeney, M., et al. (2008). FOXO1

regulates L-Selectin and a network of human T cell homing molecules downstream of phosphatidylinositol 3-kinase. J Immunol 181, 2980-2989.

Fainaru, O., Shseyov, D., Hantisteanu, S., and Groner, Y. (2005). Accelerated chemokine receptor 7-mediated dendritic cell migration in Runx3 knockout mice and the spontaneous development of asthma-like disease. Proc Natl Acad Sci U S A 102, 10598-10603.

Fimia, G.M., De Cesare, D., and Sassone-Corsi, P. (2000). A family of LIM-only transcriptional coactivators: tissue-specific expression and selective activation of CREB and CREM. Mol Cell Biol 20, 8613-8622.

Finlay, D., and Cantrell, D. (2010). Phosphoinositide 3-kinase and the mammalian target of rapamycin pathways control T cell migration. Ann N Y Acad Sci 1183, 149-157.

Friedl, P. (2004). Prespecification and plasticity: shifting mechanisms of cell migration. Curr Opin Cell Biol 16, 14-23.

Friedl, P., and Brocker, E.B. (2000). The biology of cell locomotion within three-dimensional extracellular matrix. Cell Mol Life Sci 57, 41-64.

Friedl, P., and Weigelin, B. (2008). Interstitial leukocyte migration and immune function. Nat Immunol 9, 960-969.

Friedl, P., Zanker, K.S., and Brocker, E.B. (1998). Cell migration strategies in 3-D extracellular matrix: differences in morphology, cell matrix interactions, and integrin function. Microsc Res Tech 43, 369-378.

Fukui, Y., Hashimoto, O., Sanui, T., Oono, T., Koga, H., Abe, M., Inayoshi, A., Noda, M., Oike, M., Shirai, T., et al. (2001). Haematopoietic cell-specific CDM family protein DOCK2 is essential for lymphocyte migration. Nature 412, 826-831.

Garrett, W.S., Chen, L.M., Kroschewski, R., Ebersold, M., Turley, S., Trombetta, S., Galan, J.E., and Mellman, I. (2000). Developmental control of endocytosis in dendritic cells by Cdc42. Cell 102, 325-334.

Genini, M., Schwalbe, P., Scholl, F., Remppis, A., Mattei, M., and Schäfer, B. (1997). Subtractive cloning and characterization of DRAL, a novel LIM-domain protein down-regulated in rhabdomyosarcoma. DNA Cell Biol 16(4), 433-442.

Gil, P.R., Japtok, L., and Kleuser, B. (2010). Sphingosine 1-phosphate mediates chemotaxis of human primary fibroblasts via the S1P-receptor subtypes S1P and S1P and Smad-signalling. Cytoskeleton (Hoboken) 67, 773-783.

Gittes, F., Mickey, B., Nettleton, J., and Howard, J. (1993). Flexural rigidity of microtubules and actin filaments measured from thermal fluctuations in shape. J Cell Biol 120, 923-934.

Graeler, M., and Goetzl, E.J. (2002). Activation-regulated expression and chemotactic function of sphingosine 1-phosphate receptors in mouse splenic T cells. FASEB J 16, 1874-1878.

Grakoui, A., Bromley, S.K., Sumen, C., Davis, M.M., Shaw, A.S., Allen, P.M., and Dustin, M.L. (1999). The immunological synapse: a molecular machine controlling T cell activation. Science 285, 221-227.

Granucci, F., Vizzardelli, C., Virzi, E., Rescigno, M., and Ricciardi-Castagnoli, P. (2001). Transcriptional reprogramming of dendritic cells by differentiation stimuli. Eur J Immunol 31, 2539–2546.

Guermonprez, P., Valladeau, J., Zitvogel, L., Thery, C., and Amigorena, S. (2002). Antigen presentation and T cell stimulation by dendritic cells. Annu Rev Immunol 20, 621-667.

Gunther, T., Poli, C., Muller, J.M., Catala-Lehnen, P., Schinke, T., Yin, N., Vomstein, S., Amling, M., and Schule, R. (2005). Fhl2 deficiency results in osteopenia due to decreased activity of osteoblasts. EMBO J 24, 3049-3056.

Hamidouche, Z., Hay, E., Vaudin, P., Charbord, P., Schule, R., Marie, P.J., and Fromigue, O. (2008). FHL2 mediates dexamethasone-induced mesenchymal cell differentiation into osteoblasts by activating Wnt/beta-catenin signaling-dependent Runx2 expression. FASEB J 22, 3813-3822.

Hargreaves, D.C., Hyman, P.L., Lu, T.T., Ngo, V.N., Bidgol, A., Suzuki, G., Zou, Y.R., Littman, D.R., and Cyster, J.G. (2001). A coordinated change in chemokine responsiveness guides plasma cell movements. J Exp Med 194, 45-56.

Hinman, R.M., Nichols, W.A., Diaz, T.M., Gallardo, T.D., Castrillon, D.H., and Satterthwaite, A.B. (2009). Foxo3-/- mice demonstrate reduced numbers of pre-B and recirculating B cells but normal splenic B cell sub-population distribution. Int Immunol 21, 831-842.

Hirata, N., Yanagawa, Y., Satoh, M., Ogura, H., Ebihara, T., Noguchi, M., Matsumoto, M., Togashi, H., Seya, T., Onoe, K., et al. (2010). Dendritic cell-derived TNF-alpha is responsible for development of IL-10-producing CD4+ T cells. Cell Immunol 261, 37-41.

Hotulainen, P., and Lappalainen, P. (2006). Stress fibers are generated by two distinct actin assembly mechanisms in motile cells. J Cell Biol 173, 383-394.

Idzko, M., Panther, E., Corinti, S., Morelli, A., Ferrari, D., Herouy, Y., Dichmann, S., Mockenhaupt, M., Gebicke-Haerter, P., Di Virgilio, F., et al. (2002). Sphingosine 1-phosphate induces chemotaxis of immature and modulates cytokine-release in mature human dendritic cells for emergence of Th2 immune responses. FASEB J 16, 625-627.

Ishizaki, T., Uehata, M., Tamechika, I., Keel, J., Nonomura, K., Maekawa, M., and Narumiya, S. (2000). Pharmacological properties of Y-27632, a specific inhibitor of rho-associated kinases. Mol Pharmacol 57, 976-983.

Jaffe, A.B., and Hall, A. (2005). Rho GTPases: biochemistry and biology. Annu Rev Cell Dev Biol 21, 247-269.

Janeway, C.A., Jr., and Medzhitov, R. (2002). Innate immune recognition. Annu Rev Immunol 20, 197-216.

Janeway, C.A., Travers, P., and Walport, M. (2005). Immunobiology: The Immune System in Health and Disease. Garland Science Publishing, New York, USA, . 116-130.

Jensen, P.E. (2007). Recent advances in antigen processing and presentation. Nat Immunol 8, 1041-1048.

Johannessen, M., Moller, S., Hansen, T., Moens, U., and Van Ghelue, M. (2006). The multifunctional roles of the four-and-a-half-LIM only protein FHL2. Cell Mol Life Sci 63, 268-284.

Kahl, P., Gullotti, L., Heukamp, L.C., Wolf, S., Friedrichs, N., Vorreuther, R., Solleder, G., Bastian, P.J., Ellinger, J., Metzger, E., et al. (2006). Androgen receptor coactivators lysine-specific histone demethylase 1 and four and a half LIM domain protein 2 predict risk of prostate cancer recurrence. Cancer Res 66, 11341-11347.

Kapsenberg, M.L. (2003). Dendritic-cell control of pathogen-driven T-cell polarization. Nat Rev Immunol 3, 984-993.

Keren, K., Pincus, Z., Allen, G.M., Barnhart, E.L., Marriott, G., Mogilner, A., and Theriot, J.A. (2008). Mechanism of shape determination in motile cells. Nature 453, 475-480.

Kikuchi, K., Yanagawa, Y., and Onoe, K. (2005). CCR7 ligand-enhanced phagocytosis of various antigens in mature dendritic cells-time course and antigen distribution different from phagocytosis in immature dendritic cells. Microbiol Immunol 49, 535-544.

Kindberg, G.M., Magnusson, S., Berg, T., and Smedsrod, B. (1990). Receptor-mediated endocytosis of ovalbumin by two carbohydrate-specific receptors in rat liver cells. The intracellular transport of ovalbumin to lysosomes is faster in liver endothelial cells than in parenchymal cells. Biochem J 270, 197-203.

Kirfel, J., Pantelis, D., Kabba, M., Kahl, P., Roper, A., Kalff, J.C., and Buettner, R. (2008). Impaired intestinal wound healing in Fhl2-deficient mice is due to disturbed collagen metabolism. Exp Cell Res 314, 3684-3691.

Koestler, S.A., Rottner, K., Lai, F., Block, J., Vinzenz, M., and Small, J.V. (2009). F- and G-actin concentrations in lamellipodia of moving cells. PLoS One 4, e4810.

Kupiec-Weglinski, J.W., Austyn, J.M., and Morris, P.J. (1988). Migration patterns of dendritic cells in the mouse. Traffic from the blood, and T cell-dependent and -independent entry to lymphoid tissues. J Exp Med 167, 632-645.

Labalette, C., Nouet, Y., Levillayer, F., Armengol, C., Renard, C.A., Soubigou, G., Xia, T., Buendia, M.A., and Wei, Y. (2008a). The LIM-only protein FHL2 mediates ras-induced transformation through cyclin D1 and p53 pathways. PLoS One 3, e3761.

Labalette, C., Nouet, Y., Levillayer, F., Colnot, S., Chen, J., Claude, V., Huerre, M., Perret, C., Buendia, M.A., and Wei, Y. (2010). Deficiency of the LIM-only protein FHL2 reduces intestinal tumorigenesis in Apc mutant mice. PLoS One 5, e10371.

Labalette, C., Nouet, Y., Sobczak-Thepot, J., Armengol, C., Levillayer, F., Gendron, M.C., Renard, C.A., Regnault, B., Chen, J., Buendia, M.A., et al. (2008b). The LIM-only protein FHL2 regulates cyclin D1 expression and cell proliferation. J Biol Chem 283, 15201-15208.

Labalette, C., Renard, C.A., Neuveut, C., Buendia, M.A., and Wei, Y. (2004). Interaction and functional cooperation between the LIM protein FHL2, CBP/p300, and beta-catenin. Mol Cell Biol 24, 10689-10702.

Lad, Y., Harburger, D.S., and Calderwood, D.A. (2007). Integrin Cytoskeletal Interactions. Methods Enzymol 426, 69-84.

Ladwein, M., and Rottner, K. (2008). On the Rho'd: the regulation of membrane protrusions by Rho-GTPases. FEBS Lett 582, 2066-2074.

Lai, C.F., Bai, S., Uthgenannt, B.A., Halstead, L.R., McLoughlin, P., Schafer, B.W., Chu, P.H., Chen, J., Otey, C.A., Cao, X., et al. (2006). Four and half lim protein 2 (FHL2) stimulates osteoblast differentiation. J Bone Miner Res 21, 17-28.

Lammermann, T., Bader, B.L., Monkley, S.J., Worbs, T., Wedlich-Soldner, R., Hirsch, K., Keller, M., Forster, R., Critchley, D.R., Fassler, R., et al. (2008). Rapid leukocyte migration by integrin-independent flowing and squeezing. Nature 453, 51-55.

Landi, A., Babiuk, L.A., and van Drunen Littel-van den Hurk, S. (2010). Dendritic cells matured by a prostaglandin E2-containing cocktail can produce high levels of IL-12p70 and are more mature and Th1-biased than dendritic cells treated with TNF-alpha or LPS. Immunobiology.

Lanzavecchia, A. (1996). Mechanisms of antigen uptake for presentation. Curr Opin Immunol 8, 348-354.

Lauffenburger, D.A., and Horwitz, A.F. (1996). Cell migration: a physically integrated molecular process. Cell 84, 359-369.

Le Clainche, C., and Carlier, M.F. (2008). Regulation of actin assembly associated with protrusion and adhesion in cell migration. Physiol Rev 88, 489-513.

Li, H.Y., Kotaka, M., Kostin, S., Lee, S.M., Kok, L.D., Chan, K.K., Tsui, S.K., Schaper, J., Zimmermann, R., Lee, C.Y., et al. (2001). Translocation of a human focal adhesion LIM-only protein, FHL2, during myofibrillogenesis and identification of LIM2 as the principal determinants of FHL2 focal adhesion localization. Cell Motil Cytoskeleton 48, 11-23.

Li, M., Wang, J., Ng, S.S., Chan, C.Y., Chen, A.C., Xia, H.P., Yew, D.T., Wong, B.C., Chen, Z., Kung, H.F., et al. (2008). The four-and-a-half-LIM protein 2 (FHL2) is overexpressed in gliomas and associated with oncogenic activities. Glia 56, 1328-1338.

Liu, X., Yue, S., Li, C., Yang, L., You, H., and Li, L. (2010). Essential roles of sphingosine 1-phosphate receptor type 1 and 3 in human hepatic stellate cells motility and activation. J Cell Physiol.

Luna, A., Matas, O.B., Martinez-Menarguez, J.A., Mato, E., Duran, J.M., Ballesta, J., Way, M., and Egea, G. (2002). Regulation of protein transport from the Golgi complex to the endoplasmic reticulum by CDC42 and N-WASP. Mol Biol Cell 13, 866-879.

Lutz, M.B., and Rossner, S. (2007). Factors influencing the generation of murine dendritic cells from bone marrow: the special role of fetal calf serum. Immunobiology 212, 855-862.

Lutz, M.B., and Schuler, G. (2002). Immature, semi-mature and fully mature dendritic cells: which signals induce tolerance or immunity? Trends Immunol 23, 445-449.

Lyons, A.B., and Parish, C.R. (1994). Determination of lymphocyte division by flow cytometry. J Immunol Methods 171, 131-137.

Macatonia, S.E., Hosken, N.A., Litton, M., Vieira, P., Hsieh, C.S., Culpepper, J.A., Wysocka, M., Trinchieri, G., Murphy, K.M., and O'Garra, A. (1995). Dendritic cells produce IL-12 and direct the development of Th1 cells from naive CD4+ T cells. J Immunol 154, 5071-5079.

Maeda, Y., Matsuyuki, H., Shimano, K., Kataoka, H., Sugahara, K., and Chiba, K. (2007). Migration of CD4 T cells and dendritic cells toward sphingosine 1-phosphate (S1P) is mediated by different receptor subtypes: S1P regulates the functions of murine mature dendritic cells via S1P receptor type 3. J Immunol 178, 3437-3446.

Malek, T.R., and Castro, I. (2010). Interleukin-2 receptor signaling: at the interface between tolerance and immunity. Immunity 33, 153-165.

MartIn-Fontecha, A., Sebastiani, S., Hopken, U.E., Uguccioni, M., Lipp, M., Lanzavecchia, A., and Sallusto, F. (2003). Regulation of dendritic cell migration

to the draining lymph node: impact on T lymphocyte traffic and priming. J Exp Med 198, 615-621.

Martin, B., Schneider, R., Janetzky, S., Waibler, Z., Pandur, P., Kuhl, M., Behrens, J., von der Mark, K., Starzinski-Powitz, A., and Wixler, V. (2002). The LIM-only protein FHL2 interacts with beta-catenin and promotes differentiation of mouse myoblasts. J Cell Biol 159, 113-122.

Martin, B.T., Kleiber, K., Wixler, V., Raab, M., Zimmer, B., Kaufmann, M., and Strebhardt, K. (2007). FHL2 regulates cell cycle-dependent and doxorubicin-induced p21Cip1/Waf1 expression in breast cancer cells. Cell Cycle 6, 1779-1788.

Matloubian, M., Lo, C.G., Cinamon, G., Lesneski, M.J., Xu, Y., Brinkmann, V., Allende, M.L., Proia, R.L., and Cyster, J.G. (2004). Lymphocyte egress from thymus and peripheral lymphoid organs is dependent on S1P receptor 1. Nature 427, 355-360.

Mattila, P.K., and Lappalainen, P. (2008). Filopodia: molecular architecture and cellular functions. Nat Rev Mol Cell Biol 9, 446-454.

Medzhitov, R. (2001). Toll-like receptors and innate immunity. Nat Rev Immunol 1, 135-145.

Mellman, I., and Steinman, R.M. (2001). Dendritic cells: specialized and regulated antigen processing machines. Cell 106, 255-258.

Menges, M., Rossner, S., Voigtlander, C., Schindler, H., Kukutsch, N.A., Bogdan, C., Erb, K., Schuler, G., and Lutz, M.B. (2002). Repetitive injections of dendritic cells matured with tumor necrosis factor alpha induce antigen-specific protection of mice from autoimmunity. J Exp Med 195, 15-21.

Mitchison, T.J., and Cramer, L.P. (1996). Actin-based cell motility and cell locomotion. Cell 84, 371-379.

Moissoglu, K., and Schwartz, M.A. (2006). Integrin signalling in directed cell migration. Biol Cell 98, 547-555.

Morgan, M.J., and Madgwick, A.J. (1996). Slim defines a novel family of LIM-proteins expressed in skeletal muscle. Biochem Biophys Res Commun 225, 632-638.

Morlon, A., and Sassone-Corsi, P. (2003). The LIM-only protein FHL2 is a serum-inducible transcriptional coactivator of AP-1. Proc Natl Acad Sci U S A 100, 3977-3982.

Moser, M., and Leo, O. (2010). Key concepts in immunology. Vaccine 28 Suppl 3, C2-13.

Muller, J.M., Isele, U., Metzger, E., Rempel, A., Moser, M., Pscherer, A., Breyer, T., Holubarsch, C., Buettner, R., and Schule, R. (2000). FHL2, a novel tissue-specific coactivator of the androgen receptor. EMBO J 19, 359-369.

Muller, J.M., Metzger, E., Greschik, H., Bosserhoff, A.K., Mercep, L., Buettner, R., and Schule, R. (2002). The transcriptional coactivator FHL2 transmits Rho signals from the cell membrane into the nucleus. EMBO J 21, 736-748.

Mullins, R.D., Heuser, J.A., and Pollard, T.D. (1998). The interaction of Arp2/3 complex with actin: nucleation, high affinity pointed end capping, and formation of branching networks of filaments. Proc Natl Acad Sci U S A 95, 6181-6186.

Murphy, T.L., Cleveland, M.G., Kulesza, P., Magram, J., and Murphy, K.M. (1995). Regulation of interleukin 12 p40 expression through an NF-kappa B half-site. Mol Cell Biol 15, 5258-5267.

Nobes, C., and Marsh, M. (2000). Dendritic cells: new roles for Cdc42 and Rac in antigen uptake? Curr Biol 10, R739-741.

Norbury, C.C. (2006). Drinking a lot is good for dendritic cells. Immunology 117, 443-451.

Ohl, L., Mohaupt, M., Czeloth, N., Hintzen, G., Kiafard, Z., Zwirner, J., Blankenstein, T., Henning, G., and Forster, R. (2004). CCR7 governs skin dendritic cell migration under inflammatory and steady-state conditions. Immunity 21, 279-288.

Oka, M., Homma, N., Taraseviciene-Stewart, L., Morris, K.G., Kraskauskas, D., Burns, N., Voelkel, N.F., and McMurtry, I.F. (2007). Rho kinase-mediated vasoconstriction is important in severe occlusive pulmonary arterial hypertension in rats. Circ Res 100, 923-929.

Okamoto, H., Takuwa, N., Yokomizo, T., Sugimoto, N., Sakurada, S., Shigematsu, H., and Takuwa, Y. (2000). Inhibitory regulation of Rac activation, membrane ruffling, and cell migration by the G protein-coupled sphingosine-1-phosphate receptor EDG5 but not EDG1 or EDG3. Mol Cell Biol 20, 9247-9261.

Ouaaz, F., Arron, J., Zheng, Y., Choi, Y., and Beg, A.A. (2002). Dendritic cell development and survival require distinct NF-kappaB subunits. Immunity 16, 257-270.

Paik, J.H., Chae, S., Lee, M.J., Thangada, S., and Hla, T. (2001). Sphingosine 1-phosphate-induced endothelial cell migration requires the expression of EDG-1 and EDG-3 receptors and Rho-dependent activation of alpha vbeta3- and beta1-containing integrins. J Biol Chem 276, 11830-11837.

Palm, N.W., and Medzhitov, R. (2009). Pattern recognition receptors and control of adaptive immunity. Immunol Rev 227, 221-233.

Pardi, R., Inverardi, L., Rugarli, C., and Bender, J.R. (1992). Antigen-receptor complex stimulation triggers protein kinase C-dependent CD11a/CD18-cytoskeleton association in T lymphocytes. J Cell Biol 116, 1211-1220.

Park, J., Will, C., Martin, B., Gullotti, L., Friedrichs, N., Buettner, R., Schneider, H., Ludwig, S., and Wixler, V. (2008). Deficiency in the LIM-only protein FHL2 impairs assembly of extracellular matrix proteins. FASEB J 22, 2508-2520.

Paul, C., Lacroix, M., Iankova, I., Julien, E., Schafer, B.W., Labalette, C., Wei, Y., Le Cam, A., Le Cam, L., and Sardet, C. (2006). The LIM-only protein FHL2 is a negative regulator of E4F1. Oncogene 25, 5475-5484.

Petersen, M.S., Toldbod, H.E., Holtz, S., Hokland, M., Bolund, L., and Agger, R. (2000). Strain-specific variations in the development of dendritic cells in murine bone-marrow cultures. Scand J Immunol 51, 586-594.

Philippar, U., Schratt, G., Dieterich, C., Muller, J.M., Galgoczy, P., Engel, F.B., Keating, M.T., Gertler, F., Schule, R., Vingron, M., et al. (2004). The SRF target gene Fhl2 antagonizes RhoA/MAL-dependent activation of SRF. Mol Cell 16, 867-880.

Pollard, T.D., Blanchoin, L., and Mullins, R.D. (2000). Molecular mechanisms controlling actin filament dynamics in nonmuscle cells. Annu Rev Biophys Biomol Struct 29, 545-576.

Pollard, T.D., and Borisy, G.G. (2003). Cellular motility driven by assembly and disassembly of actin filaments. Cell 112, 453-465.

Qiao, L., Wang, Y., Pang, R., Wang, J., Dai, Y., Ma, J., Gu, Q., Li, Z., Zhang, Y., Zou, B., et al. (2009). Oncogene functions of FHL2 are independent from NF-kappaBIalpha in gastrointestinal cancer. Pathol Oncol Res 15, 31-36.

Quast, T., Tappertzhofen, B., Schild, C., Grell, J., Czeloth, N., Forster, R., Alon, R., Fraemohs, L., Dreck, K., Weber, C., et al. (2009). Cytohesin-1 controls the activation of RhoA and modulates integrin-dependent adhesion and migration of dendritic cells. Blood 113, 5801-5810.

Raftopoulou, M., and Hall, A. (2004). Cell migration: Rho GTPases lead the way. Dev Biol 265 23– 32.

Rathinasamy, A., Czeloth, N., Pabst, O., Forster, R., and Bernhardt, G. (2010). The origin and maturity of dendritic cells determine the pattern of sphingosine 1-phosphate receptors expressed and required for efficient migration. J Immunol 185, 4072-4081.

Ratzinger, G., Stoitzner, P., Ebner, S., Lutz, M.B., Layton, G.T., Rainer, C., Senior, R.M., Shipley, J.M., Fritsch, P., Schuler, G., et al. (2002). Matrix metalloproteinases 9 and 2 are necessary for the migration of Langerhans cells and dermal dendritic cells from human and murine skin. J Immunol 168, 4361-4371.

Renkawitz, J., Schumann, K., Weber, M., Lammermann, T., Pflicke, H., Piel, M., Polleux, J., Spatz, J.P., and Sixt, M. (2009). Adaptive force transmission in amoeboid cell migration. Nat Cell Biol 11, 1438-1443.

Rescigno, M., Martino, M., Sutherland, C.L., Gold, M.R., and Ricciardi-Castagnoli, P. (1998). Dendritic cell survival and maturation are regulated by different signaling pathways. J Exp Med 188, 2175-2180.

Ridley, A.J. (2001). Rho GTPases and cell migration. J Cell Sci 114, 2713-2722.

Ridley, A.J., Schwartz, M.A., Burridge, K., Firtel, R.A., Ginsberg, M.H., Borisy, G., Parsons, J.T., and Horwitz, A.R. (2003). Cell migration: integrating signals from front to back. Science 302, 1704-1709.

Riol-Blanco, L., Sánchez-Sánchez, N., Torres, A., Tejedor, A., Narumiya, S., Corbí, A., Sánchez-Mateos, P., and Rodríguez-Fernández, J. (2005). The chemokine receptor CCR7 activates in dendritic cells two signaling modules that independently regulate chemotaxis and migratory speed. J Immunol 174(7), 4070-4080.

Roake, J.A., Rao, A.S., Morris, P.J., Larsen, C.P., Hankins, D.F., and Austyn, J.M. (1995). Dendritic cell loss from nonlymphoid tissues after systemic administration of lipopolysaccharide, tumor necrosis factor, and interleukin 1. J Exp Med 181, 2237-2247.

Robbiani, D.F., Finch, R.A., Jager, D., Muller, W.A., Sartorelli, A.C., and Randolph, G.J. (2000). The leukotriene C(4) transporter MRP1 regulates CCL19 (MIP-3beta, ELC)-dependent mobilization of dendritic cells to lymph nodes. Cell 103, 757-768.

Roediger, B., Ng, L.G., Smith, A.L., Fazekas de St Groth, B., and Weninger, W. (2008). Visualizing dendritic cell migration within the skin. Histochem Cell Biol 130, 1131-1146.

Saeki, H., Moore, A.M., Brown, M.J., and Hwang, S.T. (1999). Cutting edge: secondary lymphoid-tissue chemokine (SLC) and CC chemokine receptor 7 (CCR7) participate in the emigration pathway of mature dendritic cells from the skin to regional lymph nodes. J Immunol 162, 2472-2475.

Sallusto, F., and Lanzavecchia, A. (1994). Efficient presentation of soluble antigen by cultured human dendritic cells is maintained by granulocyte/macrophage colony-stimulating factor plus interleukin 4 and downregulated by tumor necrosis factor alpha. J Exp Med 179, 1109-1118.

Sallusto, F., Schaerli, P., Loetscher, P., Schaniel, C., Lenig, D., Mackay, C.R., Qin, S., and Lanzavecchia, A. (1998). Rapid and coordinated switch in chemokine receptor expression during dendritic cell maturation. Eur J Immunol 28, 2760–2769.

Sampath, P., and Pollard, T.D. (1991). Effects of cytochalasin, phalloidin, and pH on the elongation of actin filaments. Biochemistry 30, 1973-1980.

Samson, T., Smyth, N., Janetzky, S., Wendler, O., Muller, J.M., Schule, R., von der Mark, H., von der Mark, K., and Wixler, V. (2004). The LIM-only proteins FHL2 and FHL3 interact with alpha- and beta-subunits of the muscle alpha7beta1 integrin receptor. J Biol Chem 279, 28641-28652.

Sánchez-Sánchez, N., Riol-Blanco, L., and Rodríguez-Fernández, J. (2006). The multiple personalities of the chemokine receptor CCR7 in dendritic cells. J Immunol 176(9), 5153-5159.

Sanna, M.G., Liao, J., Jo, E., Alfonso, C., Ahn, M.Y., Peterson, M.S., Webb, B., Lefebvre, S., Chun, J., Gray, N., et al. (2004). Sphingosine 1-phosphate (S1P) receptor subtypes S1P1 and S1P3, respectively, regulate lymphocyte recirculation and heart rate. J Biol Chem 279, 13839-13848.

Scholl, F.A., McLoughlin, P., Ehler, E., de Giovanni, C., and Schafer, B.W. (2000). DRAL is a p53-responsive gene whose four and a half LIM domain protein product induces apoptosis. J Cell Biol 151, 495-506.

Shi, X., Bowlin, K.M., and Garry, D.J. (2010). Fhl2 interacts with Foxk1 and corepresses Foxo4 activity in myogenic progenitors. Stem Cells 28, 462-469.

Shinoda, K., Nakagawa, K., Kosaka, T., Tanaka, N., Maeda, T., Kono, H., Mizuno, R., Kikuchi, E., Miyajima, A., Umezawa, K., et al. (2010). Regulation of human dendritic cells by a novel specific nuclear factor-kappaB inhibitor, dehydroxymethylepoxyquinomicin. Hum Immunol 71, 763-770.

Shortman, K., and Naik, S.H. (2007). Steady-state and inflammatory dendritic-cell development. Nat Rev Immunol 7, 19-30.

Shurin, G.V., Tourkova, I.L., Chatta, G.S., Schmidt, G., Wei, S., Djeu, J.Y., and Shurin, M.R. (2005). Small rho GTPases regulate antigen presentation in dendritic cells. J Immunol 174, 3394-3400.

Siamakpour-Reihani, S., Argiros, H.J., Wilmeth, L.J., Haas, L.L., Peterson, T.A., Johnson, D.L., Shuster, C.B., and Lyons, B.A. (2009). The cell migration protein Grb7 associates with transcriptional regulator FHL2 in a Grb7 phosphorylation-dependent manner. J Mol Recognit 22, 9-17.

Sixt, M., Bauer, M., Lammermann, T., and Fassler, R. (2006). Beta1 integrins: zip codes and signaling relay for blood cells. Curr Opin Cell Biol 18, 482-490.

Sousa, C.R.e. (2006). Dendritic cells in a mature age. Nature 6, 476-483.

Sozzani, S., Allavena, P., D'Amico, G., Luini, W., Bianchi, G., Kataura, M., Imai, T., Yoshie, O., Bonecchi, R., and Mantovani, A. (1998). Differential regulation of chemokine receptors during dendritic cell maturation: a model for their trafficking properties. J Immunol 161, 1083-1086.

Spiegel, S., and Milstien, S. (2000). Functions of a new family of sphingosine-1-phosphate receptors. Biochim Biophys Acta 1484, 107-116.

Steinman, R.M., Hawiger, D., and Nussenzweig, M.C. (2003). Tolerogenic dendritic cells. Annu Rev Immunol 21, 685-711.

Stilo, R., Leonardi, A., Formisano, L., Di Jeso, B., Vito, P., and Liguoro, D. (2002). TUCAN/CARDINAL and DRAL participate in a common pathway for modulation of NF-kappaB activation. FEBS Lett 521, 165-169.

Sugimoto, N., Takuwa, N., Okamoto, H., Sakurada, S., and Takuwa, Y. (2003). Inhibitory and stimulatory regulation of Rac and cell motility by the G12/13-Rho and Gi pathways integrated downstream of a single G protein-coupled sphingosine-1-phosphate receptor isoform. Mol Cell Biol 23, 1534-1545.

Sullivan, S.J., Daukas, G., and Zigmond, S.H. (1984). Asymmetric distribution of the chemotactic peptide receptor on polymorphonuclear leukocytes. J Cell Biol 99, 1461-1467.

Svitkina, T.M., and Borisy, G.G. (1999). Arp2/3 complex and actin depolymerizing factor/cofilin in dendritic organization and treadmilling of actin filament array in lamellipodia. J Cell Biol 145, 1009-1026.

Svitkina, T.M., Bulanova, E.A., Chaga, O.Y., Vignjevic, D.M., Kojima, S., Vasiliev, J.M., and Borisy, G.G. (2003). Mechanism of filopodia initiation by reorganization of a dendritic network. J Cell Biol 160, 409-421.

Swetman, C.A., Leverrier, Y., Garg, R., Gan, C.H., Ridley, A.J., Katz, D.R., and Chain, B.M. (2002). Extension, retraction and contraction in the formation of a dendritic cell dendrite: distinct roles for Rho GTPases. Eur J Immunol 32, 2074-2083.

Takashima, S., Sugimoto, N., Takuwa, N., Okamoto, Y., Yoshioka, K., Takamura, M., Takata, S., Kaneko, S., and Takuwa, Y. (2008). G12/13 and Gq mediate S1P2-induced inhibition of Rac and migration in vascular smooth muscle in a manner dependent on Rho but not Rho kinase. Cardiovasc Res 79, 689-697.

Takuwa, Y. (2002). Subtype-specific differential regulation of Rho family G proteins and cell migration by the Edg family sphingosine-1-phosphate receptors. Biochim Biophys Acta 1582, 112-120.

Takuwa, Y., Takuwa, N., and Sugimoto, N. (2002). The Edg family G protein-coupled receptors for lysophospholipids: their signaling properties and biological activities. J Biochem 131, 767-771.

Tan, J.K.H., and O'Neill, H.C. (2005). Maturation requirements for dendritic cells in T cell stimulation leading to tolerance versus immunity. J Leukoc Biol 78, 319-324.

Trombetta, E.S., and Mellman, I. (2005). Cell biology of antigen processing in vitro and in vivo. Annu Rev Immunol 23, 975-1028.

Turley, S.J., Inaba, K., Garrett, W.S., Ebersold, M., Unternaehrer, J., Steinman, R.M., and Mellman, I. (2000). Transport of peptide-MHC class II complexes in developing dendritic cells. Science 288, 522-527.

van Helden, S.F., Krooshoop, D.J., Broers, K.C., Raymakers, R.A., Figdor, C.G., and van Leeuwen, F.N. (2006). A critical role for prostaglandin E2 in podosome dissolution and induction of high-speed migration during dendritic cell maturation. J Immunol 177, 1567-1574.

Wang, J., Yang, Y., Xia, H.H., Gu, Q., Lin, M.C., Jiang, B., Peng, Y., Li, G., An, X., Zhang, Y., et al. (2007). Suppression of FHL2 expression induces cell differentiation and inhibits gastric and colon carcinogenesis. Gastroenterology 132, 1066-1076.

Wei, Y., Renard, C.A., Labalette, C., Wu, Y., Levy, L., Neuveut, C., Prieur, X., Flajolet, M., Prigent, S., and Buendia, M.A. (2003). Identification of the LIM protein FHL2 as a coactivator of beta-catenin. J Biol Chem 278, 5188-5194.

Welch, M.D., and Mullins, R.D. (2002). Cellular control of actin nucleation. Annu Rev Cell Dev Biol 18, 247-288.

Wennerberg, K., and Der, C.J. (2004). Rho-family GTPases: it's not only Rac and Rho (and I like it). J Cell Sci 117, 1301-1312.

West, M.A., Antoniou, A.N., Prescott, A.R., Azuma, T., Kwiatkowski, D.J., and Watts, C. (1999). Membrane ruffling, macropinocytosis and antigen presentation in the absence of gelsolin in murine dendritic cells. Eur J Immunol 29, 3450-3455.

West, M.A., Prescott, A.R., Eskelinen, E.L., Ridley, A.J., and Watts, C. (2000). Rac is required for constitutive macropinocytosis by dendritic cells but does not control its downregulation. Curr Biol 10, 839-848.

Wixler, V., Geerts, D., Laplantine, E., Westhoff, D., Smyth, N., Aumailley, M., Sonnenberg, A., and Paulsson, M. (2000). The LIM-only protein DRAL/FHL2 binds to the cytoplasmic domain of several alpha and beta integrin chains and is recruited to adhesion complexes. J Biol Chem 275, 33669-33678.

Wixler, V., Hirner, S., Muller, J.M., Gullotti, L., Will, C., Kirfel, J., Gunther, T., Schneider, H., Bosserhoff, A., Schorle, H., et al. (2007). Deficiency in the LIM-only protein Fhl2 impairs skin wound healing. J Cell Biol 177, 163-172.

Yanagawa, Y., and Onoe, K. (2002). CCL19 induces rapid dendritic extension of murine dendritic cells. Blood 100, 1948-1956.

Yanagawa, Y., and Onoe, K. (2003). CCR7 ligands induce rapid endocytosis in mature dendritic cells with concomitant up-regulation of Cdc42 and Rac activities. Blood 101, 4923-4929.

Yang, Y., Hou, H., Haller, E.M., Nicosia, S.V., and Bai, W. (2005). Suppression of FOXO1 activity by FHL2 through SIRT1-mediated deacetylation. EMBO J 24, 1021-1032.

Zhang, J.S., Feng, W.G., Li, C.L., Wang, X.Y., and Chang, Z.L. (2000). NF-kappa B regulates the LPS-induced expression of interleukin 12 p40 in murine peritoneal macrophages: roles of PKC, PKA, ERK, p38 MAPK, and proteasome. Cell Immunol 204, 38-45.

Zhang, W., Jiang, B., Guo, Z., Sardet, C., Zou, B., Lam, C.S., Li, J., He, M., Lan, H.Y., Pang, R., et al. (2010). Four-and-a-half LIM protein 2 promotes invasive potential and epithelial-mesenchymal transition in colon cancer. Carcinogenesis 31, 1220-1229.

# Abbreviations

| | |
|---|---|
| aa | amino acids |
| ab | antibody |
| ABTS | 2,2'-azino-bis(3-ethylbenzo-thiazoline-6-sulphonic acid) |
| ACT | Activator of CREM in testis |
| ADAM | A Disintegrin And Metalloproteinase |
| APC | Allophycocyanin |
| APC | antigen presenting cell |
| Arp | Actin-Related Proteins |
| ATP | Adenosine-5'-triphosphate |
| β-ME | β-mercaptoethanol |
| BM | bone marrow |
| BMDC | bone marrow-derived dendritic cells |
| Bp | base pairs |
| BSA | Bovine serum albumin |
| C | celsius |
| cDNA | complementary DNA |
| CFSE | Carboxyfluorescein succinimidyl ester |
| CCL19 | chemokine, CC MOTIF, ligand 19 |
| CCR7 | Chemokine, CC Motif, receptor 7 |
| CD | cluster of differentiation |
| Cdc42 | cell division cycle 42 |
| cm | centimeter |
| DAPI | 4',6-diamidino-2-phenylindole |
| DC | dendritic cell |
| $ddH_2O$ | double destilled water |
| DMSO | Dimethyl sulfoxide |
| DNA | Deoxyribonucleic acid |
| dNTP | di-Nucleoside triphosphate |
| DTT | Dithiothreitol |
| ECL | Electrochemiluminescence |
| ECM | extracellular matrix |
| EDG | endothelial differentiation gene |

| | |
|---|---|
| e.g. | Latin exempli gratia (for example) |
| ELISA | Enzyme-linked immunosorbent assay |
| ER | endoplasmatic reticulum |
| et al. | Latin et alia (and others) |
| F | forward |
| F-actin | filamentous actin |
| FACS | Fluorescence-activated cell sorting |
| FCS | Fetal calf serum |
| Fig | Figure |
| FITC | fluorescein isothiocyanate |
| Foxo1 | Forkhead Box O1 |
| FSC | Forward scatter |
| g | gram |
| G-actin | globular actin |
| GAP | GTPase activating protein |
| GDI | Guanine nucleotide dissociation inhibitors |
| GDP | Guanosine diphosphate |
| GEF | Guanine nucleotide exchange factors |
| GFP | green fluorescent protein |
| GMCSF | Granulocyte macrophage colony-stimulating factor |
| GTP | Guanosine triphosphate |
| i.e. | Latin id est (that is) |
| HPLC | high performance liquid chromatography |
| HRP | Horseradish peroxidase |
| Hrs | hours |
| IF | intermediate filaments |
| IgG | Immunoglobin |
| IL | Interleukin |
| IMDM | Iscove's Modified Dulbecco's Media |
| IP | Immunoprecipitation |
| IRS | insulin receptor tyrosine kinase substrate |
| kDa | kilo Dalton |
| KLF2 | Kruppel-like factor 2 |
| KO | knock out |

| | |
|---|---|
| l | liter |
| LN | lymph node |
| LPS | lipopolysaccharides |
| LSD1 | Lysine specific demethylase 1 |
| M | molar |
| mAB | monoclonal antibody |
| MACS | Magnetic Activated Cell Sorting |
| MFI | mean fluorescence intensity |
| mg | milligram |
| $MgCl_2$ | Magnesium chloride |
| MHC | major histocompatibility complex |
| Min | minute |
| miRNA | microRNA |
| ml | milliliter |
| mM | millimolar |
| MMP | Matrix metalloproteinases |
| MP | Milk powder |
| mRNA | messenger RNA |
| ms | milliseconds |
| MT | microtubules |
| MTT | 3-(4,5-Dimethylthiazol-2-yl)-2,5-diphenyltetrazolium bromide |
| NADH | Nicotinamide adenine dinucleotide plus hydrogen (reduced) |
| NADPH | Nicotinamide adenine dinucleotide phosphate (reduced) |
| NF-κB | nuclear factor–κB |
| ng | nanogram |
| NP-40 | Nonidet P-40 |
| NK | Natural Killer |
| NKT | Natural Killer T |
| NS | not significant |
| OVA | ovalbumin |
| P | Penicillin |
| PAGE | polyacrylamide gel electrophoresis |
| PAMP | pathogen-associated molecular patterns |
| PBS | Phosphate buffered saline |

| | |
|---|---|
| PCR | Polymerase chain reaction |
| PDGF | platelet-derived growth factor |
| PE | Phycoerythrin |
| Percp | Peridinin-chlorophyll-protein complex |
| PFA | Paraformaldehyde |
| PRR | Pattern recognition receptors |
| qRT-PCR | Quantitative Real-Time PCR |
| R | reverse |
| RAC | Ras-related C3 botulinum toxin substrate |
| RBD | Rac binding domain |
| RhoA | Ras homolog gene family, member A |
| RIPA | Radioimmunoprecipitation assay |
| RLU | Relative Luminescence Units |
| RNA | ribonucleic acid |
| Rpm | rounds per minute |
| mm | milimeter |
| RPMI | Roswell Park Memorial Institute |
| RT-PCR | reverse transcriptase-PCR |
| s | seconds |
| S | Streptomycin |
| S1P | Sphingosin-1-phosphate |
| S1PR | Sphigosine-1-Phosphate Receptor |
| SDS | Sodium dodecyl sulfate |
| SEM | Standard error of the mean |
| siRNA | small interfering RNA |
| SIRT1 | Sirtuin1 |
| SNARF-1 | carboxylic acid, acetate, succicimidyl ester SNARF |
| SPF | specific pathogen free |
| SSC | Side Scatter |
| T | Tween |
| TAE | Tris-acetate-EDTA |
| TAP | transporters associated with antigen processing |
| Taq | *Thermus aquaticus* |
| TBS | Tris Buffered Saline |

| | |
|---|---|
| TCR | T cell receptor |
| TLR | Toll-like receptor |
| TNF | tumor necrosis factor |
| TRIS | Tris(hydroxymethyl)aminomethane |
| U | units |
| µl | microliter |
| µm | micrometer |
| µM | micromolar |
| V | Volt |
| VEGF | vascular endothelial growth factor |
| WASp | Wiskott-Aldrich Syndrome Protein |
| WAVE | WASP-family verprolin-homologous protein |
| w/o | without |
| wt | wild type |

# List of Figures

# List of Tables